

Development of Advanced Multi Stage Adsorption Refrigeration Cycles

**DISSERTATION
A.F.M. MIZANUR RAHMAN**

March 2013

**GRADUATE SCHOOL OF BIO-APPLICATIONS AND SYSTEMS ENGINEERING
TOKYO UNIVERSITY OF AGRICULTURE AND TECHNOLOGY, JAPAN**

Development of Advanced Multi Stage Adsorption Refrigeration Cycles

**A dissertation submitted in partial fulfillment of the requirements for the
award of the degree**

of

Doctor of Engineering (Dr. Eng.)

by

A.F.M. MIZANUR RAHMAN

Supervisor

Professor Atsushi Akisawa

Co-supervisor

Associate Professor Yuki Ueda

**GRADUATE SCHOOL OF BIO-APPLICATIONS AND SYSTEMS ENGINEERING
TOKYO UNIVERSITY OF AGRICULTURE AND TECHNOLOGY, JAPAN**

Table of Contents

	Abstract	V
	Declaration	VII
	Acknowledge	VIII
	Nomenclatures	IX
	Chapter 1	1
1.1	Background	1
1.2	Introduction	1
1.3	Objectives and scopes	4
1.4	Thesis Outline	5
	Chapter 2	6
	Chronological development of adsorption system	
2.1	Conventional vapour compression system	7
2.2	Absorption system	8
2.3	Adsorption system	9
2.4	Adsorption system description	10
2.4.1.	Single-stage adsorption system	10
2.4.1.1	Single-bed adsorption system	11
2.4.1.2	Conventional two-bed adsorption system	13
2.4.1.3	Advanced two-bed adsorption system	15
2.4.1.4	Conventional three-bed adsorption system	18
2.4.1.5	Advanced three-bed adsorption system	19
2.4.1.6	Four-bed adsorption system	22
2.4.2	Two-stage adsorption system	23
2.4.2.1	Conventional two-stage adsorption system	23
2.4.2.2	Advance two-stage adsorption system	25
2.4.3	Three-stage adsorption system	27
2.4.3.1	Conventional three-stage adsorption system	27
2.4.3.2	Advance three-stage adsorption system	29
2.5	Other type of adsorption system	31
2.5.1	Cascading adsorption system	31

2.5.2	Double effect adsorption system	32
2.6	Adsorbent/adsorbate pairs	34
	Chapter 3	36
	Adsorption system modelling	
3.1	Adsorption and desorption	36
3.2	Theory of adsorption	37
3.3	Forces and energies of adsorption system	41
3.4	Heat and energy balance of adsorption system	43
3.4.1	Adsorption and desorption bed energy balance	43
3.4.2	Evaporator energy balance	44
3.4.3	Condenser energy balance	45
3.4.4	Adsorption and desorption rate	45
3.4.5	Mass balance	46
3.4.6	System performance	46
3.5.	Optimization of adsorption system	47
	Chapter 4	51
	Performance comparison of three-bed adsorption cooling system with optimal cycle time setting	
4.1	Introduction	51
4.2	Description of three-bed adsorption cooling system	52
4.3	Methods and materials	55
4.4	Results and discussion	56
4.5	Conclusion	65
	Chapter 5	67
	Innovative design and performance of three-bed two stage adsorption cycle under optimized cycle time	
5.1	Introduction	67
5.2	Description of three-bed two-stage adsorption cycle	68
5.3	Simulation methods and materials	73
5.4	Results and discussions	73
5.5	Conclusion	83
	Chapter 6	84

	Design and performance of an innovative four-bed, three stage adsorption cycle	
6.1	Introduction	84
6.2	Description of three-stage adsorption cycle	85
6.3	Simulation methods and materials	89
6.4	Results and discussions	90
6.5	Conclusion	101
	Chapter 7	102
7.1	Overall conclusion	102
7.2	Remarks	103
	Appendix A	104
	Appendix B	118
	References	129
	Dissertation related author's publication	138

Abstract

Adsorption refrigeration system is widely considered to be an environmental friendly usage, neither use CFC (Chlorofluorocarbons), HCFC (Hydro-Chlorofluorocarbons) as working fluid nor use fossil fuel or electricity as driving heat source. Therefore, this system does not contribute to global warming and Ozone layer depletion potential as prerequisite in accordance with the Kyoto Protocol. In recent years, adsorption refrigeration systems have drawn considerable attention due to their relatively lower environmental impact and large energy saving potential. The reduction of primary energy could be achieved with a reasonable utilization of waste thermal energy. Adsorption cycle has distinct advantage over other refrigeration systems in its ability to be driven by heat of relatively low, near-environment temperature. Both experimental and simulation based investigation on adsorption cooling systems shows that the performance of adsorption chillers depend highly on both the adsorbent-refrigerant pairs and cycle operation time.

Two-bed, single-stage adsorption refrigeration machine is currently available in the market which has limitation on the overall performance. Many studies were carried out to modify the system in various aspects such as three-bed, single-stage cycle and it was identified that the performance of advance three-bed, single-stage adsorption system is better than the conventional and advance two-bed, single-stage adsorption system. In this dissertation, the cycle time of two different types of silica gel-water based three-bed single-stage adsorption system employing mass recovery with heating/cooling scheme was optimized to increase the performance. It is reported that optimization procedure has not been applied on three-bed system. A new simulation program has been developed to analyze the effect of cycle time precisely on the performance of the systems. The particle swarm optimization (PSO) method has been used to optimize the cycle time and then the optimum performances of two systems are compared. Sensitive analysis of cycle time has been conducted using contour plot of specific cooling power (SCP) with a fixed driving heat source temperature at 80 °C. It is found that the center point of the contour indicates the maximum SCP value and optimal cycle time, which are comparable with the quantitative values obtained for PSO method. Both three-bed mass recovery adsorption cycles can produce effective cooling at heat source temperature as low as 50 °C along with a coolant at 30 °C. The optimal SCP is similar for both cycles and is greater than that of the conventional two-bed adsorption cooling system employing same adsorbent-refrigerant pair. Consequently, the proposed comparison

method is effective and useful to identify the best performance of adsorption cooling cycles.

Three-bed, single-stage adsorption system was further modified to four-bed, two-stage adsorption system enabling to utilize the waste heat/solar heat as low as 45 °C effectively. However, the size of the four-bed, two-stage system is larger compare to two- and three-bed systems. In the present work, an innovative design of a three-bed, two-stage silica gel-water based adsorption cycle has been proposed aiming to minimize the overall size of four-bed, two-stage cycle. One adsorber/desorber heat exchanger bed was removed from former four-bed, two-stage cooling system and operational strategy was taken to increase the adsorption time compare to desorption time in the proposed design. The cycle time was optimized to obtain the maximum SCP for different heat source temperatures using the PSO method. Sensitivity analysis of the cycle time was conducted using contour plot of SCP and chilled water outlet temperature for driving heat source temperature at 55 °C. Optimize results were compared with the results of four-bed, two-stage adsorption cooling cycle. It was found that the SCP was increased for the proposed cycle over the whole range of regeneration temperature. The proposed cycle seems advantageous from the economic viewpoint due to its improved performance and reduced volume.

Four-bed, two-stage adsorption cooling system was modified to six-bed, three-stage adsorption system, which is capable to utilize very low temperature waste heat/solar heat at near environmental temperature but size of the system is larger compare to other adsorption cooling system. In this dissertation the design of a four-bed, three-stage adsorption cycle has been proposed to reduce the volume of the six-bed, three-stage adsorption cycle. Particle swarm optimization (PSO) technique was used to optimize the cycle time enabling to maximize the SCP. PSO results showed that the optimal cycle time was decreased with heat source temperature and SCP value was proportional to heat source temperature. It was found that the proposed cycle could be driven by waste heat as low as 40°C along with coolant at 30°C. Comparative study of optimized results indicated that the proposed cycle increased the performance significantly over the whole range of temperatures from 40 to 70 °C and reduced two adsorbent beds, compared to the six-bed, three-stage adsorption cooling cycle.

The innovative designs of three-bed, two-stage and four-bed, three-stage adsorption system, commonly known as multi-stage adsorption refrigeration cycle introduced in this dissertation are simple design, optimal size and better performance. Therefore, it is expected that this multi-stage adsorption refrigeration cycle will be more attractive to the consumers.

Candidate's Declaration

I hereby declare that the work, which is being presented in the thesis entitled **“Development of Advanced Multi Stage Adsorption Refrigeration Cycle”** submitted in partial fulfilment of the requirements for the award of the degree of Doctor of Philosophy (Ph.D), Graduate School of Bio-Applications and Systems Engineering, Tokyo University of Agriculture and Technology, Japan is an authentic record of my own research work.

The research work presented in the thesis has not been submitted by me for the award of any other degree in this or any other university.

November 2012

(A.F.M. Mizanur Rahman)

Acknowledgement

I would like to express my sincere gratitude and appreciation to my research supervisor **Professor Atsushi Akisawa** and co-supervisor **Associate Professor Yuki Ueda** for their thorough help, constant encouragement, advice and guidance through the progress of my work. I am highly grateful to them for their earnest feeling and help in matters concerning my research work.

I would like to express my heartiest gratitude to **Professor Bidyut Baran Saha**, Mechanical Engineering Department, Faculty of Engineering and International Institute for Carbon-Neutral Energy Research (WPI-I2CNER), Kyushu University and **Associate Professor Takahiko Miyazaki**, Faculty of Engineering Science, Kyushu University, Japan for their indispensable encouragement, assistance and guidance in every steps of my research work.

I also would like to express my heartiest gratitude to Dr. Mazibur Rahman, International Atomic Energy Agency, Vienna (during his visit of Tokyo) and Dr. Yaron Silberberg, Research Fellow, Tokyo University of Agriculture and Technology for their guidance to write the thesis paper.

All students of Akisawa and Ueda Laboratories, specially Ishii Yuji, Muhammad Umair, Shoaib Ahmad Lutfi and I Gusti Agung Bagus Wirajati, are gratefully acknowledged, for their co-operation and help during my research work.

I would like to express love and sincere gratitude to my beloved parents, son, daughter and wife for their deep understanding and moral support throughout the study in Japan. Moreover, I would like to thank to all Bangladeshi and foreign friends for their help, supports and cooperation throughout my study in Japan.

Finally, Bangladesh Atomic Energy Commission (BAEC) is appreciatively acknowledged for allowing me to carry out research work in Japan. Ministry of Education, Culture, Sports, Science and Technology (MEXT), Japan is also thankfully acknowledged for their provision of scholarship and all other assistances.

Nomenclatures

A	Heat transfer area (m^2)
C	specific heat ($\text{J kg}^{-1} \text{K}^{-1}$)
D_{so}	surface specific heat ($\text{m}^2 \text{s}^{-1}$)
E_a	activation energy (J kg^{-1})
L	latent heat of vaporization (J kg^{-1})
\dot{m}	mass flow rate (kg s^{-1})
P_s	saturated vapour pressure (Pa)
q	fraction of refrigerant that can be adsorbed by the adsorbent (kg kg^{-1})
q^*	fraction of refrigerant that can be adsorbed by the adsorbent under saturation condition (kg kg^{-1})
Q_{st}	isosteric heat of adsorption (J kg^{-1})
R	gas constant ($\text{J kg}^{-1} \text{K}^{-1}$)
R_p	average radius of silica gel particles (m)
T	temperature (K)
t	time (s)
U	overall heat transfer coefficient ($\text{W m}^{-2} \text{K}^{-1}$)
W	mass (kg)
Col	cooling water
Hot	hot water
V	valve
n	number of particles
k	number of iteration
z	dimension or number of variables

Superscripts

b	adsorption/desorption bed
c	condenser
e	evaporator
ads	adsorption
des	desorption
col	cooling water
hot	hot water

chil chilled water

Subscripts

hex heat exchanger (copper or aluminium)

in inlet

out outlet

s silica gel

tot total

cycle total cycle

w water

wv water vapour

Chapter 1

1.1 Background

Heat pump technique is considered as one of the modern technology in the contemporary era. Among different techniques, vapor-compression system is well-established for using in most household refrigerators, air conditioners, and many large commercial and industrial refrigeration systems. According to environmental aspect of the Kyoto Protocol, the vapor-compression systems are not recommended due to its use of non-natural working fluids such as chlorofluorocarbon (CFC), hydro-chlorofluorocarbon (HCFC) and hydro-fluorocarbon (HFC), which are responsible for ozone layer depletion and/or global warming. Additionally, the Montreal protocol 1987 also recommended reducing the emissions of these refrigerants. Not only that, the traditional systems are driven by electricity or heat, which increases the consumption of electricity and fossil energy. It is reported that approximately 15% of all the electricity produced in the whole world is employed for refrigeration and air-conditioning processes of various kinds, and the energy consumption for air-conditioning systems has recently been estimated to 45% of the whole households and commercial buildings (Santamouris et al., 1994). Nowadays, global demand of some other technologies to utilize renewable energy source either waste heat or solar heat that will be directly contribute to reduce the consumption of primary energy sources and to avoid the emission of green house gasses. Thermally driven adsorption heat pump is one of the key technologies, which can utilize renewable energy sources and use natural adsorbent-adsorbate pair. Subsequently, there is no chance for emission of green house gasses. Therefore, ozone layer depletion potential and global warming potential both are zero. It is widely accepted that thermally driven refrigeration technologies are attractive alternatives for simple design and lower cost. It can not only serve the needs for air-conditioning, refrigeration, ice making and congelation purposes, but also can meet the demand for energy conservation and environment protection.

1.2 Introduction

Adsorption is the accumulation of vapour molecules at the surface of a solid or liquid rather than in the bulk. This process was commercially used in refrigeration equipment in the late 1920s, where as patent literature of refrigeration cycle has existed since at least 1909, as reported by Hulse, 1929. The silica gel-sulphur dioxide pair was applied to propane-fired,

air-cooled cargo train refrigeration system. In 1929, Miller described several systems which utilized silica gel and sulfur dioxide as an adsorbent/adsorbate pair (Miller, 1929). Adsorption system is driven by external heat source, which can be chosen as waste heat of industries and machines or solar heat. Most fundamental adsorption system consists of a adsorption/desorption bed, a condenser and a evaporator, which is known as single-bed single-stage system. A solar powered single-bed refrigerator was invented by Critoph, 2002, which was recommended by the U.N. for vaccine storage in poor area. Patzer, 2001, Hidaka et al., 2005 and Monma et al., 2005 also invented other different type of single-bed adsorption refrigeration systems. Performance of single-bed adsorption system is very low but it is advantageous in simple structure and low initial cost.

Two-bed single-stage adsorption system is a basic adsorption system and comprises of two adsorption/desorption beds, one condenser and an evaporator. The system has some limitation on performance. Many researchers study on advanced single-stage adsorption systems such as two-bed mass recovery, three-bed, three-bed mass recovery, and three-bed heat recovery adsorption cycle to improve the performance of the single-stage adsorption system. A few examples of remarkable studies were demonstrated as in the field of solar cooling (Pons et al., 1986, Critoph, 1988, Sakoda et al., 1984, Wang et al., 2009), automobiles cooling system (Suzuki, 1993, Zhang et al., 1997) and in the field of waste heat utilization (Saha et al., 1995a, Chua et al., 1999). Silica gel-water based two-bed adsorption system powered by heat source of temperature as low as 70 °C is commercialized in Japan (Critoph et al., 2005).

Design of three-bed adsorption system was proposed to increase the performance and to produce continuous cooling load compare to two-bed adsorption system (Saha et al. 2003a). The systems consist of three heat exchanger beds, one evaporator and one condenser. The system was further modified considering mass recovery scheme by Khan et al., (2006a, 2007a) and Uyun et al., (2009a, 2009b). It was shown that appropriate cycle time setting provided better performance of a system and a fitting cycle time of a system is not suitable for other system. To compare different adsorption cycles fairly, it is emphasized that the best performance of each cycle should be compared. From this point of view, optimizing the cycle performance is quite important. Miyazaki et al., 2009 succeeded the optimization of cycle time to maximize the cooling effect of two-bed, single-stage adsorption cycle by the particle swarm optimization (PSO) method. It is reported that optimization technique was not applied on the three-bed adsorption system and also in comparison of different type of adsorption

system. This study, focused on optimization technique for Khan and Uyun three-bed non-regenerative silica gel-water adsorption cycle with mass recovery heating/cooling. Although both system have same number of adsorption/ desorption beds but the cycles have different behavior. Although the three-bed cycles are established and studied, but the simulated performance didn't reflect the optimal results because of the limitation of the simulation methods. In order to overcome this problem, the PSO method is applied to simulate the best performance.

Performance of three-bed single-stage adsorption system is better than two-bed adsorption system. However, the required driving temperature for the systems is 60 °C or higher. In order to utilize solar/waste heat with temperature below 70 °C, Saha et al., 2001 proposed a prototype design of a four-bed two-stage adsorption cycle. Later, an extensive study was conducted (Alam et al., 2004 and Hamamoto et al., 2005) to identify the influence of design and operating conditions on the system performance. Moreover, the modification of the system in terms of operating condition such as re-heat scheme was investigated by Khan et al., (2005, 2006b, 2007c), Alam et al., 2007 and Farid et al., 2011. These investigations identified that it can work with heat source temperature as low as 45°C. Therefore, a two-stage adsorption cycle is effective to utilize low grade heat sources.

The above mentioned studies on two-stage cycle, two pairs of adsorption/desorption heat exchanger beds were used in the higher temperature and pressure cycle (i.e., upper cycle) and lower temperature and pressure (i.e., lower cycle). However, the larger size of this adsorption cycle needs further modifications to make it more attractive to the users. In this study, it has focused on the reduction of the size of the four-bed two-stage adsorption cycle through reduce of a heat exchanger bed. Accordingly, a design was proposed via replacing the upper cycle two heat exchanger beds with one bed, whereas the lower cycle two beds were kept similar to the previous cycle. It can be said that the proposed cycle is the three-bed two-stage cycle, which is newly approached design with operational strategy. Investigation on the performance of the proposed cycle has been carried and then it has been compared with the conventional four-bed two-stage cycle. It can be noted that cycle performance strongly depends on heat source temperature and cycle time that needs to be adjusted to maximize the performance in accordance with the temperature. The PSO method was adopted to obtain the maximum cooling output. Finally, the results obtained from the proposed cycle were compared with the former four-bed two-stage cycle in order to investigate the influence of heat source temperature on specific cooling power (SCP) and coefficient of performance (COP).

To increase the performance while keeping the heat source temperature around 45 °C, Saha et al., 1997b proposed a design of six-bed three-stage adsorption system and then investigated the effect of different parameters (e.g. cycle time, heat exchanger flow rate and temperature) on system performance. Khan et al., 2008 improved system performance by adding a re-heat scheme. It was shown that the COP of three-stage adsorption system reaches up to 0.3 at 70 °C heat source temperature with cycle time of 4400 s and longer, the heat source temperature can be reduced to as low as 40 °C along with a coolant at 30 °C.

The three-stage adsorption system has six beds (i.e., a pair of beds in each stage) and these beds occupy large space of the system. Accordingly, the footprint of the three-stage machine is larger than that of the single- and two-stage adsorption machine for the same cooling capacity. This is the drawback of three-stage system. Therefore, the reduction of the number of adsorbent beds directly contributes to the reduction of system volume.

In the present study, first a design of a four-beds three-stage adsorption system was proposed, instead of six-beds three-stage adsorption system. Second, cycle time was optimized to maximize the performance of the proposed and former six-bed system to identify the best performance. The particle swarm optimization method was used to obtain the maximum cooling output under standard working conditions. Finally, the performance of the proposed cycle was compared with the optimal performance of former six-bed three-stage adsorption systems.

1.3 Objectives and Scopes

The main objective of the present research work is to develop an advanced multi-stage adsorption refrigeration cycles which can be powered by low grade renewable energy or waste heat sources. The scopes of the present work are:

1. to improve the performance of three-bed single-stage adsorption systems through optimization of cycle time using particle swarm optimization process;
2. to establish the appropriate method for comparing different adsorption system, which can be achieved through comparison of best performance of each system taking into account standard working condition and same input parameters;
3. to minimize the of overall size of four-bed two-stage adsorption system without changing its original performance;
4. to find out the optimal cycle time of different heat source temperature of three-bed two-stage adsorption system, which is the modified innovative design of former four-bed

- two-stage adsorption system;
5. to minimize the overall size of six-bed three-stage adsorption system; and
 6. to find out the optimal cycle time of different heat source temperature of four-bed three-stage adsorption system, which is the proposed modified design of former six-bed three-stage adsorption system.

This study aims to examine the optimal performance of proposed two innovative systems known as three-bed two-stage and four-bed three-stage adsorption refrigeration system.

1.4 Thesis Outline

This thesis comprises 7 chapters describing the various theories of adsorption and simulations to achieve the research objectives. The following is a brief description of the contents of each chapter.

Chapter 1 gives a scientific background of adsorption system and the goal of the research. The mechanism of different types of adsorption systems are discussed in chapter 2. A literature review on the advanced adsorption cooling systems and types of adsorbent/refrigerant pairs which are commonly used in adsorption cooling and heat pump systems are presented therein. Adsorption/desorption phenomena, theory of adsorption and mathematical expression for heat and energy balance of adsorption system are described in Chapter 3. Chapter 4 presents the performance comparison of three-bed single-stage adsorption cooling system with optimal cycle time setting whereas silica gel water as chosen as adsorbent-refrigerant pair. In Chapter 5 describes the innovative design and performance of three-bed two-stage adsorption cycle under optimized cycle time. Design and performance of an innovative four-bed three-stage adsorption cycle are described in chapter 6. Finally, overall conclusions and remarks on the further development of the adsorption refrigerator are presented in Chapter 7.

Chapter 2

Chronological Development of Adsorption System

Heat pump technology is widely used in refrigeration, air conditioning and other heating mechanism. It works against the normal heat flow principle which allows heat flows from higher temperature to lower temperature and consequently heat pump drives heat from lower temperature to higher temperature. Simply it can be said that a heat pump is a device that is able to transfer heat from one fluid at a lower temperature to another at a higher temperature.

Conventional vapour compressor heat pump is well established for consumer use. The main drawback is that it not environmental friendly. That is why nowadays sorption heat pump systems becoming more attractive than conventional one. It can be simply classified into absorption (liquid-gas) and adsorption (solid gas). Absorption process in which material transferred from one phase to another (e.g., liquid) interpenetrates the second phase to form a solution (Papadopoulos et al., 2003). On the other hand, adsorption (solid-vapor) phenomenon concerns a separation of a substance (adsorbate) from one phase, accompanied by its accumulation or concentration of another (adsorbent). The adsorbing substance is the adsorbent and the material adsorbed on that substance is the adsorbate. Generally, the main difference between absorption and adsorption is the nature of the sorbent pair as well as the cycle duration time (Fan et al., 2007). It is reported that absorption cycle performance is higher than that of adsorption cycle. However, the main drawback of absorption cycles is that it needs a high temperature heat source to maintain its operation. All absorption cycles are closed cycles. On the other hand adsorption cycles can be classified into open and closed cycles. The open cycle is applied in the field of desiccant cooling and dehumidification applications. Calcium chloride, lithium bromide and silica gel are commonly used as desiccants. Closed adsorption systems can be classified into high pressure (above atmospheric pressure) and low pressure (sub-atmospheric pressure) depending on the type of adsorbent-refrigerant employed in the system as well as the system application. Flowchart of simple classification of heat pump system is shown in Fig. 2.1. A short description of vapour compression, absorption and adsorption systems is given below:

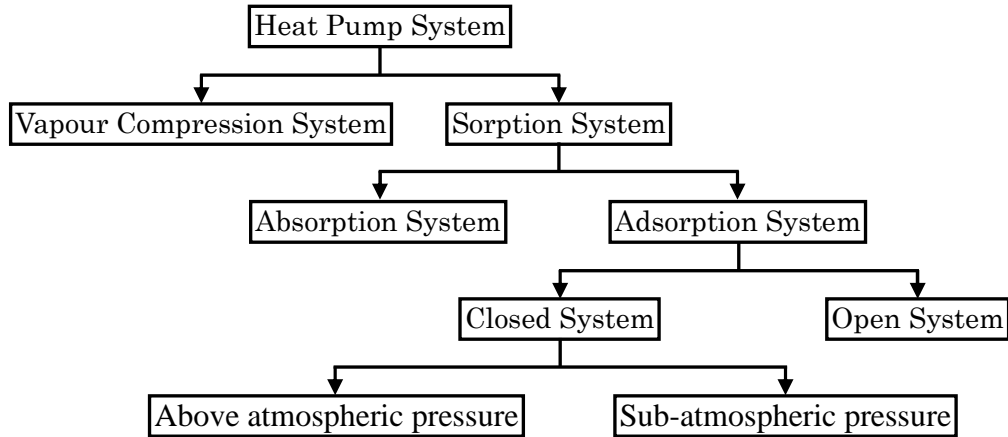


Fig. 2.1: Classification of Heat Pump System

2.1 Conventional Vapour Compression System

A simple vapour compressor system consists of four basic components, namely, 1) evaporator, 2) compressor, 3) condenser and 4) expansion valve. The schematic diagram of the arrangement is as shown in Fig.2.2. Except these, a heat transfer fluid known as refrigerant is required to transfer heat. The refrigerant passes through these four components of the system and performs compression, condensation, expansion and evaporation, respectively. Liquid refrigerant is allowed to evaporate in the evaporator at low temperature and pressure. Heat is required for vaporization and hence, a refrigerating effect is produced during the vaporization. After evaporating vapor into evaporator, it enters to the compressor and compressed by mechanical compressor to increase the pressure as well as temperature. When the pressure of vapor reaches at the pressure of condenser, the vapor is allowed to condense in condenser. The pressure at this state is sufficiently high and vapor is condensed into high pressure liquid in the condenser where heat is removed from it by either water or air. After the condensation, the liquid refrigerant passes through the expansion valve. Here, the vapor is throttled down to a low pressure liquid and goes to the evaporator. The cycle repeats again and again. The exchange of energy is as follows:

- a) During evaporation, heat which is equivalent to latent heat of vaporization is absorbed by the refrigerant.
- b) Compressor requires work, which is supplied to the system from the surroundings.
- c) During condensation, heat, equivalent of latent heat of condensation etc, is lost from the refrigerator.
- d) There is no exchange of heat during throttling process through the expansion valve as this process occurs at constant enthalpy.

The performance of a vapor-compression system is defined as the coefficient of performance (COP), which can be calculated as follows;

$$COP = \frac{\text{refrigeration effect}}{\text{work input}}$$

Typically, for domestic refrigeration, the coefficient of performance (COP) of vapour compression system lies around 3. Up to the recent regulation, the usual refrigerant was CFC's. However, because of the ozone layer depletion and global warming problems, more and more substitutes are under development.

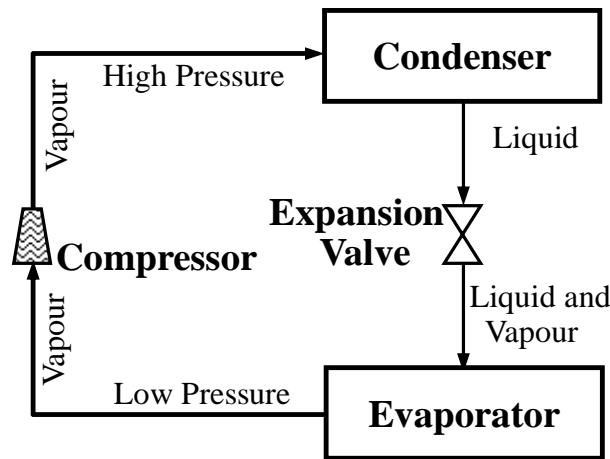


Fig.2.2: Typical vapour compressor refrigeration system.

2.2 Absorption System

The absorption system differs from the vapour compression system in a way that it uses heat energy instead of mechanical energy to make a change in the conditions necessary to complete the refrigeration cycle. It can be said that absorption system is heat powered system in which a secondary fluid, known as sorbent, is used to absorb the primary fluid i.e., gaseous refrigerant, which has been vaporized in the evaporator. A basic absorption system consists of one or more absorber, a pump, a generator, a condenser and an evaporator. Schematic of a basic absorption system is shown in Fig. 2.3.

Condenser and evaporator of absorption system act as similar as the condenser and evaporator of compression system. In compression system only one suitable refrigerant is used whereas in absorption system sorbent and refrigerant pair is needed. In absorber, at low pressure sorbent absorb the refrigerant vapour of evaporator. Pump is used to send low pressure sorbent-refrigerant solution to the generator, which works at higher temperature and pressure. Pump is similar as the compressor of vapour compression system. Generator

separate the solution into liquid sorbent and refrigerant vapour through heating and rectification process and then refrigerant vapour goes to the condenser and liquid sorbent return to the absorber. At the same time refrigerant vapour condense in the condenser and then go to the evaporator through expansion valve. The cycle is repeats.

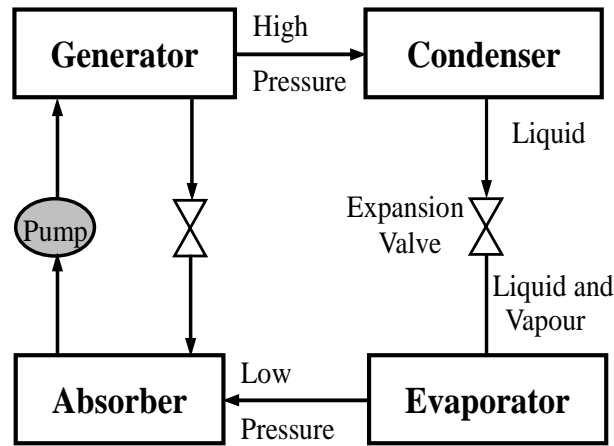


Fig.2.3: Typical absorption refrigeration system.

2.3 Adsorption System

Adsorption system is environmental friendly whereas vapour compression system has weakness in this point. It can work at lower heat source temperature compare to absorption system. Adsorption system is very simple compare to compression and absorption system because it has no extra component such as compressor, generator and pump. The simplest heat powered adsorption system composes of three heat exchangers namely, sorption bed or adsorber/desorber bed, condenser and evaporator, as shown in Fig. 2.4. Adsorber/desorber bed can compare with compressor of compression system but electric power is needed to operate compressor whereas heat power is used in bed to change it mode from adsorber to desorber. Adsorption system needed adsorbent-adsorbate pair similar as sorbent-refrigerant pair of absorption system. Adsorption system will be described elaborately in subsequent sections.

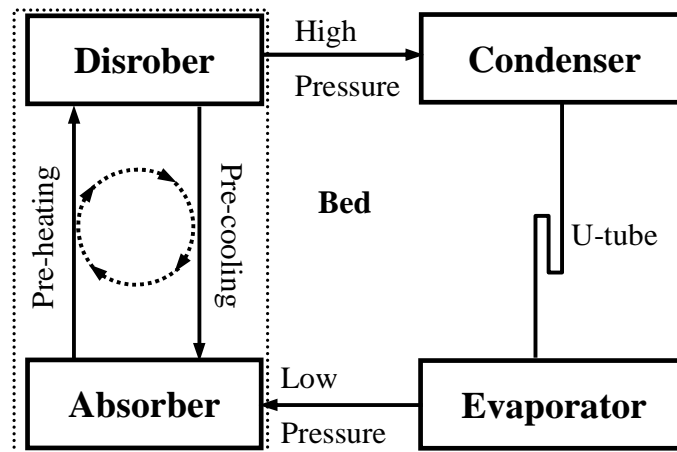
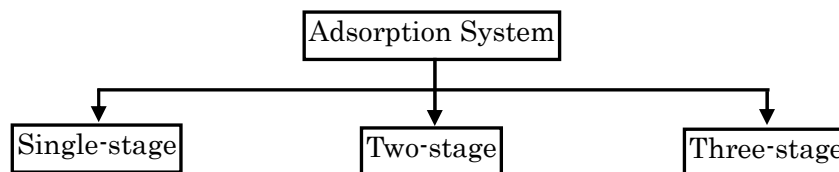


Fig.2.4: Typical adsorption refrigeration system.

2.4 Adsorption System Description

A conventional adsorption heat pump functions in a manner similar to a vapor compression cycle (Sun et al., 1997), except that the refrigerant is compressed thermally in batch-wise fashion by controlling the sorption bed temperature as well as pressure. Sorption bed works between condenser (works at higher temperature/pressure) and evaporator (works at lower temperature/ pressure) pressure. Higher heat source temperature can easily drive refrigerant vapour from evaporator to condenser pressure but when temperature is lower then it is not sufficient enough to drive vapour from evaporator to condenser pressure. That is why need staging to drive vapour step by step. Based on staging, adsorption system can be divided into three types such as single-stage, two-stage and three-stage system. Flow chart of classification is give below;



2.4.1. Single-stage adsorption system

Single-stage adsorption system works with higher heat source temperature and all adsorption systems available in the market are single-stage. Most fundamental single-stage adsorption system is the single-bed adsorption system and two-bed adsorption system is known as conventional adsorption system. Advance single-stage adsorption systems are two-bed bed mass recovery, three bed, three-bed mass recovery/heat recovery, four bed, four

bed mass recovery/heat recovery and six bed adsorption system. Description of different types of single-stage adsorption system is given below:

2.4.1.1 Single-bed adsorption system

A single-bed single-stage adsorption system is shown in Fig. 2.5, which is the most fundamental system. It has one adsorber/desorber bed, one condenser and one evaporator. Sorption element or adsorber/desorber bed simply called as bed and filled with adsorbent, which is fixed all time but heat transfer fluid know as adsorbate moves inside the system through different thermodynamically process.

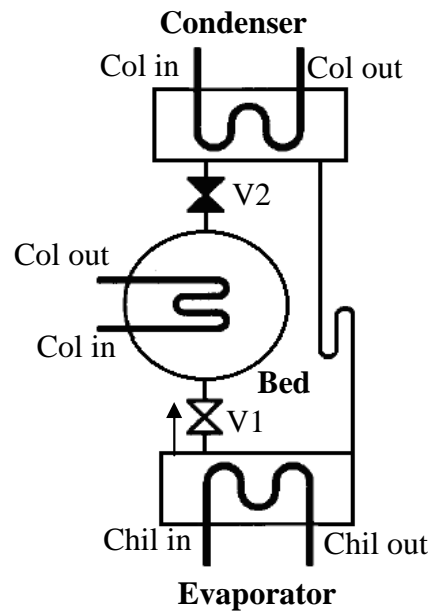


Fig. 2.5: Schematic of single-bed single-stage adsorption system.

The cycle consists of four batch-operated thermodynamic processes i.e., adsorption, pre-heating, desorption and pre-cooling process, which are shown on in Fig. 2.6. The graph representing pressure-temperature-concentration of the system is known as Dühring diagram. The processes can be explained briefly as follows where the subscripts a , b , c and d indicate the states of processes a - b , b - c , c - d and d - a , respectively.

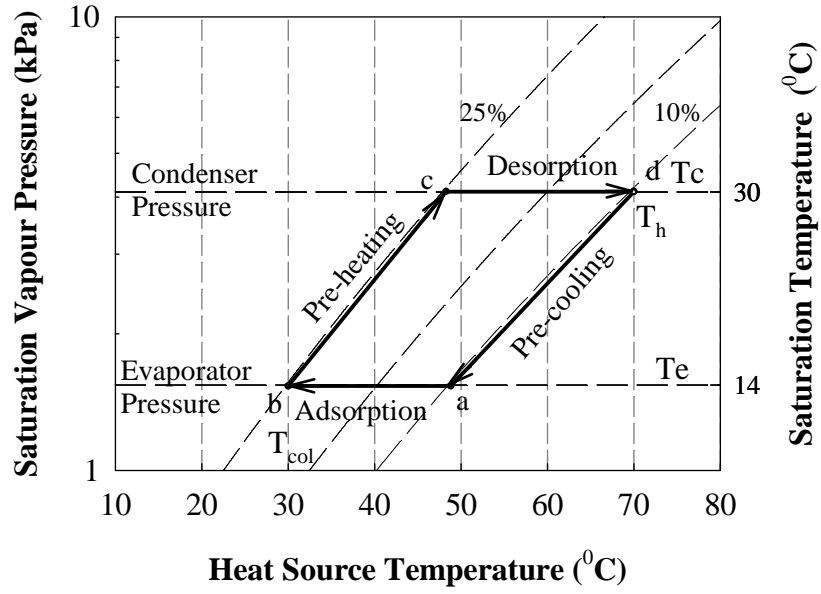


Fig. 2.6: Dühring diagram of single-bed single-stage adsorption system.

Adsorption and evaporation process (a-b): The bed is connected to the evaporator through opening the valve, V1, which makes it possible to adsorb the refrigerant vapor of the evaporator. At this time, it is disconnected from condenser by closing the V2 valve (Fig. 2.5). Adsorption heat is removed by coolant temperature, T_{col} that flows inside the sorption element. Refrigerant concentration in the bed increases until reaches saturation level.

Pre-heating process (b-c): During this period, bed is isolated from both of the evaporator and the condenser by closing the both valve V1 and V2. At the same time bed is heated by external heat source to the sorption element at constant refrigerant concentration. As a result the temperature increase as well as bed pressure from evaporator to the condenser pressure.

Desorption and condensation process (c-d): The bed is connected to the condenser by opening the valve V2 and the heat input from external source continues in this process. The refrigerant vapor is desorbed at constant condenser pressure, while the temperature increases until it reaches the heat source temperature, T_h . The desorbed refrigerant is continually provided to the condenser where condensation takes place at T_c . Condensation heat is removed by coolant that flows inside the condenser heat transfer tubes. In this process, the concentration decreases until reaching the equilibrium temperature at T_h .

Pre-cooling process (d-a): the bed is disconnected from both the evaporator and the condenser. It is cooled down at constant refrigerant concentration by coolant. The bed pressure decreases from condenser pressure to the evaporator pressure. Generally, the

specific cooling load equal to the mass of refrigerant evaporated and circulated through the system time its latent heat. The mass of evaporated refrigerant is equal to the concentration change during adsorption process which can be calculated by using Dühring diagram if ideal cycle is considered. The amount of heat addition depends on the heat of adsorption. However, both of the concentration change and heat of adsorption can be extracted from the adsorption isotherms.

Performance of single bed adsorption system is very low but it is advantageous in simple structure and lower initial cost. It can be used in applications when continuous cooling or higher cooling capacity is not required, such as cooling drinks, storage of vaccine. A solar powered single-bed refrigerator was invented by Critoph, 2002, which was recommended by the U.N. for vaccine storage in poor area. Various type of single-bed adsorption refrigerator system also was invented by Patzer, 2001, Hidaka et al., 2005 and Monma et al., 2005.

2.4.1.2 Conventional two-bed adsorption system

A conventional two-bed adsorption system consist of two adsorber/desorber bed, namely, Bed 1 and Bed 2, one condenser and one evaporator. Schematic diagram and Dühring diagram of convention two-bed adsorption system are shown in Figs. 2.7 and 2.8, respectively. The system functions like two single-bed devices operating one-half cycle out of phase. One adsorber adsorbs refrigerant vapor from the evaporator under low temperature and pressure, while another adsorber discharges refrigerant vapor into the condenser under high temperature and pressure. In complete cycle operation, one undergoes adsorption, pre-heating, desorption and pre-cooling, while another bed completes desorption, pre-cooling, adsorption and pre-heating over the same time increments. Because one bed can adsorb while the other desorbs, there is less non-productive time than with the single-bed module. Having less non-productive time reduces evaporator temperature fluctuation and utilizes the condenser and evaporator components better. Performance of conventional two-bed system is better than the single single-bed adsorption system. A number of investigations have been performed on two-bed adsorption system based on different type of adsorbent-adsorbate pair (Table 2.1).

Table 2.1: Conventional two-bed adsorption system investigation.

Source	Pair	Type of work	Remarks
Cacciola et al., 1995.	Zeolite-water and carbon -methanol	Simulation	Specific for southern Europe
Zhang et al., 1997	Zeolite-water	Simulation	Lumped parameter simulation
Marletta et al., 2002	Zeolite- water	Simulation	Zeolite compacted in binder
Chua et al., 2004	Silica gel- water	Experimental	--
Critoph et al., 2004	Monolithic carbon-Ammonia	Simulation	Plate-type sorption bed heat exchanger
Kubota et al., 2008	Silica gel water	Experimental	Finned-tube sorption bed heat exchanger
Clausse et al., 2008	Silica gel(RD) - water	Simulation	Powered by PEM fuel cell exhaust burn
Mittelbach et al., 2008	Silica gel - water	Experimental	Commercially available chiller
Schicktanz et al., 2008	Silica gel - water	Simulation & experiment	Lumped parameter simulation
Vasta et al., 2008	FAM-ZO2 - water	Experiment	Mobile applications
Khalifa A.H.N., 2011	Active carbon - methanol	Experimental	---

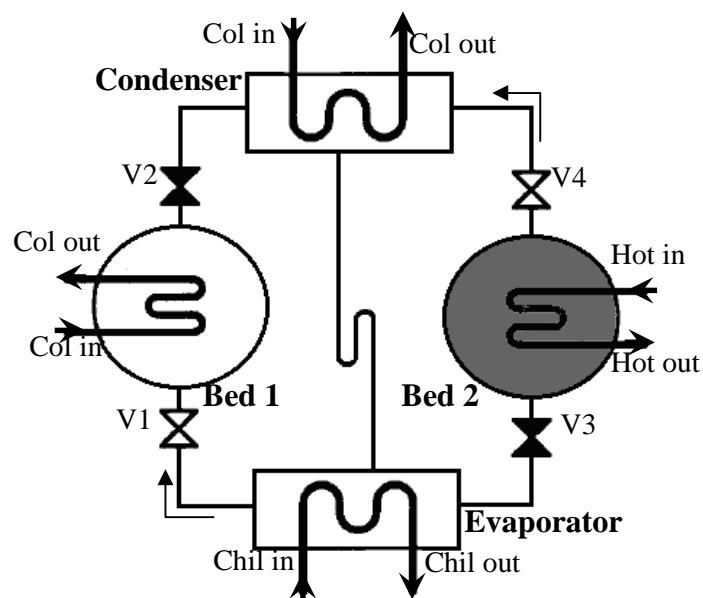


Fig. 2.7: Schematic of conventional two-bed single-stage adsorption system.

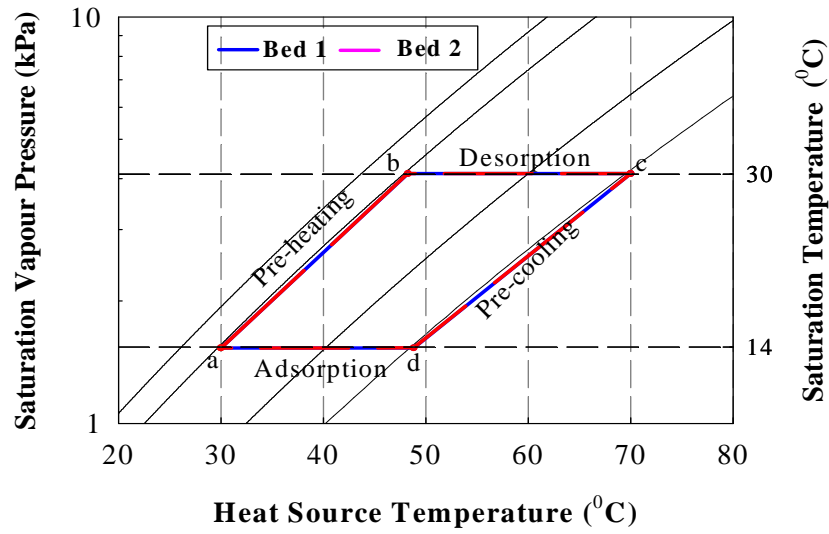


Fig. 2.8: Dühring diagram of conventional two-bed single-bed adsorption system.

2.4.1.3 Advanced two-bed adsorption system

Advanced two-bed adsorption mainly known as two-bed mass recovery, heat recovery and thermal wave system. A typical two-bed mass recovery system and its Dühring diagram are shown in Figs. 2.9 and 2.10, respectively. Similar as conventional system, the advanced mass recovery system has two heat exchanger beds, one condenser and one evaporator. In addition, there is an option for connecting two beds. Conventional system each bed needs four thermodynamical processes to complete a full cycle operation, but in the advanced mass recovery system, six thermodynamical processes are required: (i) adsorption; (ii) mass recovery cooling; (iii) pre-heating; (iv) desorption; (v) mass recovery heating; and (vi) pre-cooling process. Mass recovery is a partial automatic pressurization and depressurization process. When Bed 1 is at the end of the adsorption process (at point 'b' of Fig. 2.10) at the same time Bed 2 is at the end of the desorption position (at point 'e'). Bed 1 is at a lower temperature and pressure, and Bed 2 is at a higher temperature and pressure. Bed 1 needs heat to increase pressure, and Bed 2 needs cooling to decrease pressure. If both beds are connected to each other, then the pressure of both beds will equalize within a very short time. As a result, gaseous refrigerant in the high-pressure bed flows to the low-pressure bed, which is known as the mass recovery process. It supplies a pumping effect to the high-temperature desorption bed, thereby introducing more desorption. In contrast, the low-temperature adsorption bed is pressurized somewhat to get more adsorption. Thus, the cooling capacity of the advanced system is better than the conventional system. Respectively, if the cooling and heating of Bed 1

and Bed 2 after adsorption and desorption are continuing to the mass recovery mode then it is identify as mass recovery with cooling/heating process, if not then it is called mass recovery without cooling/heating process.

Two-bed heat recovery system is similar as two-bed mass recovery system but main difference, in mass recovery system refrigerant vapour transfers from higher temperature to lower temperature bed whereas in heat recovery system heat exchanger fluid transfer. When the two beds complete one process and start to change their working states, the bed that has just finished the desorbing process will be cooled so that it will release a lot of heat, meanwhile the bed that has just finished the adsorbing process will be heated so that it needs a lot of heat. Therefore, the heat discharged by the bed to be cooled can be partly recovered and, thus, used to heat the other bed if the two beds are connected. This process is a heat recovery process. More explicitly it can be explain as, when the adsorbing process of Bed 1 and desorbing process of Bed 2 are completed, Bed 1 and the heat transfer medium inside Bed 1 are at the adsorption temperature, meanwhile Bed 2 and the heat transfer medium inside it are at the desorption temperature. By opening and closing the valves in the pipes, the heat transfer mediums of the two beds are connected, and then the low temperature and high temperature mediums are mixed to an intermediate temperature. The high temperature bed transfers its heat to the low temperature bed through flow of the thermal medium. There is also some system where is mass recovery and heat recovery both process are work simultaneously.

It is found that a combined recovery cycle can effectively utilize the advantages of both heat recovery and mass recovery. Investigation on silica gel-water advance adsorption system has been done by Chua et al., (1999, 2004) and Wang et al., 2007. Shanghai Jiao Tong University has investigated adsorption refrigerator with CaCl_2 /activated carbon-ammonia, CaCl_2 / graphite-ammonia and physical adsorbent (zeolite, silica gel, etc.) - water (Li et al., 2011, Chen et al., 2007, Gong et al., 2011, Yang et al., 2006, Lu et al., 2003 Wu et al, 2003, Wang et al., 2005). It was observed that the performance of advance two-bed adsorption (mass/heat recovery) system is better than conventional two-bed adsorption system. It is also noted that mass recovery with heating/cooling system is better than mass recovery without heating/cooling system.

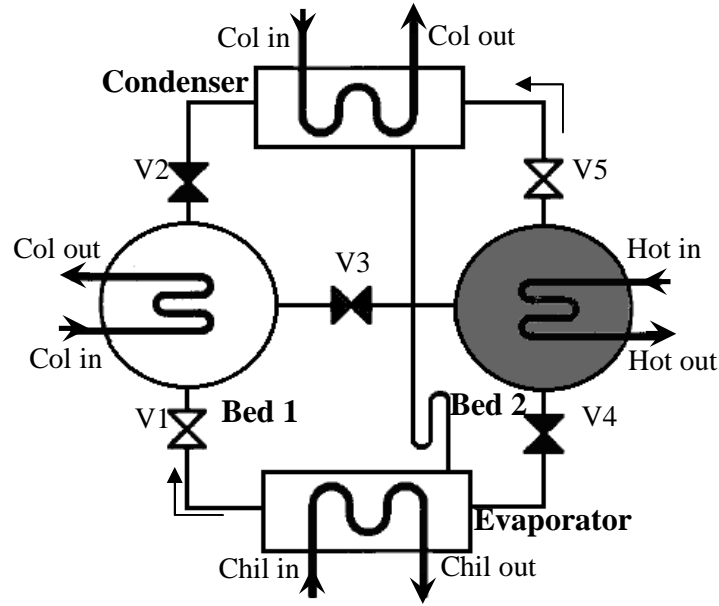


Fig. 2.9: Schematic of two-bed single-stage mass recovery adsorption system.

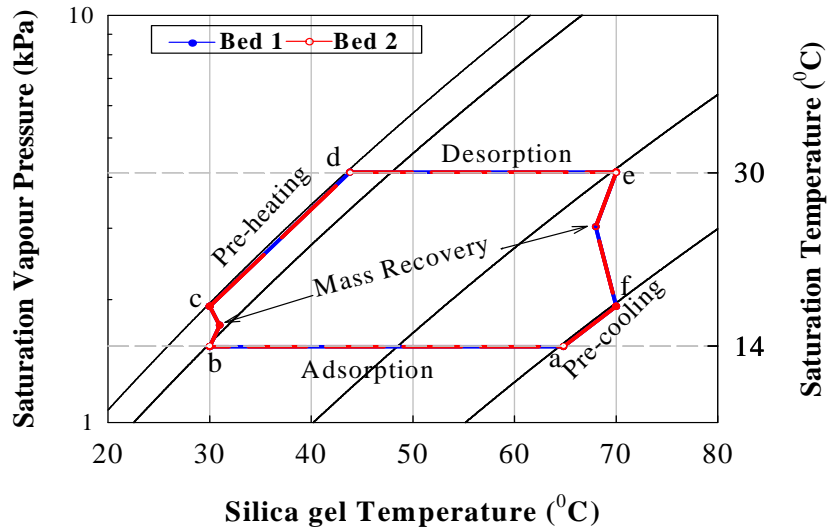


Fig.2.10: Dühring diagram of two-bed single-stage mass recovery adsorption system.

Two-bed thermal wave adsorption system was proposed by Miles et al., 1996 to improve the performance of adsorption system. The schematic of the system is shown in Fig. 2.11, which employs activated carbon-ammonia as an adsorbent-refrigerant pair. In the thermal process, only a single heat transfer fluid loop exists. A reversible pump is placed in the closed heat transfer fluid loop to invert the circulation of fluid flow. The system operation

can be described as follows; initially, heat transfer fluid is heated in the heat exchanger (HFX) to a high temperature (T_h), and then it enters Bed 1 to regenerate the refrigerant (ammonia), which evaporates and goes to the check valve and condensed in the condenser. Heat transfer fluid flows from Bed 1 to the cooler, which is a finned tube heat exchanger. After that enters Bed 2, which adsorbs ammonia from the evaporator through the check valve. After finishing the first half cycle, the Bed 1 is sufficiently heated and Bed 2 is sufficiently cooled, all the check valves are shut down and the direction of the heat transfer fluid is reserved by the reversible pump. In the second half cycle, the regeneration process begins at Bed 2 and adsorption process begins at Bed 1. It is reported that the proposed system achieves a cooling COP as high as 1.9. Similar cycles have been investigated theoretically by Sward et al., 2000.

A related concept, convective thermal wave, has been lunched by Critoph, R.E., (1994, 1998) and Critoph et al., (1996, 2004). In this cycle refrigerant works as the heat transfer medium and activated carbon/ammonia is used as an adsorbent/refrigerant pair.

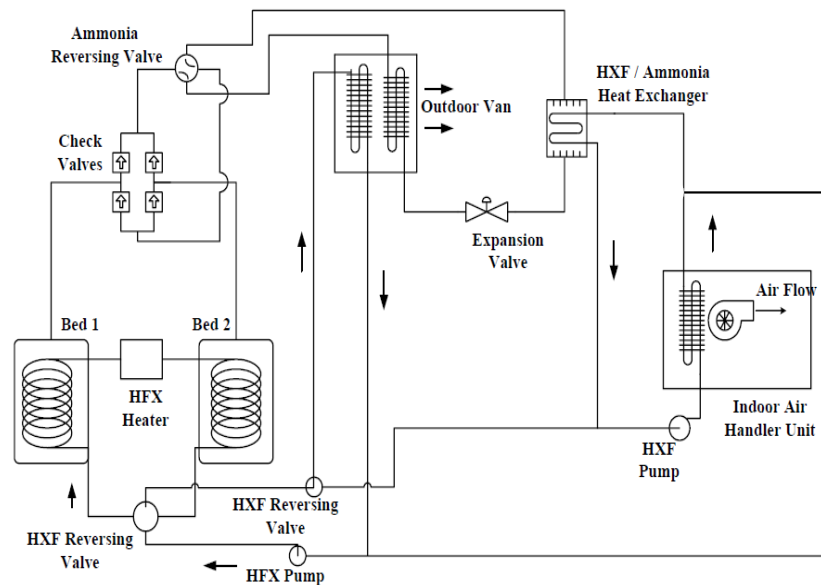


Fig. 2.11: Wave air solid sorption heat pump in cooling mode (Miles et al., 1996).

2.4.1.4 Conventional three-bed adsorption system

Conventional three-bed adsorption system consist of three heat exchanger bed, namely Bed 1, Bed 2 and Bed 3, one condenser and one evaporator. Schematic of the system is shown in Fig. 2.12, which is proposed by Saha et al., 2003. One side of each bed is connected with evaporator and another side is connected with condenser. So, all are working between

the pressure of condenser and evaporator and function of each bed is similar as single bed adsorption system, which was described in section 2.4.1.1. Dühring diagram is shown in Fig. 13, which indicated that each bed follows adsorption, pre-heating, desorption and pre-cooling modes in cyclic order. Operation strategy is taken so that continuous cooling load produces to the evaporator and some time more than one bed also produce cooling load at the same time. Thus the performance of three-bed adsorption system is better than two-bed adsorption system.

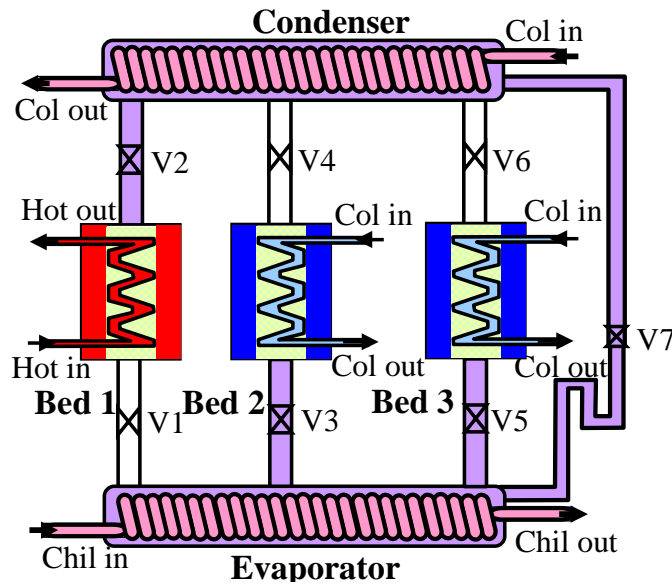


Fig.2.12: Schematic of three-bed single-stage adsorption system (Saha et al., 2003).

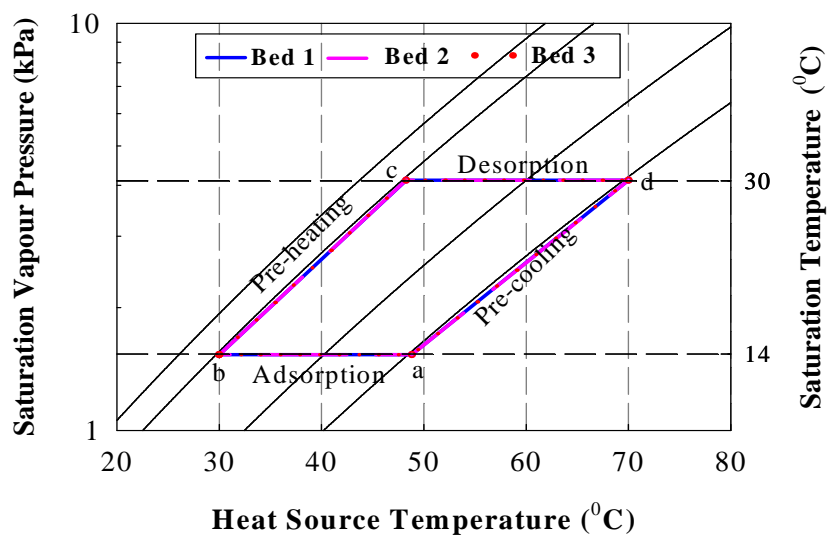


Fig.2.13: Dühring diagram of conventional three-bed single-stage adsorption system.

2.4.1.5 Advanced three-bed adsorption system

To increase the performance of conventional three-bed adsorption system mass recovery and heat recovery processes between beds was applied, which is known as advanced three-bed adsorption system. Schematic of three-bed mass recovery adsorption system and its Dühring diagram are shown in Figs. 2.14 and 2.15. Fig. 2.14 indicates that mass recovery process only takes place between Bed 1 and Bed 2. That is why Bed 3 completing adsorption, pre-heating, desorption and pre-cooling process whereas Bed 1 and 2 completing adsorption, mass recovery cooling, pre-heating, desorption, mass recovery heating and pre-cooling modes (Fig. 2.15). It was observed that performance of three-bed mass recovery is better than conventional three-bed adsorption system. Uyun et al., 2009 introduces different type of three-bed adsorption system with mass recovery (with and out heating/cooling) and heat recovery process, which is shown in Fig. 2.16. Bed 3 of Uyun cycle is fully disconnected from condenser whereas Khan cycle it is connected with condenser. As a result Bed 3 of Uyun cycle desorb the refrigerant vapour to the Bed 1 and Bed 2 through mass recovery heating process. Heat recovery arrangement was not shown in this figure. Dühring diagram (Fig. 2.17) indicates that Bed 3 only follows adsorption, mass recovery with heating and pre-cooling process whereas Bed 1 and Bed 2 follow adsorption, mass recovery cooling, pre-heating, desorption and pre-cooling modes. Details of advanced three bed mass recovery system will be described in chapter 4.

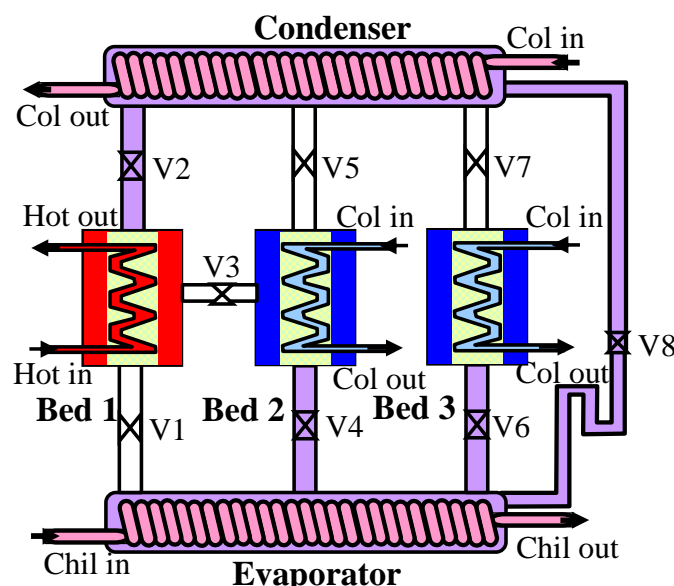


Fig. 2.14: Schematic of three-bed single-stage mass recovery adsorption system (Khan et al., 2005a).

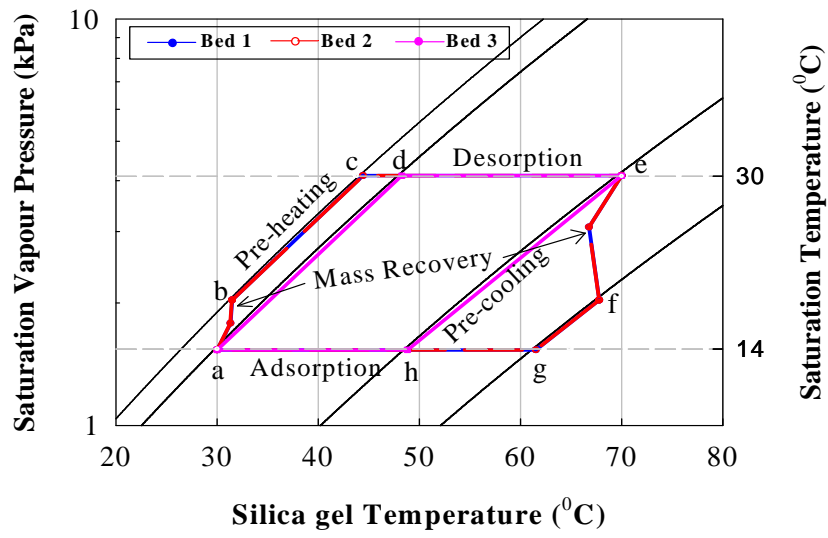


Fig. 2.15: Dühring diagram of three-bed single-stage mass recovery system (Khan cycle).

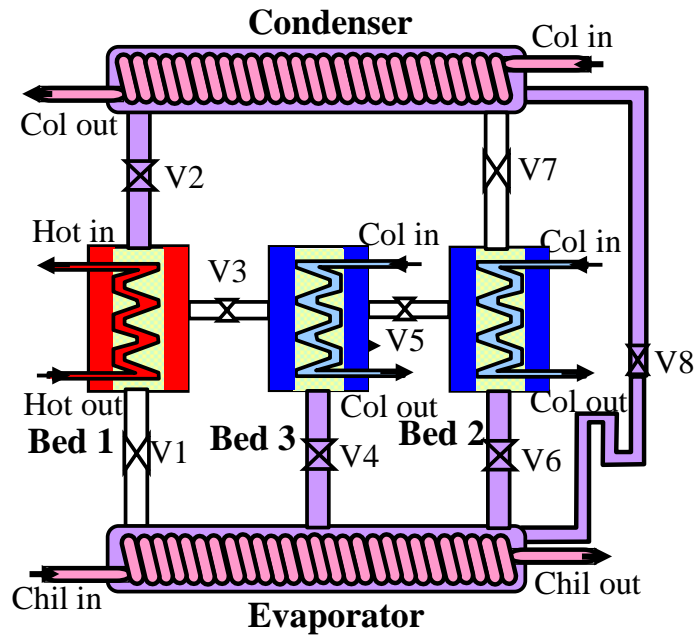


Fig. 2.16: Schematic of three-bed single-stage mass recovery adsorption system (Uyun et al., 2009a).

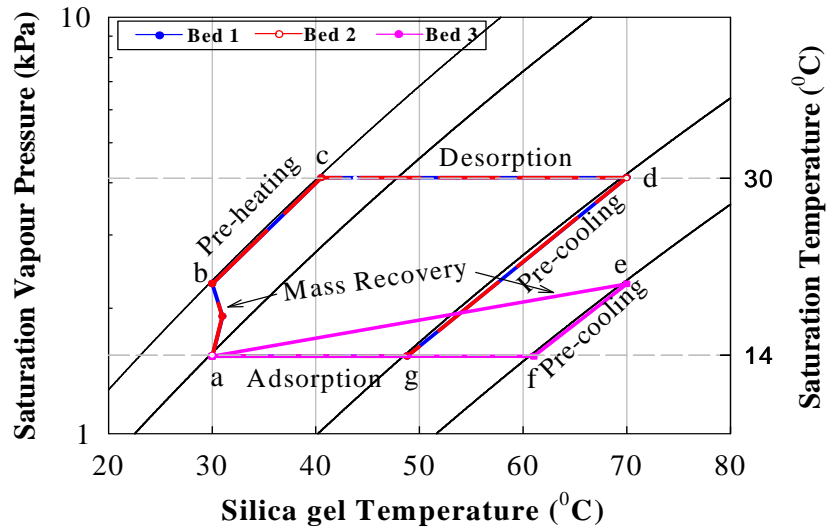


Fig. 2.17: Dühring diagram of three-bed single-stage mass recovery system (Uyun cycle).

2.4.1.6 Four-bed adsorption system

A design of four bed adsorption system proposed by Chua et al, 2001 to extract the most enthalpy from the low-grade waste heat before it is purged into the drain. The system is capable to minimize the chilled water fluctuation and avoids a master-and-slave configuration. Schematic of four-bed adsorption system is shown in Fig. 2.18. It indicates that four-bed system comprises of four adsorption/desorption beds, one condenser and one evaporator. Function of four-bed system is similar to conventional two-bed adsorption system whereas more two-bed was added. In two-bed adsorption when one bed is in adsorption at the same time another bed is in desorption mode. But in four-bed adsorption when Bed 1 is at the end of the adsorption, Bed 2 is in the pre-heating, Bed 3 is at the end of desorption and Bed 4 is in the pre-cooling mode. Also at this instant, Beds 2 and 4 are isolated from the evaporator and condenser. Bed 1 is connected to the evaporator, while Bed 3 is connected to the condenser. As a result continuous cooling effect produces to the evaporator. It was found that for the same waste heat source flow rate and inlet temperature, a four-bed adsorption system generates 70% more cooling capacity than a typical two-bed adsorption system (Chua et al., 2001). Four bed adsorption system also investigated by San J.Y., 2006 considering methanol and an activated carbon as the adsorption pair. Experimental investigation on four-bed mass recovery and heat recovery was done by Ng et al., 2006. It was noted that through heat and mass recovery COP of the system could be increased as much as 48% without additional

hardware changing.

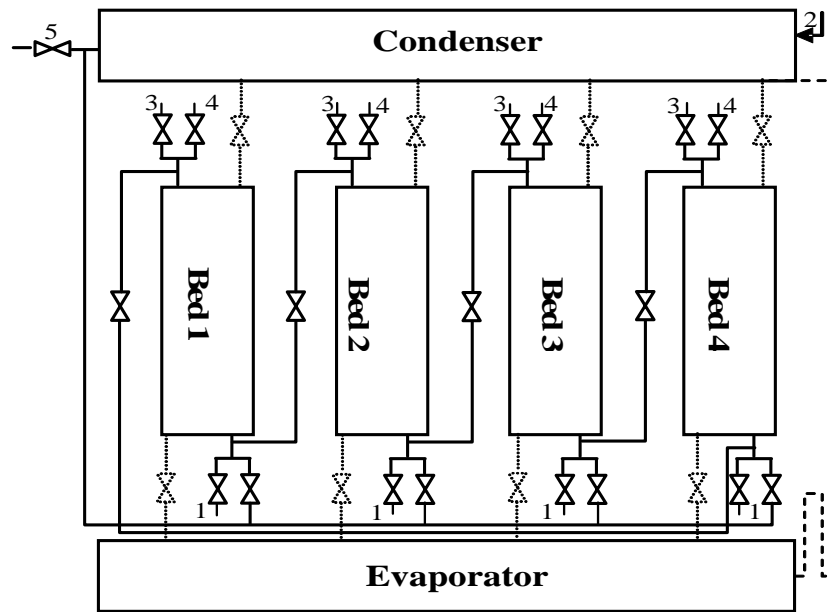


Fig. 2.18: Schematic of four-bed single-stage adsorption system (Chua et al., 2001).

2.4.2 Two-stage Adsorption System

Two-stage adsorption system can be divided as conventional two-stage and advance two-stage system. Details of the system are given below;

2.4.1 Conventional two-stage adsorption system

Saha et al., 2001 proposed two-stage adsorption system to utilized waste heat /solar heat of temperature below 70 °C because single-stage adsorption system has some shortcoming in this temperature region. Schematic of two-stage adsorption system and its Dühring diagram is shown in Figs. 2.19 and 2.20, respectively. When heat source temperature is lower it is not sufficient enough to drive refrigerant vapour from evaporator pressure to condenser pressure. That is why two regeneration temperate lift is necessary to be driven at low heat source temperature. The system allows reducing regeneration temperature lift of the adsorbent ($T_{des}-T_{ads}$) by dividing the evaporating temperature lift (T_c-T_e) into two smaller lifts. Thus, refrigerants vapour pressure rises into two consecutive steps from evaporation to condensation pressure level. In first step refrigerant vapour drive from evaporator pressure to intermediate pressure level and then in second step vapour drive from intermediate pressure level to condenser pressure level (Fig. 2.20). For this reason two pair of beds is necessary (Fig. 2.19), where Bed 1 and Bed 2 work at lower pressure cycle and, Bed 3 and Bed 4 work in upper temperature level. Thus, two-stage adsorption system consists of four beds, one

evaporator and one condenser. In single-stage system one side of each bed is connected with evaporator and another side is connected with condenser as a result beds adsorb vapour from evaporator and desorb to the condenser. But in two-stage cycle, one side of lower cycle two beds is connected with evaporator and another side is connected with the lower side of upper cycle two beds. Opposite side of upper cycle two beds is connected with evaporator. As a result, lower cycle beds adsorb refrigerant vapour from evaporator and desorb to upper cycle beds and finally upper cycle beds desorb to the condenser. Both upper and lower cycle beds have to complete four thermodynamical process, such as adsorption, pre-heating, desorption and pre-cooling process (Fig. 2.20).

At the beginning of cycle operation the desorbers (Bed 1 and Bed 4) are heated by hot water while adsorbers (Bed 2 and Bed 3) are cooled by cooling water. This time valves 2, 4 and 6 are opened and refrigerant vapour transfer from Bed 1 to Bed 3, evaporator to Bed 2 and Bed 4 to condenser. During a short intermediate process (pre-cooling/ heating), all valves are closed and no adsorption/desorption occurs. After this short period, valves 1, 3, and 5 are opened to allow refrigerant from evaporator to Bed 1, Bed 3 to condenser, and Bed 2 to Bed 4. When refrigerant concentration in the adsorber and desorber is near their equilibrium level, hot and cooling flows are redirected by switching the valves so that desorber can change its mode into adsorber and adsorber into desorber. The adsorption/desorption process can be continued by changing the direction of hot and cooling water flow. It is noted that coefficient of performance of two-stage adsorption system is lower than the single-stage adsorption system. Performance of a two-stage adsorption system with different mass allocation between upper and bottom beds was investigated numerically by Hamamoto et al., 2005. It was shown that cooling capacity can be improved with the optimum allocation of adsorbent mass to the bottom beds than that to the upper beds. The influence of design and operation condition on the performance of two beds adsorption system was also investigated by Alam et al., 2011. It was shown that the operating conditions such as cycle time and hot and cooling water inlet temperature have an influential effect on cooling capacity and COP. COP is proportional to cycle time and heat transfer coefficient as well as inversely proportional to the cooling water inlet temperature.

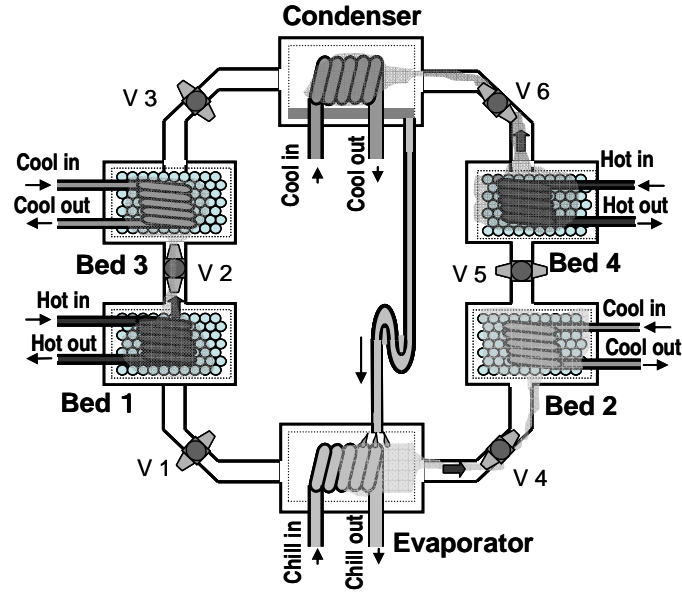


Fig. 2.19: Schematic of four-bed two-stage adsorption system.

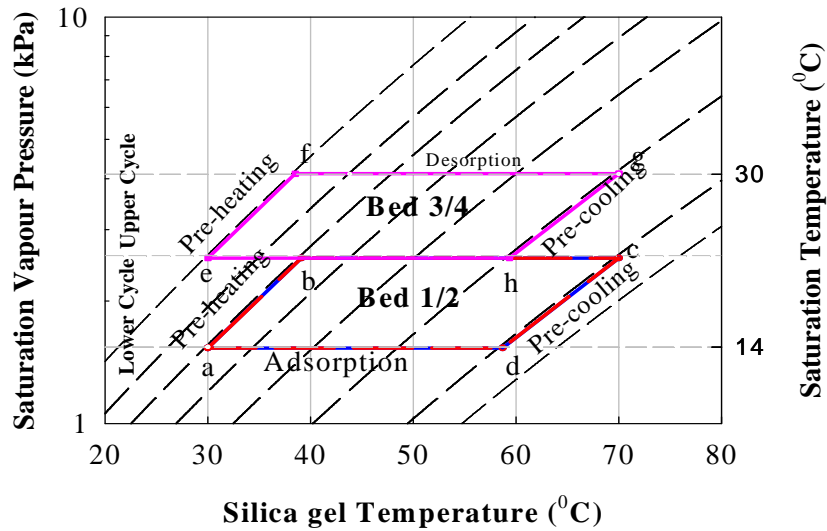


Fig. 2.20: Dühring diagram of four-bed two-stage adsorption system.

2.4.2.1 Advance two-stage adsorption system

To increase the performance of two-stage adsorption system Khan et al., 2006b introduce re-heat two-stage adsorption system, which can be identified as the advance two-stage adsorption system. After that elaborate investigation on the system was done by Khan et al. 2007c, Alam et al., 2007 and Farid et al., 2011. Schematic diagram of the re-heat two-stage adsorption system is shown in Fig. 2.21. It consists of four heat exchanger beds, condenser and evaporator. Main structural different form conventional system each bed is connected with evaporator and condenser and there is option to connect each pair of bed for mass recovery process. Dühring diagram of the system is shown in Fig. 2.22. When one bed

is in the end position of adsorption process and another bed is in the end position of desorption process, those two beds can be connected with each other by continuing heating and cooling and that was done in the two-bed mass recovery with heating process. Thus, the system can be compared with two-bed mass recovery with heating adsorption system where two pair of beds are working between condenser and evaporator.

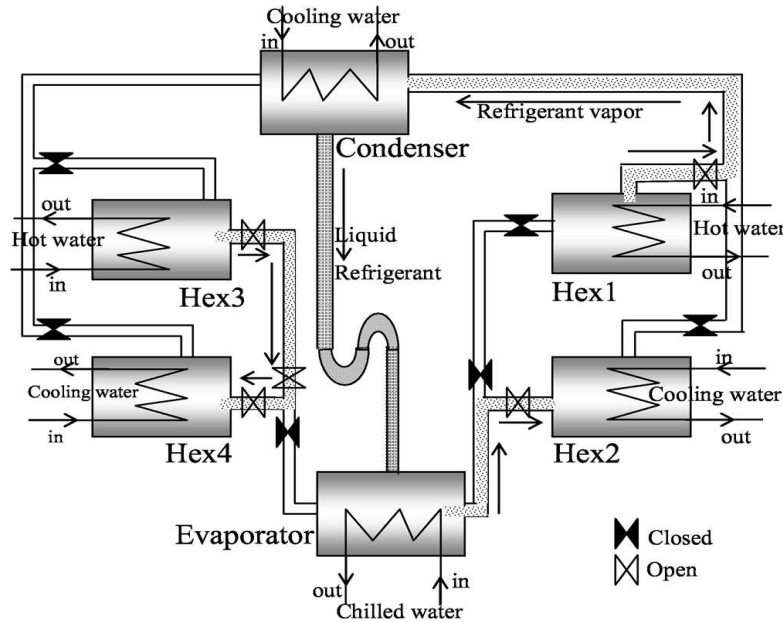


Fig. 2.21: Schematic of re-heat two-stage adsorption system (Khan et al., 2006b)

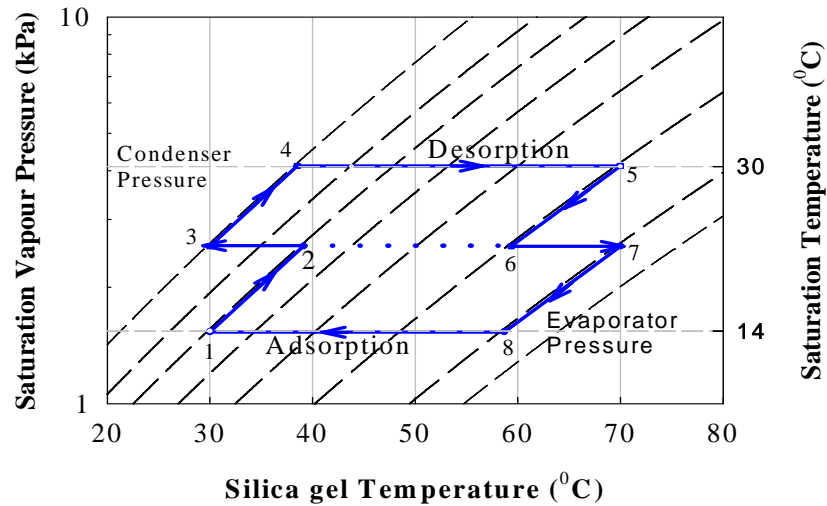


Fig. 2.22: Dühring diagram of re-heat two-stage adsorption system.

2.4.3 Three-stage adsorption system

Three-stage adsorption system can be divided into two groups such as conventional and advance three-stage adsorption system. Description of these adsorption system are given below;

2.4.3.1 Conventional three-stage adsorption system

Strategy of three-stage adsorption system is similar as two-stage system. With the decreasing of regeneration/heat source temperature higher degree of staging will be needed. Two-stage of adsorption system can be utilized as low as 45 °C heat source temperature whereas Saha et al., 1995 shown that three-stage adsorption system capable to utilize heat source as low as 40 °C heat source temperature. Three pair of heat exchanger beds needed in each stage of three-stage adsorption system. Thus, the three-stage adsorption system consists of six beds, (i.e., Bed 1 Bed 2 Bed 3 Bed 4 Bed 5 and Bed 6) one condenser and one evaporator, which is shown in Fig. 2.23. Bed 1 and Bed 2 work at lowest temperature and pressure (near to evaporator pressure), Bed 3 and Bed 4 work in intermediated pressure level and, Bed 5 and Bed 6 work in heights temperature and pressure (near to condenser pressure) level (Fig. 2.24). Each pair of bed in each stage follows adsorption, pre-heating, desorption and pre-cooling process. Bed 1 adsorbs refrigerant vapour from evaporator (where liquid refrigerant evaporate through seizing heat of chilled water) and desorbs to Bed 3. Finally, Bed 3 sends the vapour to the condenser through Bed 5. Similarly, Bed 2 adsorbs vapour from evaporator and sends to the condenser through Bed 4 and Bed 6. Coefficient of performance of three-stage adsorption is quit lower compare to single and two-stage adsorption system, however, the system is effective to utilize very low grade waste/renewable heat source, which finally contributes to mitigation of global warming. The system consists of six beds that why it is little bit bulky compare to other systems. More study will be needed to make it more attractive dimensionally and economically.

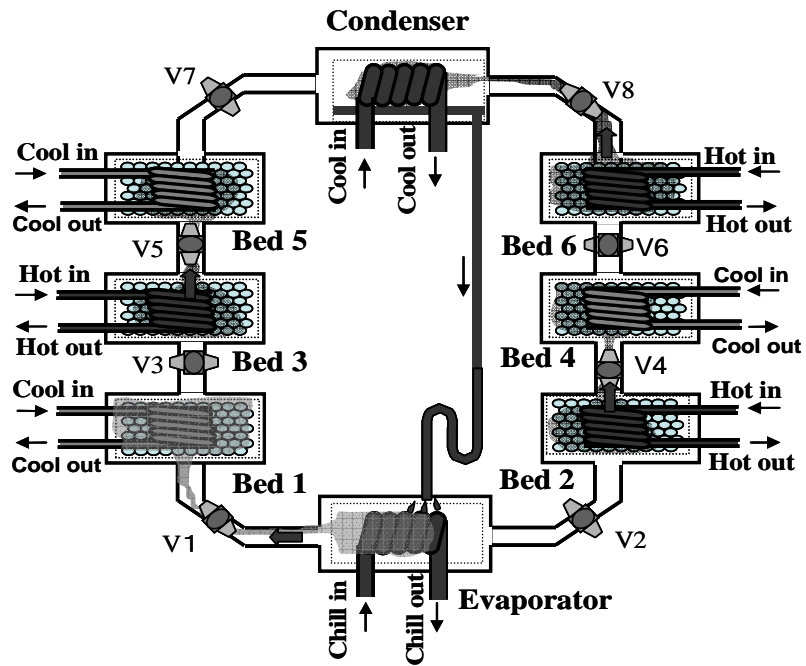


Fig. 2.23: Schematic of six-bed three-stage adsorption system.

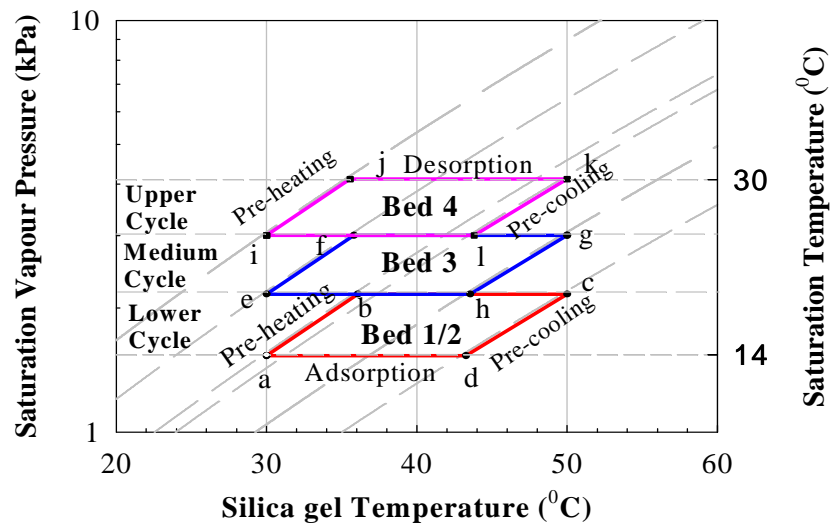


Fig. 2.24: Dühring diagram of six-bed three-stage adsorption system.

2.4.3.2 Advance three-stage adsorption system

Khan et al., 2008 proposed advance three-stage adsorption system, which is known as re-heat three-stage system (Fig. 2.25). The re-heat three-stage system is similar as re-heat two-stage system whereas one pair of beds and one stage were increased. But the operation strategy of three-stage re-heat scheme is fully different from without re-heat scheme. To complete one full cycle of re-heat scheme, all beds pass through six consecutive steps: (i) desorption, (ii) mass recovery process with heating, (iii) pre-cooling, (iv) adsorption, (v) mass recovery process with cooling, and (vi) pre-heating. The adsorbent is packed in the adsorber/desorber heat exchanger, which undergo alternate cooling and heating to allow refrigerant adsorption and desorption. In the adsorption-evaporation process, refrigerant in evaporator is evaporated at evaporation temperature and seized heat from the chilled water. The evaporated vapor is adsorbed by adsorbent (e.g., silica gel), at which cooling water removes the adsorption heat. The desorption-condensation process takes place at condenser pressure. The desorber is heated up to temperature of heat source. The resulting refrigerant is cooled down by temperature T_{cond} in the condenser by the cooling water, which removes condensation heat Q_{cond} . The resulting condensate flows back to the evaporator via a capillary tube connecting the condenser and the evaporator, to complete the cycle. It was shown that re-heat scheme of three-stage adsorption system increased the cooling capacity (CC) and coefficient of performance (COP) compare to without re-heat scheme.

Saha et al., 2003 proposed a dual mode adsorption system, which will work in single-stage as well as three-stage (Fig. 2.28). This adsorption could be utilized effectively low temperature solar or waste heat sources of temperature between 40 and 95 °C. Single-stage operation mode will be to work as a highly efficient conventional chiller where the driving source temperature is between 60 and 95 °C. Three-stage operation mode will be work as an advanced three-stage adsorption chiller where the available driving source temperature is very low (between 40 and 60 °C). With this very low driving source temperature in combination with a coolant at 30 °C, no other cycle except an advanced adsorption cycle with staged regeneration will be operational.

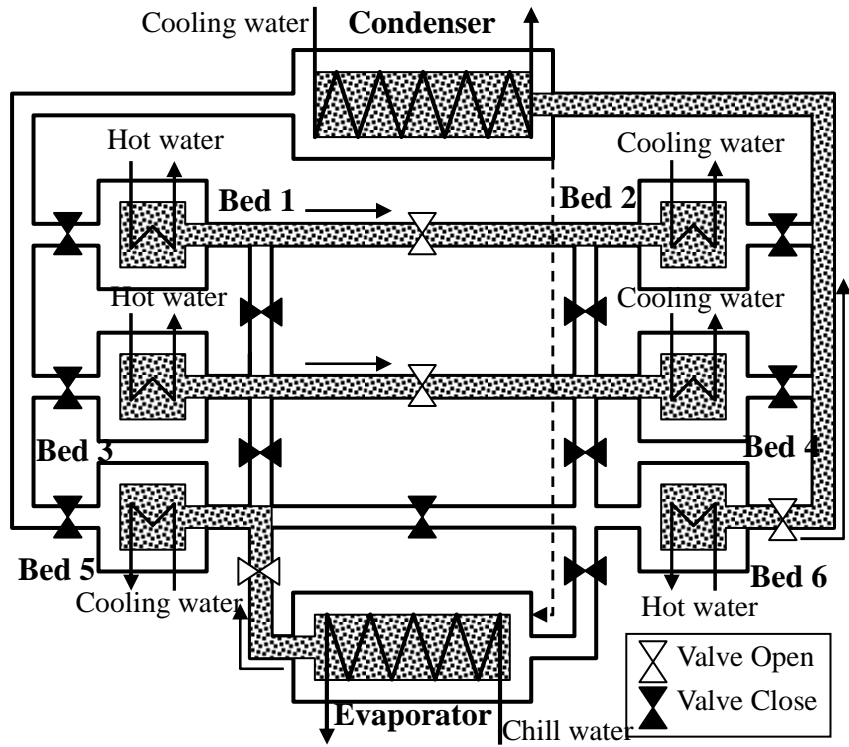


Fig. 2.25: Schematic of re-heat three-stage adsorption system.

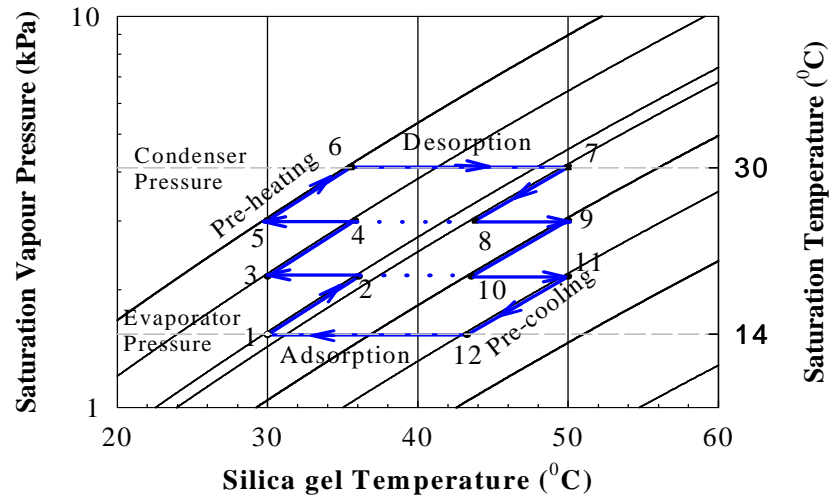


Fig. 2.26: Conceptual Dühring diagram of re-heat three-stage adsorption system.

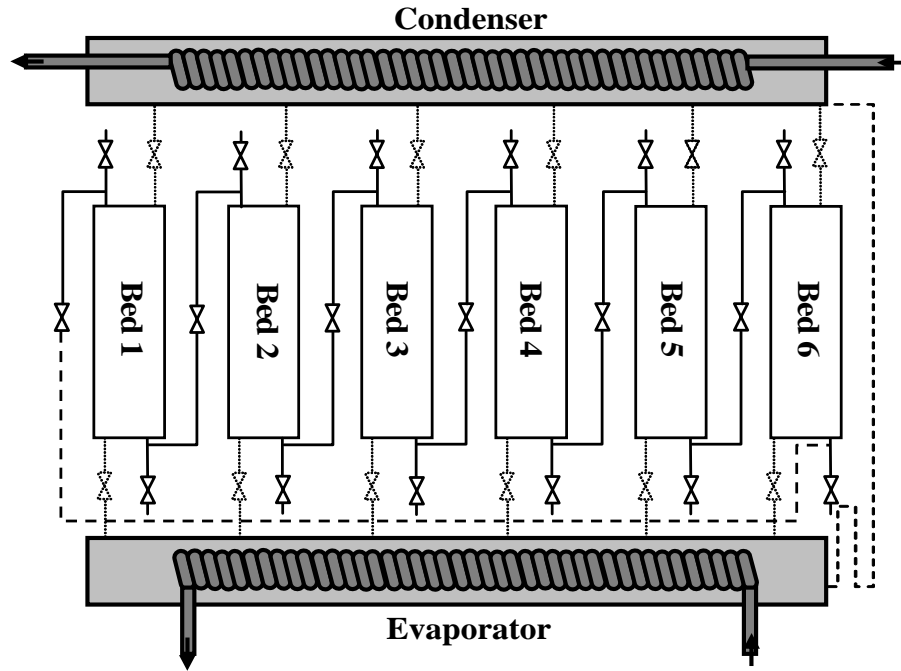


Fig. 2.27: Schematic of six-bed dual mode adsorption system.

2.5 Other Types of Adsorption System

Except of aforementioned systems other different type of adsorption system was proposed and investigation by different researchers. Some of them are describe in following section.

2.5.1 Cascading adsorption system

A novel cascading adsorption system was proposed by Liu et al., 2006. Schematic of cascading system is shown in Fig.2.28. It consists of three heat exchanger bed, one condenser and one evaporator. Two suitable different types of adsorbent and single refrigerant are used in this system. Both heat and mass recovery technique was applied in this system. Bed 1 and Bed 2 work in higher temperature/pressure and Bed 3 work in lower temperature/pressure. Mass and heat recovery happened between Bed 1 and Bed 2 as well as heat is flow from higher temperature bed to lower temperature bed. Liu et al. chosen zeolite adsorbent for high temperature stage while the silica-gel adsorbent for lower temperature stage. Using lumped model it was shown that the COP of cascading cycle 1.35, which is much higher than the COP of an intermittent cycle (about 0.5) and a two-bed combined heat and mass recovery cycle (about 0.8). Uyun et al., 2009c proposed and investigate four bed cascading cycle, where two adsorption/desorption beds were added in higher temperature cycle and two beds

in lower temperature cycle. Two beds of high temperature cycle works in mass recovery process and driven by waste heat while other two beds work in a single-stage cycle that is driven by an external heat source of higher temperature cycle. Better coefficient of performance was observed for cascading cycle but higher heat source is needed for this system.

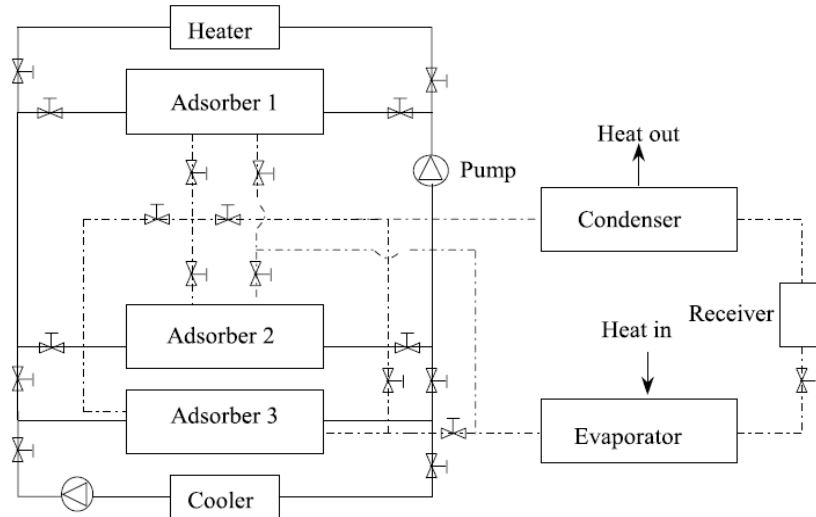


Fig. 2.28: Schematic of cascading adsorption system (Liu et al., 2006).

2.5.2 Double effect adsorption system

Based on cascading adsorption system, Marlinda et al., 2010 proposed double effect adsorption system. Schematic of double effect system and the conceptual Dühring diagram are shown in Figs. 2.29 and 2.30, respectively. It consist of four heat exchanger (HX) bed namely HHX1, HHX 2, LHX1 and LHX 2, one condenser and one evaporator. Similar as the cascading cycle, double effect cycle is divided into two-stages: a high temperature cycle (HTC) as the top cycle and a low temperature cycle (LTC) as the bottom cycle (Fig.2.30). The heat exchanger HHX1 and HHX2 work in high temperature cycle and, LHHX1 and LHX2 works in low temperature cycle. The working principle of the LTC cycle is the same as that of the conventional two bed single-stage cycle; the only difference is the heat source. In a single-stage cycle, the cycle is driven by external heat; however, in a double-effect cycle, the LTC is driven by condensation heat from the top cycle (the HTC). Because the HTC cycle operates at high temperatures, the waste heat from the desorption-condensation process can be re-used to generate the LTC. This relationship is the basic principle of the double-effect adsorption system. Because the condensation heat from the HTC is directly

transferred to the LTC beds and is used to generate the desorption process of the LTC, the condensing pressure of the HTC side is influenced by latent heat on the LTC.

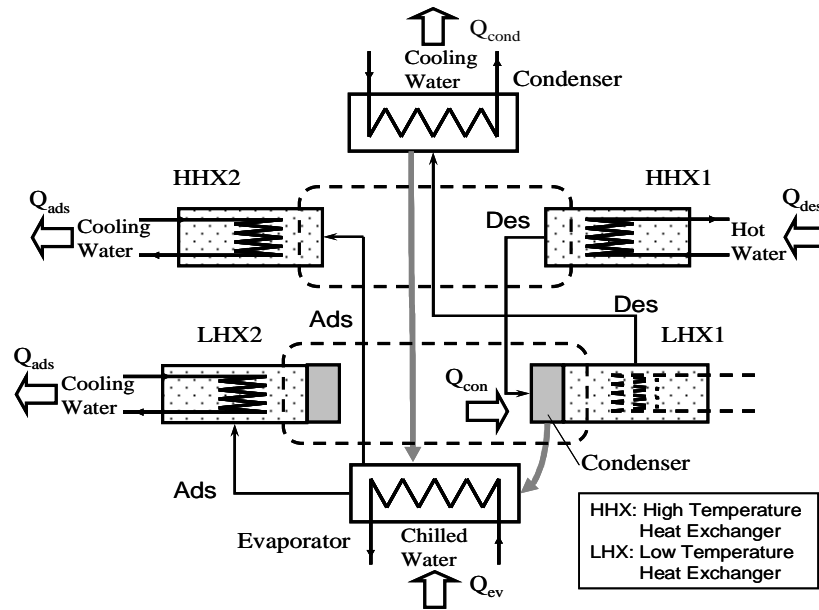


Fig. 2.29: Schematic of double effect adsorption system (Marlinda et al., 2010).

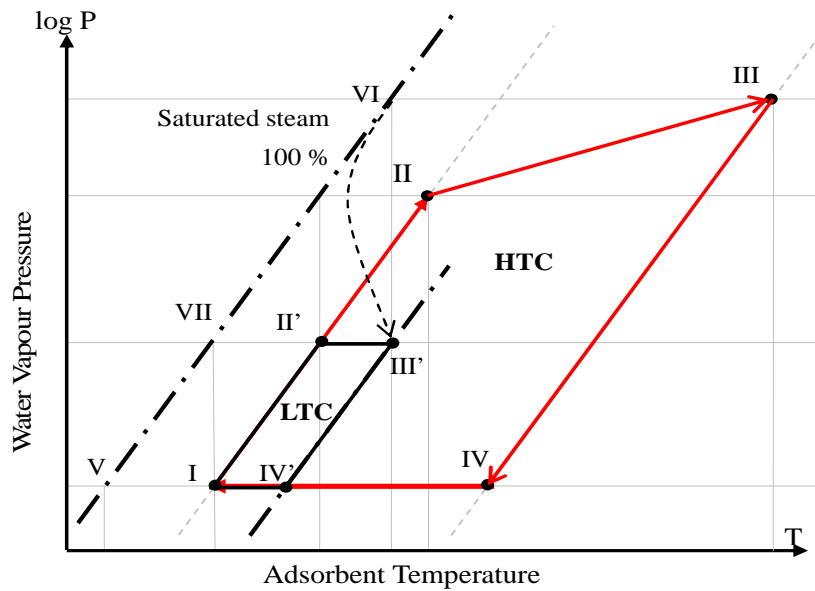


Fig.2.29: Conceptual Dühring diagram of double-effect adsorption system.

2.6 Adsorbent/Adsorbate Pairs

Many kinds of adsorbate-adsorbent pairs have been developed and still in development. Zeolite/water, activated carbon/methanol, and silica/water, are most commonly used adsorbent/adsorbate pairs. Srivastava et al., 1998 described in detail about adsorbate-adsorbent pair used in adsorption refrigeration and heat pump system. Working pairs can be described as three categories such as physical, chemical and composite adsorbent pair, according to the nature of the forces involved in the adsorption process. Simply it can be expressed as

❖ **Physical adsorbent pair**

The physical adsorbents that are used in adsorption heat pumps rely on van der Waal's forces to contain adsorbate. Common examples include silica gel, zeolite, activated carbon and activated carbon fiber and their pairs are given below.

- Silica gel/water
- Zeolite/water
- Activated carbon/ethanol
- Activated carbon/ammonia
- Activated carbon/methanol
- Monolithic carbon /ammonia
- Activated carbon fiber/ammonia
- Activated carbon fiber/methanol
- Activated carbon fiber/Alcohol

❖ **Chemical adsorbent pair**

Chemical adsorbents chemically combine with an adsorbate and there is a transfer or sharing of electron, or breakage of the adsorbate into atoms or radicals which are bound separately. Pair of chemical adsorbents are given below.

- Metal chloride/ ammonia
- Metal hydrides/hydrogen
- Metal oxides/water

❖ **Composite adsorbent pair**

Composite adsorbents are combination of physical and chemical adsorbent and example of some pairs are given below.

- Silica gel and chlorides/water
- Silica gel and chlorides/methanol
- Chlorides and porous media/ammonia

- Zeolite and foam aluminum/water

Extensive studies have been conducted to investigate the performance of adsorption cooling and heat pump systems considering various types of adsorbent/refrigerant pairs, some example of investigation are given below (Saha et al.,2007).

Adsorbent/adsorbate pair	System Type	Remarks
Silica gel - water	Non-regenerative system	Three-bed system
	Non-regenerative system	Multi-bed, dual-mode system
	Multi-stage system	Can operate with regeneration temperature of 40 °C
Zeolite-water	Cascaded cycles	Heating application; adsorption heat is 3700 kJ/kg ⁻¹
	Combination of two independent single adsorption systems	Locomotive cooling application
Activated carbon - ammonia	Regenerative system	Four-bed system
	Regenerative system	Thermal wave system, required regeneration temperature is very high
	Regenerative system	Convective thermal wave system
Activated carbon-methanol	Solid adsorption refrigerator	Solar powered system with very low efficiency.
	Solar ice maker	Solar refrigeration COP is between 0.1 and 0.12
	Adsorption ice maker driven by diesel engine waste heat	System COP is between 0.085 and 0.179
Activated carbon fiber- methanol	Cooling applications	Refrigeration capacity is about three folds higher than that of the AC- methanol system.
Zeolite-water and Activated carbon fiber “Bisofit”- ammonia	Combined solar adsorption cycles	Topping cycle regeneration at 280 °C and bottoming cycle regeneration at 150 °C
Activated carbon fiber “Bisofit”- ammonia	Two-bed solar-gas heat pump	Solar COP is around 0.3

Chapter 3

Adsorption System Modelling

Adsorption system works with mainly two natural phenomena consisting of adsorption and desorption. The mechanism of such phenomena are described below.

3.1 Adsorption and Desorption

Adsorption is a surface phenomenon occurring at the interface of refrigerant phase (gas phase) and adsorbent phase (solid phase) in such a way that Van der Waals forces and hydrogen bonding act between the molecules of substances, irrespective of their state of aggregation. The substance on whose surface the adsorption occurs is known as adsorbent and whose molecules get adsorbed on the surface of the adsorbent (i.e., solid or liquid) is known as adsorbate. Depending upon the nature of forces existing between adsorbate molecules and adsorbent, the adsorption occurs through physical (Vander Waal's forces which is weak) and chemical sorption (chemical bonds known as Langmuir adsorption). Physical adsorption can be easily reversed by heating or by decreasing the pressure. In chemical sorption, the force of attraction is very strong, therefore adsorption cannot be easily reversed.

Adsorption is different from absorption. In absorption, the molecules of a substance are uniformly distributed in the bulk of the other, whereas in adsorption molecules of one substance are present in higher concentration at the surface of the other substance.

Desorption is a phenomenon whereby a substance is released from or through a surface. It is exactly opposite of either adsorption or absorption. The adsorption and desorption process is simply shown in Fig. 2.1. During adsorption water vapour molecules attach to the surface of silica-gel particle, where as during desorption it is removing from the surface.

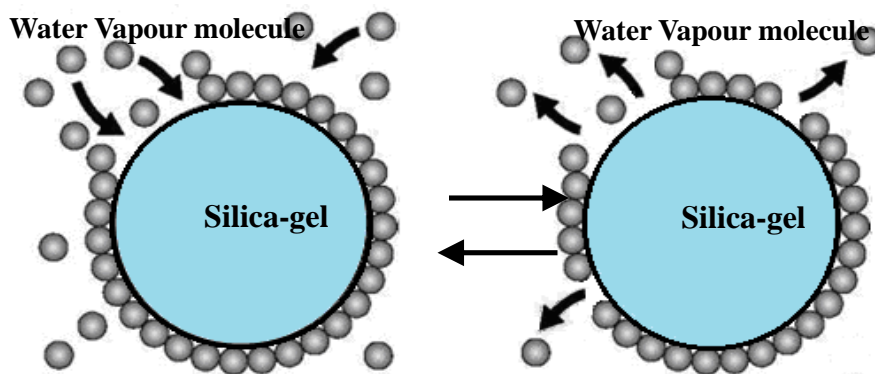


Fig 3.1: Adsorption and desorption process.

The use of solids for removing substances from either gaseous or liquid solutions has been widely used since biblical times. This process is known as adsorption, involves nothing more than the preferential partitioning of substances from the gaseous or liquid phase onto the surface of a solid substrate. Therefore, the adsorption process is essentially an attraction of a gaseous or liquid adsorbate molecules into a porous adsorbent surface. From the early days of using bone char for decolorization of sugar solutions and other foods, to the later implementation of activated carbon for removing nerve gases from the battlefield to today's thousands of applications, the adsorption phenomenon has become a useful tool for purification, separation and refrigeration. Adsorption phenomena are operative in most natural, physical, biological, and chemical systems, and adsorption operations employing solids such as activated carbon and synthetic resins are used widely in industrial applications and for purification of waters and waste water. The process of adsorption involves separation of a substance from one phase accompanied by its accumulation or concentration at the surface of another. Adsorption is thus different from absorption, a process in which material transferred from one phase to another (e.g. liquid) interpenetrates the second phase to form a "solution". The term sorption is a general expression encompassing both processes.

The principle of adsorption is employed,

1. in heterogeneous catalysis.
2. in gas masks where activated charcoal adsorbs poisonous gases.
3. in the refining of petroleum and decoloring cane juice.
4. in creating vacuum by adsorbing gases on activated charcoal.
5. in chromatography to separate the constituents of a mixture.
6. to control humidity by the adsorption of moisture on silica gel.
7. in certain titrations to determine the end point using an adsorbent as indicator (Example: Fluorescein).

3.2 Theory of Adsorption

If adsorbent is in direct contact with the certain surrounding fluid (usually vapor) adsorption phenomenon takes place and after a sufficient long time, both of the adsorbent and the surrounding fluid reach the equilibrium. The extent of adsorption depends upon the following factors:

1. Nature of adsorbate and adsorbent.
2. The surface area of adsorbent.

3. Activation of adsorbent.
4. Experimental conditions. e.g., temperature, pressure, etc.

The process of adsorption is usually studied through graphs known as adsorption isotherm (Fig. 3.2). From the graph, it can be seen that after saturation pressure P_s , adsorption does not occur anymore. This can be explained by the fact that there are limited numbers of vacancies on the surface of the adsorbent. At high pressure a stage is reached when all the sites are occupied and further increase in pressure does not cause any difference in adsorption process. So, at high pressure, adsorption is independent of pressure. It can also explain as, according to Le-Chatelier principle, the direction of equilibrium would shift in that direction where the stress can be relieved. In case of application of excess of pressure to the equilibrium system, the equilibrium will shift in the direction where the number of molecules decreases. Since number of molecules decreases in forward direction, with the increases in pressure, forward direction of equilibrium will be favored. There are different adsorption isotherms such as Freundlich, Langmuir and BET isotherm.

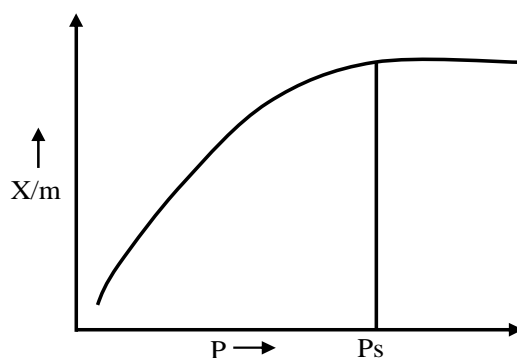


Fig. 3.2: Basic adsorption isotherm.

Freundlich adsorption isotherm

In 1909, Freundlich established an empirical expression representing the isothermal variation of adsorption of a quantity of gas adsorbed by unit mass of solid adsorbent with pressure. This equation is known as Freundlich adsorption isotherm or Freundlich adsorption equation or simply Freundlich isotherm.

$$\frac{X}{m} = kP^{\frac{1}{n}} \quad (3.1)$$

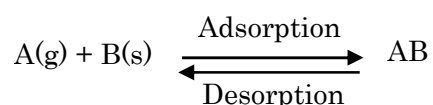
where X is the mass of the gas adsorbed on mass m of the adsorbent at pressure p and k , n are constants whose values depend upon adsorbent and gas at particular temperature. The isotherm correctly established the relationship of adsorption at lower pressure but it failed to predict value of adsorption at higher pressure.

Langmuir adsorption isotherm

Irving Langmuir (Langmuir, 1918) proposed another adsorption isotherm known as Langmuir adsorption isotherm. The Langmuir isotherm is

"Whenever a gas is in contact with a solid there will be an equilibrium established between the molecules in the gas phase and the corresponding adsorbed species (molecules or atoms) which are bound to the surface of the solid".

This isotherm was based on different assumptions one of which is that dynamic equilibrium exists between adsorbed gaseous molecules and the free gaseous molecules.



Where A(g) is unadsorbed gaseous molecule, B(s) is unoccupied metal surface and AB is adsorbed gaseous molecule. The basic assumptions on which the model is based are:

1. Molecules are adsorbed at a fixed number of wall-defined localized sites.
2. Each site can hold one adsorbate molecule;
3. All sites are energetically equivalent; and
4. There is no interaction between molecules adsorbed on neighboring sites.

Based on assumption, Langmuir derived a equation which depicted a relationship between the number of active sites of the surface undergoing adsorption and pressure.

$$\theta = \frac{bP}{1 + bP} \quad (3.2)$$

where θ is the number of sites of the surface which are covered with gaseous molecule, P represents pressure and b is the equilibrium constant for distribution of adsorbate between the surface and gas phase. The limitation of Langmuir adsorption equation is that it is valid at low pressure only. At lower pressure, bP is so small, that factor $(1+bP)$ in denominator can almost be ignored. So Langmuir equation reduces to $\theta = bP$. At high pressure bP is so large, that factor $(1+bP)$ in denominator is nearly equal to bP . So Langmuir equation reduces to $\theta = bP/bP = 1$.

BET Adsorption Isotherm

Brunauer, Emmett and Teller (BET) (Brunauer et al., 1938) were developed a simple model of isotherm to explain multilayer adsorption which is the true picture of physical adsorption whereas Langmuir adsorption isotherm was monolayer adsorption in nature. Under the condition of high pressure and low temperature, thermal energy of gaseous

molecules decreases and more and more gaseous molecules would be available per unit surface area. Due to this multilayer adsorption would occur. Multilayer adsorption presents formidable problems since it is necessary to take account not only of the interactions between sorbate molecules and the adsorbent surface but also of the sorbate-sorbate interactions which are often of comparable magnitude. This model is based on a number of rather serious idealizations which can be at best no more than a first approximation. The BET equation is given as

$$\frac{q}{q_s} = \frac{b(P/P_s)}{(1 - P/P_s)(1 - (P/P_s) + b(P/P_s))} \quad (3.3)$$

Where p_s represent the saturation vapour pressure of the saturated liquid sorbate at the relevant temperature, q represents the sorbate concentration and b is the equilibrium constant.

Types of adsorption isotherm

According to Brunauer (Brunauer et al., 1940), adsorption isotherms can be classified into five types, as shown in Fig. 3.3. Type-I isotherm is generally true for microporous adsorbents, in which the pore size is not very much greater than the molecular diameter of the sorbate molecule. This can be easily explained using Langmuir adsorption isotherm. If $P/P_s \ll 1$ and $b \gg 1$ then BET equation leads to monolayer formation and Type-I adsorption isotherm is obtained. Example of Type-I adsorption is adsorption of Nitrogen (N_2) or Hydrogen (H) on charcoal at temperature near to -1800°C . Type II is observed in adsorbents having a wide range of pore sizes, with either mono or multi-molecular adsorption layers. In BET equation, value of b has to be very large in comparison to 1. Adsorption of benzene vapor on graphite carbon represents an example of this type of isotherms. Type III is uncommon and it includes capillary condensation in addition to the multi-molecular adsorption layer. In BET equation if value of $b \ll 1$ then Type-III adsorption isotherm obtained. Adsorption of bromine on silica gel is an example of this type of isotherms. An isotherm of Type-IV suggests the formation of two surface layers either on a plane surface or on the wall of a pore very much wider than the molecular diameter of the sorbate. Type-V is observed on the adsorbents involving large forces produced by intermolecular attraction such as adsorption of phosphorus on NaX (Barrer et al., 1967).

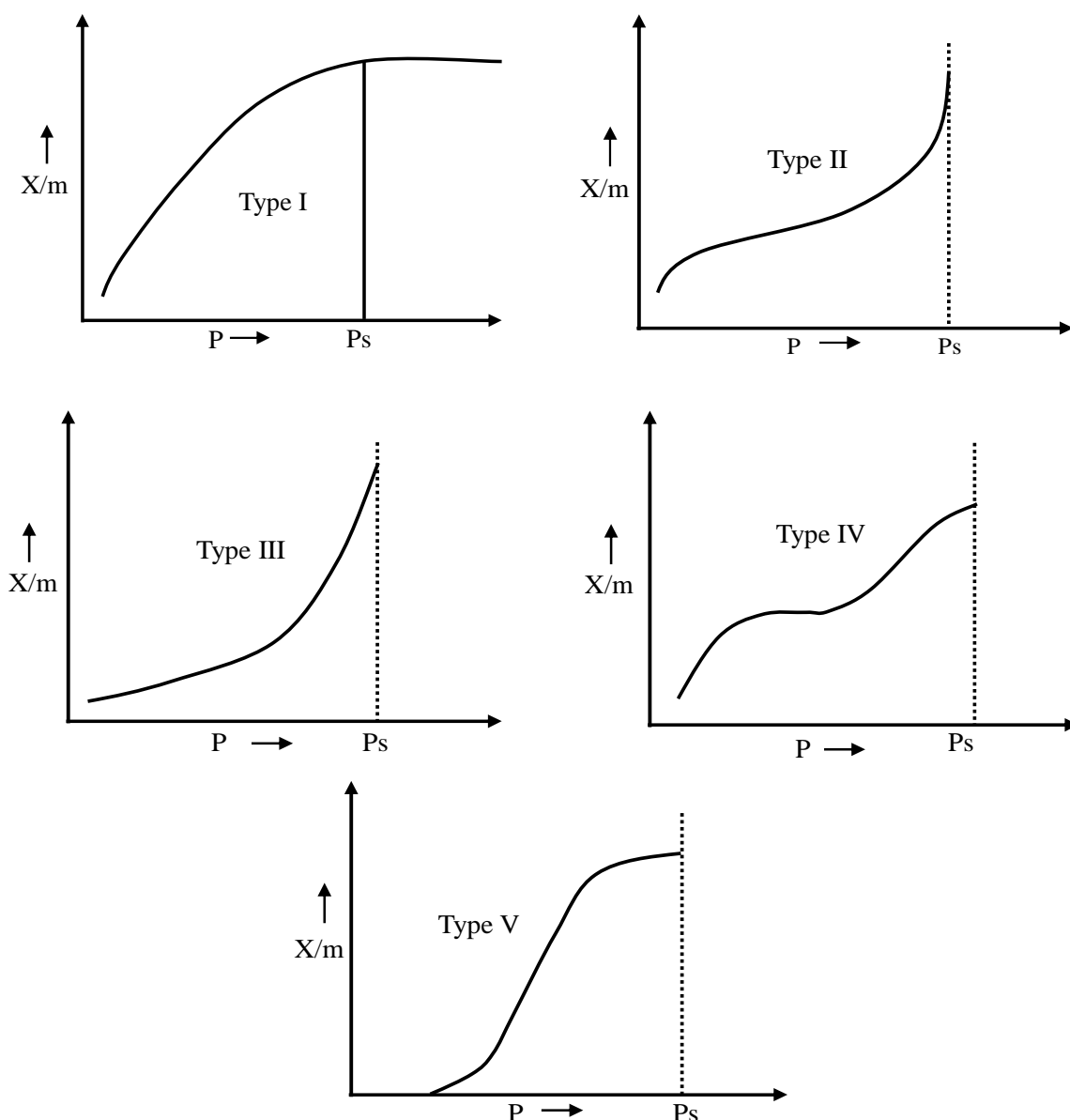


Fig.3.3: Five different Brunauer adsorption Isotherm.

3.3 Forces and Energies of Adsorption System

In physical adsorption two forces involved such as Van der Waals forces (dispersion-repulsion) and electrostatic interactions comprising polarization, dipole and quadrupole interactions. The Van der Waals contribution is always present while the electrostatic contribution are significant only for the case of ionic structure adsorbents such as Zeolites. In the adsorption of small dipolar molecules such as H_2O and NH_3 on zeolite adsorbents the electrostatic contribution may be vary large, giving rise to unusually high heats of adsorption (25-30 kcal/mol). This type interactions are properly regarded as physical adsorption, the heat of adsorption may be well of a magnitude generally associated with chemisorption. More over the adsorption system is quite specific and the rate is controlled by

an activated diffusion process, which is giving the appearance of a slow activated chemisorption, even though the actual surface adsorption is quite rapid. Thus, the systems may appear to exhibit many of the characteristic features generally associated with chemisorption.

Dispersion-repulsion energy

The attractive potential arising from dispersion forces between two isolated molecules may be written in the form (Ruthven, 1984)

$$\phi_D = -\frac{A_1}{r_{12}^6} - \frac{A_2}{r_{12}^8} - \frac{A_3}{r_{12}^{10}} \quad (3.4)$$

where r_{12} is the distance between the centres of the interacting molecules and A_1, A_2, A_3 are constants. The expression of first term of Eq 3.4 is always dominant, which arises from the coupling between instantaneous induced dipoles. Second and third terms represent induced dipole-induced quadrupole and induced quadrupole-induced quadrupole interactions, respectively. For finite size of molecules the short-range repulsive energy generally represented as semi empirically by the twelfth-order inverse power expression;

$$\phi_R = \frac{B}{r_{12}^{12}} \quad (3.5)$$

Neglecting the higher order contributions to the dispersion energy and combining the inverse sixth-power attraction with the inverse twelfth-power repulsion leads to the familiar Lennard-Jones potential function:

$$\phi = 4\epsilon \left[\left(\frac{\sigma}{r} \right)^{12} - \left(\frac{\sigma}{r} \right)^6 \right] \quad (3.6)$$

which is sketched in Fig.3.4. The force constants ϵ and σ are characteristics of the particular molecular species and tabulated values for many common molecules are available.

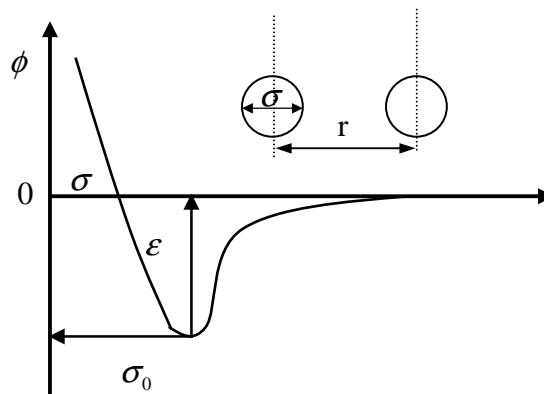


Fig.3.4: The Lennard-Jones Potential.

Electrostatic energies

There is a significant electric field in the surface region of ionic adsorbent such as Zeolites, which will be additional contribution to the adsorption energy. It may arise from polarization (ϕ_p), field-dipole (ϕ_μ), and field gradient-quadrupole (ϕ_Q) interactions. These are given by the following expressions:

$$\phi_p = -\frac{1}{2}\alpha E^2 \quad (3.7)$$

$$\phi_\mu = -\mu E \quad (3.8)$$

$$\phi_Q = \frac{1}{2}Q \frac{\partial E}{\partial r} \quad (3.9)$$

where E is the electric field, α the polarizability, μ the dipole and Q the quadrupole moment, defined by

$$Q = \frac{1}{2} \int q(\rho, \theta) (3 \cos^2 \theta - 1) \rho^2 dV \quad (3.10)$$

where $q(\rho, \theta)$ is the local charge density at the point (ρ, θ) with the origin at the center of the molecule, and the integration is carried out over the entire volume of the molecule. Thus, the overall potential for an ionic adsorbent is given by the sum of six terms:

$$\phi = \phi_D + \phi_R + \phi_P + \phi_\mu + \phi_Q + \phi_s \quad (3.11)$$

where ϕ_s represents the contribution from sorbate-sorbate interaction.

3.4 Heat and Energy Balance of Adsorption System

During the operation of the system, refrigerant vapour of evaporator goes to condenser through adsorption/desorption bed and return after condensation in condenser via U-shape tube. Heat and energy are balancing in every aspect whereas temperature, pressure and refrigerant concentration throughout system are assumed uniform. Heat transfer and energy balance of the system are described in the following sections.

3.4.1 Adsorption and desorption bed energy balance

The heat transfer and energy balance equations for the adsorption/desorption bed are given below;

$$T_{out}^{col/hot} = T^b + (T_{in}^{col/hot} - T^b) \cdot \exp\left(-\frac{(U.A)_{hex}^b}{\dot{m}_w^{col/hot} \cdot C_w}\right) \quad (3.12)$$

$$\begin{aligned}
W_s^b C_s \frac{dT^b}{dt} + W_s^b C_w \frac{d(q^{ads/des} \cdot T^b)}{dt} + (W \cdot C)_{hex}^b \frac{dT^b}{dt} = \dot{m}_w^{col/hot} c_w (T_{in}^{col/hot} - T_{out}^{col/hot}) \\
+ W_s^b Q_{st} \frac{dq^{ads/des}}{dt} - \alpha W_s^b C_{wv} \{ \beta (T^b - T^e) + (1 - \beta) (T^b - T_{wv}) \} \frac{dq^{ads/des}}{dt}
\end{aligned} \quad (3.13)$$

Both identical equations are used for adsorption and desorption purposes, where heat transfer fluid temperature $T_{in}^{col/hot}$ and $T_{out}^{col/hot}$ denote cooling water temperature upon adsorption and hot water temperature upon desorption. T^b stands for adsorption/desorption bed temperature. Heat transfer is fully depending on heat transfer coefficient U_{hex}^b and heat transfer area A_{hex}^b of bed. Left-hand side of Eq. 3.13 indicates the amount of sensible heat required to cool or heat the adsorbent (e.g. silica-gel), adsorbate (e.g., water) as well as metallic parts of the heat exchanger (*hex*) during adsorption or desorption. First term of right hand side stands for the total amount of heat released to the cooling water upon adsorption or provided by the hot water upon desorption, the second term for the adsorption heat release or desorption heat input and last two terms for the sensible heat of the adsorbed vapour. α is either 0 or 1 depending on whether bed is working as desorber or adsorber and β is either 1 or 0 depending on whether bed is connected with evaporator or other bed. Heat and energy balance equation does not consider the external heat losses to the environment.

3.4.2 Evaporator energy balance

The heat transfer and energy balance equations of evaporator are given below;

$$T_{out}^{chil} = T^e + (T_{in}^{chil} - T^e) \cdot \exp\left(-\frac{(U \cdot A)_{hex}^e}{\dot{m}_w^{chil} \cdot C_w}\right) \quad (3.14)$$

$$\begin{aligned}
(W_w^e C_w + (W \cdot C)_{hex}^e) \frac{dT^e}{dt} = -L_w W_s^b \frac{dq^{ads}}{dt} - W_s^b C_w (T^c - T^e) \frac{dq^{des}}{dt} \\
+ \dot{m}_w^{chil} c_w (T_{in}^{chil} - T_{out}^{chil})
\end{aligned} \quad (3.15)$$

where A_{hex}^e and U_{hex}^e are the heat transfer area and heat transfer coefficient of evaporator, respectively and L_w is the latent heat of vaporization. Left hand side of Eq. 3.15 indicates the sensible heat required by the liquid refrigerant (water) and the metal of heat exchanger tube of evaporator. First term of right hand side represents the latent heat for adsorbed refrigerant; second term represents the sensible heat required to cool down the incoming condense refrigerant from the condensation temperature; and the last term represents the total amount

of heat loss by the chilled water.

3.4.3 Condenser energy balance

The heat transfer and energy balance equations of the condenser are as follows:

$$T_{out}^{c,col} = T^c + (T_{in}^{c,col} - T^c) \cdot \exp\left(-\frac{(U \cdot A)_{hex}^c}{\dot{m}_w^{c,col} \cdot C_w}\right) \quad (3.16)$$

$$\begin{aligned} (W_w^c C_w + (W \cdot C)_{hex}^c) \frac{dT^c}{dt} = & \{-L_w - C_{wv}(T^b - T^c)\} W_s^b \frac{dq^{des}}{dt} \\ & + \dot{m}_w^{c,col} C_w (T_{in}^{c,col} - T_{out}^{c,col}) \end{aligned} \quad (3.17)$$

where A_{hex}^c and U_{hex}^c is the heat transfer area and heat transfer coefficient of condenser, respectively. The left hand side of Eq. 3.17 represents the sensible heat required by the liquid refrigeration and the metallic parts of heat exchanger tubes due to the temperature variations in the condenser. First part of write hand side represents the latent heat of vaporization (L_w) for desorbed refrigerant; the second term represents the sensible heat due to vapour transfer from desorber to the condenser and the last term taken into account of total amount of heat released to the cooling water.

3.4.4 Adsorption and desorption rate

The adsorption/desorption rate can be express as

$$\frac{dq^{ads/des}}{dt} = ksap(q^* - q^{ads/des}) \quad (3.18)$$

where the overall mass transfer coefficient (ksap) for adsorption is given by

$$ksap = 15 \cdot D_s / (R_p)^2 \quad (3.19)$$

Here R_p denotes the average radius of silica gel particle. The adsorption rate is controlled by surface diffusion inside gel particle and surface diffusivity (D_s), which can be expressed by Arrhenius equation as a function of temperature as

$$D_s = D_{so} \exp\left(\frac{-E_a}{R \cdot T}\right) \quad (3.20)$$

where D_{so} is a pre-exponential term whose value is taken as $2.54 \times 10^{-4} \text{ m}^2 \text{ s}^{-1}$; E_a denotes activation energy; R denotes gas constant and T stands for temperature.

where q^* is adsorption uptake at equilibrium state that can be expressed as (Akahira A., 2004)

$$q^* = \frac{0.8 \times [P_s(T_w) / P_s(T_s)]}{1 + 0.5 \times [P_s(T_w) / P_s(T_s)]} \quad (3.21)$$

where $P_s(T_w)$ and $P_s(T_s)$ are the saturation vapour pressure at temperatures T_w (water vapour) and T_s (silica gel), respectively. Antoine correlates the saturation pressure and temperature, which can be expressed as

$$P_s = 133.32 \times \exp(18.3 - 3820 / (T - 46.1)) \quad (3.22)$$

3.4.5 Mass balance

Total mass of refrigerant, W_w^e of the system is constant. The rate of change of the mass of liquid refrigerant (due to adsorption and desorption process) can be expressed through the following equation;

$$\frac{dW_w^e}{dt} = -W_s^b \left(\frac{dq^{des-con}}{dt} + \frac{dq^{ads-evp}}{dt} \right) \quad (3.23)$$

where W_s^b is the weight of silica gel packed in each bed and superscript *des-con* and *ads-evp* are indicating the vapour flow rate from desorber to condenser and evaporator to adsorber bed, respectively.

3.4.6 System performance

The performance of adsorption system is mainly characterized by specific cooling power (SCP), which is the cooling capacity per unit mass of adsorbent and coefficient of performance (COP), which is the ratio between heat released by the evaporator and heat source input to the bed, these can be calculated by using the following equations:

Specific cooling power (SCP);

$$SCP = \dot{m}_w^{chil} C_w \int_0^{t_{cycle}} (T_{in}^{chil} - T_{out}^{chil}) dt / t_{cycle} W_{s,tot} \quad (3.24)$$

where \dot{m}_w^{chil} is the chilled water flow rate; T_{in}^{chil} and T_{out}^{chil} are indicating the chilled water inlet and outlet temperature; and t_{cycle} and $W_{s,tot}$ are indicating the total cycle time and total mass of silica-gel of the system.

Coefficient of performance (COP):

$$COP = \frac{\dot{m}_w^{chil} C_w \int_0^{t_{cycle}} (T_{in}^{chil} - T_{out}^{chil}) dt}{\dot{m}_w^{hot} C_w \int_0^{t_{cycle}} (T_{in}^{hot} - T_{out}^{hot}) dt} \quad (3.25)$$

where \dot{m}_w^{hot} is indicating the hot water flow rate in the desorption bed; and T_{in}^{hot} and T_{out}^{hot} are indicating hot water inlet and outlet temperature, respectively.

3.5. Optimization of Adsorption System

Role of optimization is to find values of the variables that minimize or maximize the objective function while satisfying the constraints. In this dissertation the objective function is chosen as specific cooling power (SCP), variables were cycle time components and chilled water flow rate and fixed chilled water outlet temperature. It can be precise as

Objective: To maximize the objective function

Objective function: Specific cooling power (SCP)

Variables: Cycle time components such as

for three-bed mass recovery cycle: adsorption/desorption, pre-cooling/pre-heating and mass recovery time

for two- and three-stage cycle: τ_1 , τ_2 and \dot{m}_{chill}

Boundary Conditions: Chilled water outlet temperature

Input parameters: Hot and cooling water inlet temperature, chilled water inlet temperature, adsorbent mass etc. Parameters values are shown details in Tables 4.3-4, 5.2 and 6.2).

There are some methods of optimization among them particle swarm optimization (PSO) method is applied for optimizing of cycle time to maximize SCP of adsorption system. Details of PSO is given below;

Particle swarm optimization (PSO) methodology

Particle swarm optimization (PSO) is a stochastic population based optimization technique that was first introduced by James Kennedy (a Social Psychologist) and Russel Eberhart (an Electrical Engineer) in 1995 (Kennedy et al., 1995). Inspired by social behavior and movement of birds and fishes. It is an evolutionary computational technique based on the movement and intelligence of swarms looking for the most fertile feeding location and it is globally acceptable methods for optimization.

Swarm is an apparently disorganized collection (population) of moving individuals that

tend to cluster together while each individual seems to be moving in a random direction. Swarm picture of birds and fish are shown in Fig.3.5.

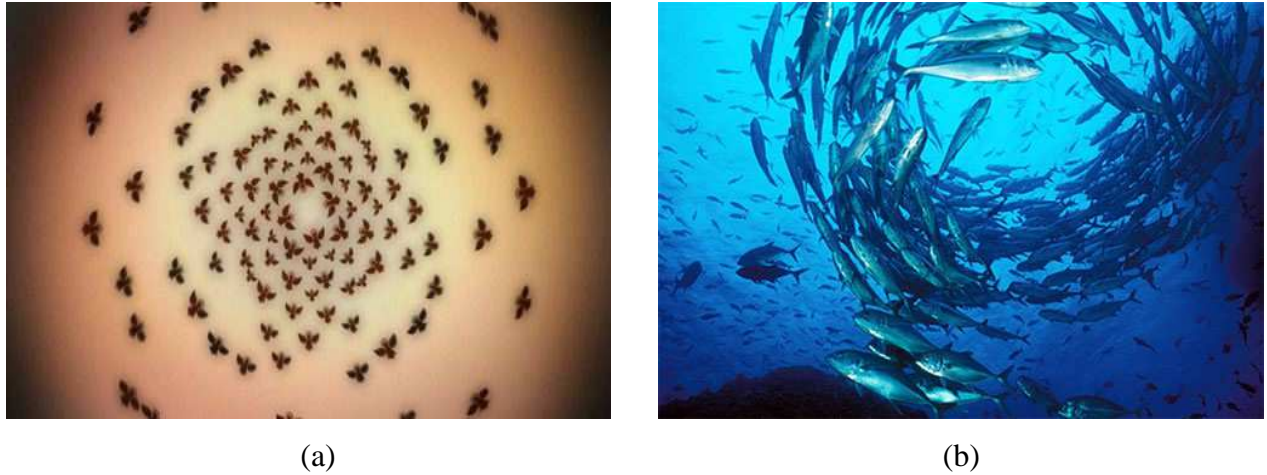


Fig. 3.5: Swarm of (a) birds and (b) fishes.

PSO applicable to optimize the nonlinear function based on swarm of particles (e.g., birds and fishes). The particle swarm consists of 'n' particles. These particles are moved around in the search space according to formulae. The dimension or number of variables are indicated by z. The particles of the swarm is represented by $x_{z1}, x_{z2}, x_{z3}, \dots, x_{zn}$ and the best particle of the swarm, i.e. the particle with the maximum function value, is denoted by index g. The best previous position (i.e. the position giving the maximum function value) of the i-th particle is recorded and represented as $p_{z1}, p_{z2}, p_{z3}, \dots, p_{zn}$ and the position change (velocity) of the particles are represented as $v_{z1}, v_{z2}, v_{z3}, \dots, v_{zn}$. The formula to update a particle's velocity and position can be written as

$$v_{zi}^{k+1} = \omega \cdot v_{zi}^k + C_1 \cdot r_1 \cdot (p_{zi}^k - x_{zi}^k) + C_2 \cdot r_2 \cdot (p_{zg}^k - x_{zi}^k) \quad (3.26)$$

$$x_{zi}^{k+1} = x_{zi}^k + v_{zi}^{k+1} \quad (3.27)$$

where x_i and v_i are the position and velocity of the ith particle. p_i is the personal best position that the ith particle had reached and p_{zg} , is the group best position that all the particles had reached. k represents the number of iteration. ω is the inertia weight; r_1 and r_2 are two random numbers either 0 or 1 and C_1 and C_2 are two positive constant, called the cognitive and social parameter, respectively.

The equation 3.26 is used to calculate at each iteration, the i-th particle's new velocity. Three terms are taken into consideration. The first term, ωv_{zi}^k is the particle's previous velocity weighted by the inertia weight ω . The second term, $(p_{zi}^k - x_{zi}^k)$, is the distance

between the particle's best previous position and its current position. Finally, the third term, $(p_{zg}^k - x_{zi}^k)$, is the distance between the swarm's best experience and the i-th particle's current position. Equation 3.27 provides the new position of the i-th particle, adding its new velocity, to its current position. The particles change its condition according to the following three principles: (1) to keep its inertia (2) to change the condition according to its most optimist position (3) to change the condition according to the swarm's most optimist position. The positions of the particles are guided by their own best known position (i.e., personal best or pbest) as well as the entire swarm's best known position (i.e., group best or gbest). When better positions are being discovered these will then come to guide the movements of the swarm. The modification of search particle position and velocity graphically shown in Fig. 3.6. In general, the performance of each particle is measured according to a fitness function, which is problem dependent. In optimization problems, the fitness function is usually the objective function under consideration. More descriptions of PSO technique are given in Fig. 3.7(a). Optimization of cycle time components to maximize the SCP based on PSO is shown in the Fig.3.7(b).

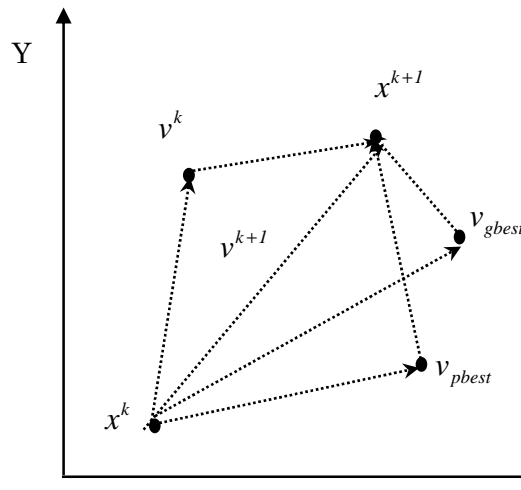


Fig. 3.6: Concept of modification of a searching position by PSO.

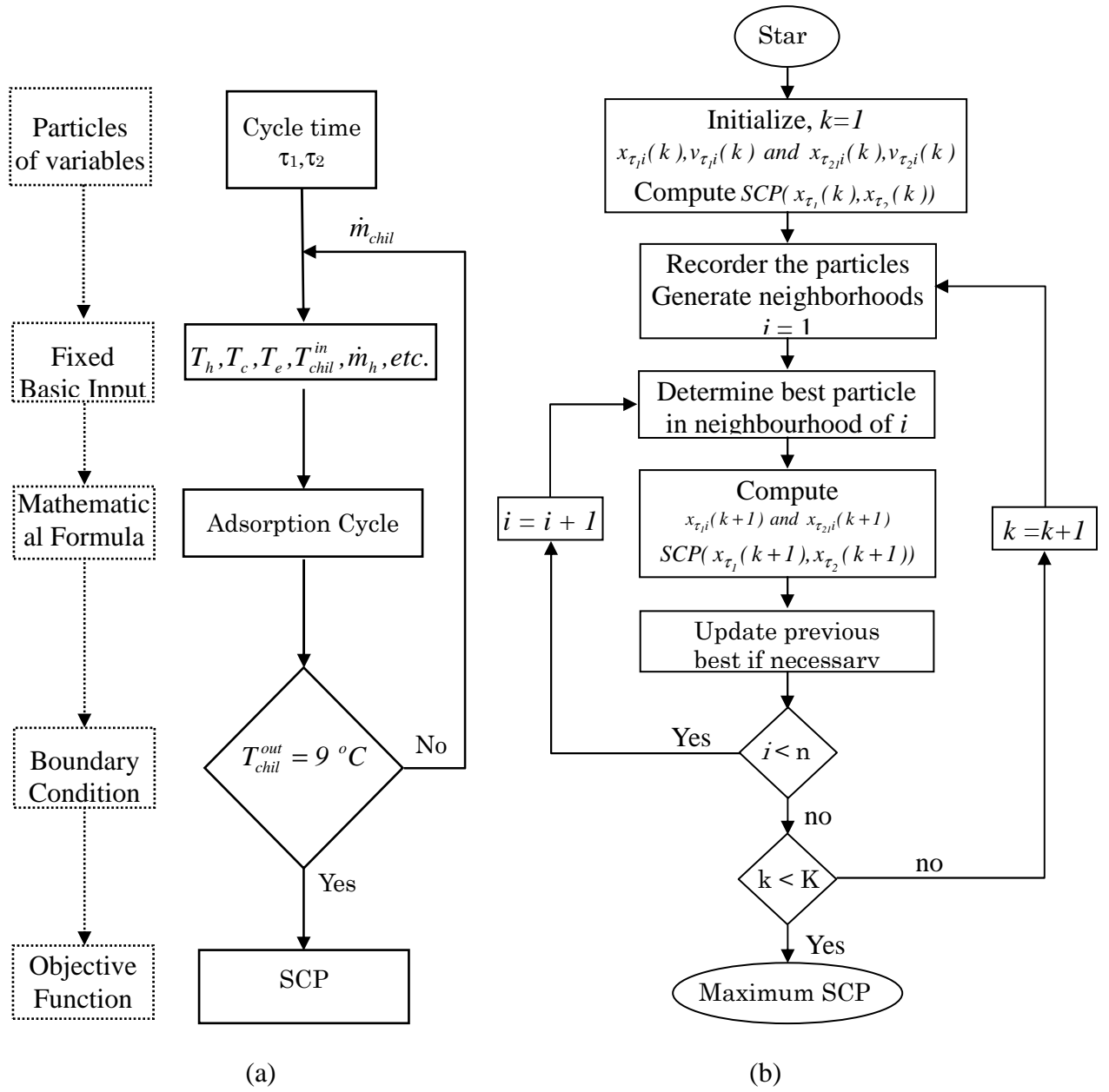


Fig. 3.7: Flow chart of (a) SCP simulation and (b) optimization of cycle time based on PSO.

Chapter 4

Performance Comparison of Three-bed Single-Stage Adsorption Cooling System with Optimal Cycle Time Setting

4.1 Introduction

Nowadays, the potential of using low-grade waste heat or renewable energy sources to generate cooling energy is attracting increasing attention. Adsorption chillers employing silica-gel and water as the adsorbent-refrigerant pair can effectively utilize heat source of temperature below 90 °C to produce cooling energy and such temperature can be easily found from industrial waste heat or renewable energy sources. A considerable number of studies have been conducted on environmental friendly adsorption heat pump systems. The followings are some representative studies. Meunier, 1978 studied a solid-vapor system using the zeolite-water pair. The same system was analytically investigated by Douss et al., 1988. Silica gel-water system was investigated analytically by Saha et al., 1995a and experimentally by Boelman et al., 1995 for adsorption cooling application. Silica gel-water based adsorption system powered by driving heat source temperature as low as 70 °C is commercialized in Japan (Critoph et al., 2005).

To improve the cooling performance and to utilize low-temperature heat source various advanced adsorption systems have been proposed such as heat and mass recovery cycles by Szarzynski et al., 1997 and Akahira et al., (2004, 2005), multi-stage cycles by Saha et al., 1995b and Alam et al., 2004, multi-bed cycles by Chua et al., 2001 and Saha et al., (2003a, 2006). It was presented that those advanced cycles would achieve better performances compared with that of the conventional two-bed adsorption cycle.

In this study, the authors focused on two kinds of three-bed non-regenerative silica gel-water adsorption chiller with mass recovery heating/cooling. One was developed by Kahn et al., (2006a, 2007a) while the other was proposed by Uyun et al., (2009a, 2009b). Although they have the same number of adsorption/desorption beds, the cycles have different behavior. It can be said that each adsorption cycle has an appropriate cycle time setting to maximize the performance. In other words, a setting of cycle time producing the best performance for one cycle dose not necessarily work well for the other cycles. To compare different adsorption cycles fairly, it is emphasized that the best performance of each cycle should be compared with each other. From this point of view, optimizing the cycle

performance is quite important. Miyazaki et al., 2009 succeeded the optimization of cycle time to maximize the cooling effect of two-bed, single-stage adsorption cycle by the particle swarm optimization (PSO) method. PSO optimizes total cycle time length as well as the allocation of time to processes of adsorption/desorption, mass recovery and pre-cooling/pre-heating to get the highest specific cooling power.

Although the three-bed cycles are established and studied, but the simulated performance didn't reflect the optimal results because of the limitation of the simulation methods. In order to overcome this problem, the PSO method is applied to simulate the performance of two different three-bed adsorption cycles with mass recovery heating/cooling. The objectives of this study consist of the following two points. One is to propose a method of comparing different adsorption refrigeration cycles from the viewpoint of optimal performance. The other is to compare cycles studied by Khan and Uyun base on the proposed method to understand advantages and disadvantages of each cycle.

4.2 Description of Three-Bed Adsorption Cooling System

The three-bed adsorption cooling system consists of three adsorber/desorber heat exchangers namely Bed 1, Bed 2 and Bed 3, one evaporator and one condenser. The schematic diagrams of two different types of mass recovery three-bed adsorption cooling systems known as Cycle A and Cycle B, respectively are shown in Figs. 4.1 and 4.2.

Silica-gel and water have chosen as adsorbent-refrigerant pair because the regenerative temperature of silica gel is lower than that of other adsorbents and water has large latent heat of vaporization. The former (cycle A) was developed by Khan et al. (2007a) through modification of Saha et al. (2003a) three-bed adsorption cooling system by adapting mass recovery process between Bed 1 and Bed 2. The mass recovery process is done by interconnecting two beds for depressurizing-pressurizing after the desorption-adsorption process. In this case mass recovery happened between Bed 1 and Bed 3, and Bed 2 and Bed 3. The physical dimension of Bed 1 and Bed 2 is chosen as uniform, but the dimension of Bed 3 is chosen as the half of that of the Bed 1 or Bed 2. To complete a full cycle, the cooling system needs 10 modes, namely A, B, C, D, E, F, G, H, I and J as can be seen from Table 4.1. In mode A, Bed 1 and Bed 3 are in heating with hot water and connected with condenser to remove all refrigerant from the beds, which called desorption mode. At the same time Bed 2 is in cooling with cooling water and connected with evaporator to adsorb the refrigerant vapor of evaporator, which is called adsorption mode. A low pressure is maintained in the evaporator so that the refrigerant can vaporize at low temperature. Bed 1 and Bed 2 remain in

desorption up to end of mode C and adsorption up to end of mode D, respectively. In mode B, Bed 3 is disconnected from the evaporator and then cooled down by cooling water, which is called pre-cooling mode. During desorption mode it was in relatively higher pressure and thereafter pressure is decreasing due to cooling by coolant supply. When pressure attains nearly equal to the pressure of the evaporator then it is connected with evaporator, which is known as mode C. In mode D, Bed 1 is heated by hot water and Bed 3 is cooled by cooling water, at the same time the beds are connected with each other by opening the connecting valve (V3), which is called the mass recovery process with heating/cooling. Mode E is called pre-heating and pre-cooling mode as the beds are isolated during this process. In this case Bed 1 is in pre-cooling mode and is cooled by cooling water, and Bed 2 and Bed 3 are in pre-heating mode and they are heated by hot water. In desorption mode, adsorbed refrigerant removed from the adsorbent beds and goes to the condenser. Refrigerant vapor condensed inside the condenser where condensation heat is removed by cooling water. Condensed refrigerant then goes to the evaporator via a U-bend tube. The mechanism of modes F, G, H, I and J are similar as the mode of A, B, C, D and E. During the F~J modes, Bed 1 is in adsorption process, while Bed 2 is in desorption process and mass recovery process takes place between Bed 2 and Bed 3.

The latter three-bed mass recovery adsorption cycle (cycle B) was proposed by Uyun et al. (2009b). However, in order to facilitate comparison, we have considered the physical dimension of Bed 3 as that of the half of Bed 1 or Bed 2. Main difference between cycle A and cycle B is that, Bed 3 is connected with condenser in cycle A, but

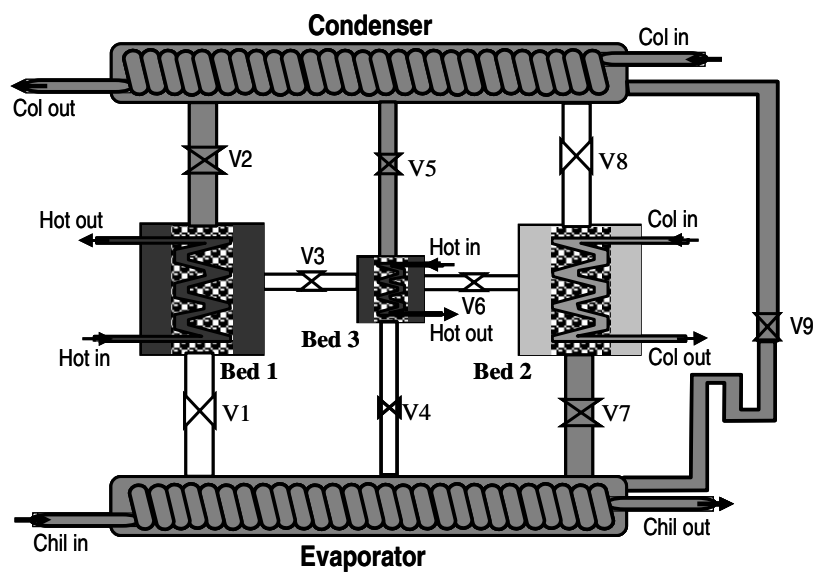


Fig. 4.1: Schematic diagram of three-bed single-stage mass recovery heating/cooling cycle A.

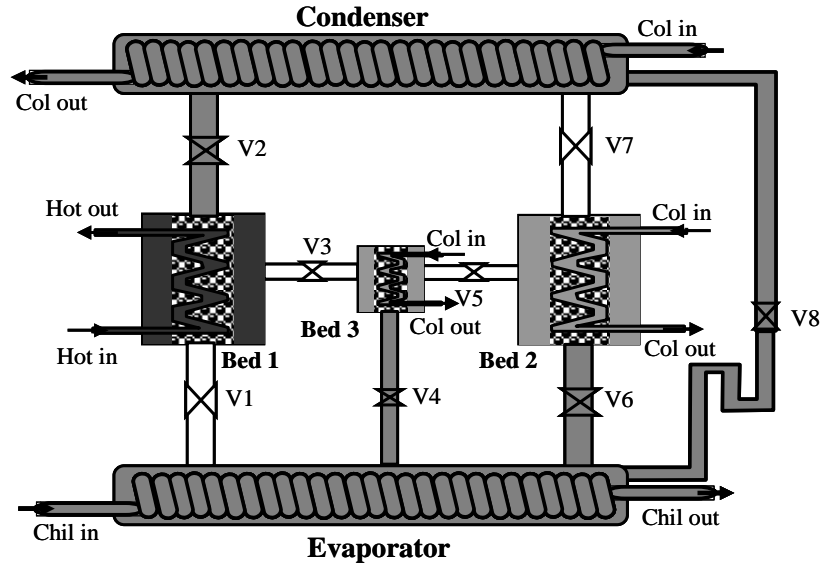


Fig. 4.2: Schematic diagram of three-bed single-stage mass recovery heating/cooling adsorption cycle B.



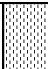



it is always disconnected from the condenser in cycle B. Different operation modes of cycle B is given in Table 4.2. To complete a full cycle, this system needs only 8 modes, i.e. A, B, C, D, E, F, G and H. In this case, both Bed 1 and Bed 2 follow desorption, pre-cooling, adsorption, mass recovery cooling and pre-heating processes, whereas Bed 3 only follows adsorption, mass recovery heating and pre-cooling processes. Desorbed water vapor from Bed 3 is adsorbed by Bed 1 or Bed 2 during mass recovery heating process. Details description of the both three-bed mass recovery cycles can be found elsewhere (Khan et al., (2006a, 2007a) and Uyun et al., (2009a, 2009b)).

Table 4.1: Operation modes and cycle time (in second) of cycle A.

Mode	A 400	B 30	C 300	D 140	E 30	F 400	G 30	H 300	I 140	J 30
Bed 1	730			140	30	870				30
Bed 2	870				30	730			140	30
Bed 3	400	30	300	140	30	400	30	300	140	30

Table 4.2: Operation modes and cycle time (in second) of cycle B.

Mode	A 400	B 30	C 170	D 30	E 400	F 30	G 170	H 30
Bed 1	400	30	600		200		30	
Bed 2	400	200	30	400	30	200		
Bed 3	400	200	30	400		200		30

	Desorption		Mass recovery with heating		Pre-heating
	Adsorption		Mass recovery with cooling		Pre-cooling

4.3 Methods and Materials

Simulation methods and materials of three-bed single-stage adsorption system with mass recovery heating/cooling are details described in chapter 3 of section 3.4. Heading of the sub-sections from 3.4.1 to 3.4.6 are given below:

- ❖ Adsorption and Desorption Energy Balance
- ❖ Condenser energy balance
- ❖ Evaporator energy balance:
- ❖ Adsorption and desorption rate
- ❖ Mass balance:
- ❖ System performance

Optimization procedure

A complete simulation program was developed based on Matlab software to solve all equations mentioned in section 3.4. Energy balance equation, mass balance equation and equation for adsorption/desorption rates have been solved simultaneously using Mathlab ode-45 solver. In the beginning of the solution process, initial values are assumed and finally, those are adjusted by the iteration process. Once the satisfactory convergence criterion is achieved, then the process goes for the next time step. All input parameters such as adsorbent-refrigerant properties, flow rates of heat transfer fluids and heat exchangers specifications initially was given for which the system cyclic operation can be realized.

In this study, PSO was applied to optimize the cycle time based on maximum value of

SCP, whereas SCP was chosen as the objective function and cycle time components (i.e., adsorption/desorption time, pre-cooling/pre-heating time and mass recovery time) were chosen as the variable. In PSO, a particle holds the values of variables and updates the values toward the optimal solution. After a number of updating calculations, all the particles hold the same value and the objective function value is maximized. In this case, the number of particles and the number of iterations were considered as 24 and 1500, respectively. It was observed that all particles reached their best position before 500 iterations.

4.4 Results and Discussion

The developed simulation program for three-bed mass recovery with heating/cooling adsorption cooling system was operated by adopting the standard working conditions and cycle time for each mode. Operation mode and cycle time for cycle A and cycle B are given in Tables 4.1 and 4.2, respectively, which has been taken from (Khan et al., 2007a and Uyun et al., 2009b). The standard working conditions and input parameters are presented in Table 4.3 and Table 4.4, respectively. Previous authors as part of their research compared the performance of three-bed adsorption system with the conventional system assuming relative cycle time, e.g. short cycle time and long cycle time, whereas, the present study demonstrates the comparison of the maximum performance of two types of three-bed adsorption chiller and a conventional two-bed adsorption chiller.

Table 4.3: Standard working conditions (Khan et al., 2007b)

Hot water inlet		Cooling water inlet		Chilled water inlet	
Temp (°C)	Flow rate (kg.s ⁻¹)	Temp (°C)	Flow rate (adsorption + condensation) (kg.s ⁻¹)	Temp (°C)	Flow rate (kg.s ⁻¹)
50-90	0.4	30	0.4+0.34	14	0.11

Table 4.4: Basic input parameters (Khan et al., 2007b)

Parameters	Value	Units
Q _{st}	2.80×10 ⁶	J.kg ⁻¹
E _a	4.2×10 ⁴	J.mol ⁻¹
D _{so}	2.54×10 ⁻⁴	m ² .s ⁻¹
R	8.314	J.mol ⁻¹ .K ⁻¹
R _p	0.35×10 ⁻³	m
C _w	4.18×10 ³	J.kg ⁻¹ .K ⁻¹

C_{wv}	1.89×10^3	$J.kg^{-1}.K^{-1}$
L_w	2.50×10^6	$J.kg^{-1}$
C_{Cu}	386.00	$J.kg^{-1}.K^{-1}$
C_{Al}	905.00	$J.kg^{-1}.K^{-1}$
C_s	924.00	$J.kg^{-1}.K^{-1}$
A_{hex}	1.45	m^2
A_e	0.665	m^2
A_c	0.998	m^2
U_c	4070.00	$W.m^{-2}.K^{-1}$
$U_{hex}(\text{desorption})$	1540.00	$W.m^{-2}.K^{-1}$
$U_{hex}(\text{adsorption})$	1380.00	$W.m^{-2}.K^{-1}$
U_e	3550.00	$W.m^{-2}.K^{-1}$
W_s	35.00	kg
$W_{hex}(Cu)$	12.67	kg
$W_{hex}(Al)$	5.33	kg
$W_{e,hex}$	4.80	kg
$W_{e,w}$	25.0	kg
$W_{c,w}$	5.00	kg
$W_{c,hex}$	6.40	kg

The cycle time means adsorption/desorption time, mass recovery time and pre-cooling/pre-heating time and it is one of the important parameters of the system that influence on the overall performance. The SCP represents the cooling capacity per unit quantity of adsorbent, and therefore, it is a useful index to minimize the size of the system. That is why the cycle time was optimized based on the maximum value of SCP using PSO procedure. PSO is newly approached for three-bed adsorption cooling system. Optimal adsorption/desorption time, mass recovery time and pre-heating/pre-cooling time of both systems were optimized for different heat source temperature from 50 °C to 90 °C, which is given in Table 4.5. Total optimal cycle time is the sum of the cycle time of all modes (Table 4.1). The cycle time ratio is defined as the ratio of each process time to the total cycle time. Figs. 4.3 and 4.4, respectively, are representing the optimal cycle time ratio of cycle A and cycle B for different heat source temperature. It is observed that adsorption/desorption time ratio and pre-cooling/pre-heating time ratio were increased, whereas mass recovery time ratio was decreased with

heat source temperature for both cycles. This effect is prominent for cycle A but less impact for cycle B. Effect of heat source temperature on total cycle time for both cycles is shown in Fig. 4.5. It is obvious that total optimal cycle time specific for each heat source temperature and was decreased with temperature. Cycle A was provided longer total cycle time compares to cycle B.

Table 4.5: Observed optimal cycle time, SCP and COP of cycle A and cycle B

Adsorption Cycle	HST	Optimized						Un-optimized		
		Ad/Ds	Pc/Ph	MR	TCT	SCP	COP	TCT	SCP	COP
Cycle A MR with heating/ cooling	50	611.87	33.98	849.55	4282.46	23.25	0.55	754	9.18	0.10
	55	418.77	30.58	517.11	2831.60	39.48	0.60		28.38	0.24
	60	329.60	24.15	371.62	2158.25	54.73	0.62		46.06	0.33
	65	269.22	22.39	268.84	1704.11	68.29	0.61		62.05	0.38
	70	223.68	20.73	208.11	1393.88	80.27	0.59		76.20	0.41
	75	196.60	18.02	164.20	1186.87	90.90	0.56		88.55	0.43
	80	164.38	17.42	128.15	983.48	100.12	0.52		99.06	0.44
	85	145.03	15.89	104.06	851.80	108.06	0.49		107.81	0.45
	90	130.32	14.39	87.47	753.79	114.87	0.45		114.87	0.45
Cycle A MR with heating/ cooling	50	991.24	44.74	420.12	3001.70	20.50	0.48	768	13.58	0.16
	55	764.29	36.44	275.61	2225.58	37.75	0.57		31.89	0.29
	60	628.89	31.43	212.24	1807.98	53.64	0.60		49.01	0.36
	65	510.45	26.89	155.88	1440.21	68.13	0.59		64.65	0.41
	70	435.93	22.86	129.60	1222.50	80.93	0.57		78.57	0.44
	75	386.51	21.16	110.30	1078.26	92.20	0.55		90.88	0.45
	80	328.88	18.84	90.40	913.90	102.07	0.51		101.41	0.46

	85	297.22	17.66	81.82	828.69	110.67	0.49		110.51	0.47
	90	276.86	16.62	73.75	767.69	118.06	0.46		118.06	0.46

Note: HST-Heat Source Temperature, Ad/Ds- Adsorption/Desorption time, Pc/Ph- Pre-heating/Pre-cooling time, MR-Mass Recovery time and TCT- total cycle time.

Sensitivity of each process time on the performance was investigated for heat source temperature of 80 °C. The search for SCP was performed with the range from 10 s to 600 s for adsorption/desorption time and from 5 s to 400 s for the pre-cooling/pre-heating and mass recovery time. The steps for searching adsorption/desorption time was 10 s and for pre-cooling/pre-heating and mass recovery time were 5 s. Contour plot of SCP is shown in Figs. 4.6 - 4.7 for cycle A and in Figs. 4.8 - 4.9 for cycle B. It is clear that with the increasing of adsorption/desorption time initially SCP was increased after that again decreased with adsorption/desorption time for both cycles. Similar, effect was also observed for mass recovery time. The SCP is not too sensitive on mass recovery time compare to adsorption/desorption time for cycle A because the mass recovery time between 85-175 s along with the adsorption/ desorption time of 160 s gives high SCP over 100 W.kg⁻¹ (Fig. 4.6). On the other hand both adsorption/desorption time and mass recovery time equally affected the SCP of cycle B (Fig. 4.8). Both cycles was indicated shorter pre-heating/pre-cooling time and SCP was decreased with pre-heating/pre-cooling time. The contour plot of SCP was provided a singular pattern with cycle time. The centre of the contour was indicated the maximum SCP and optimal cycle time, which is similar with PSO result.

Optimal performance of both cycles was obtained using particle swarm optimization, which is shown in Figs. 4.10 and 4.11. It is apparent that both cycles are fully applicable for low heat source temperature as low as 50 °C. The optimal SCP was increased with heat source temperature and both cycles were provided similar optimal specific cooling power. On the other hand, optimal COP at first was increased sharply up to 60 °C after that it was decreased with heat source temperature. It is a generally observed behavior that COP of adsorption cycle increased with longer cycle time. That is considered the reason why COPs increase as the heat source temperature decreases. When the temperature is as low as 50 °C, the cycles can not work well due to low driving power, which may be attributable to the decreasing behavior of COP at 50 °C. The maximum optimal COP was observed around 60 °C temperature for both cycles. Similarly, considering the same standard working condition

and input parameters the optimal performance of conventional two-bed adsorption system was calculated using PSO. The optimal performance of conventional system is also shown in Figs. 4.10 and 4.11. It is obvious that optimal SCP of both cycle A and cycle B is higher than conventional system over the whole range of temperature. The optimal COP also higher at lower end temperature compare to conventional system but conventional system achieved a little higher COP value at higher temperature.

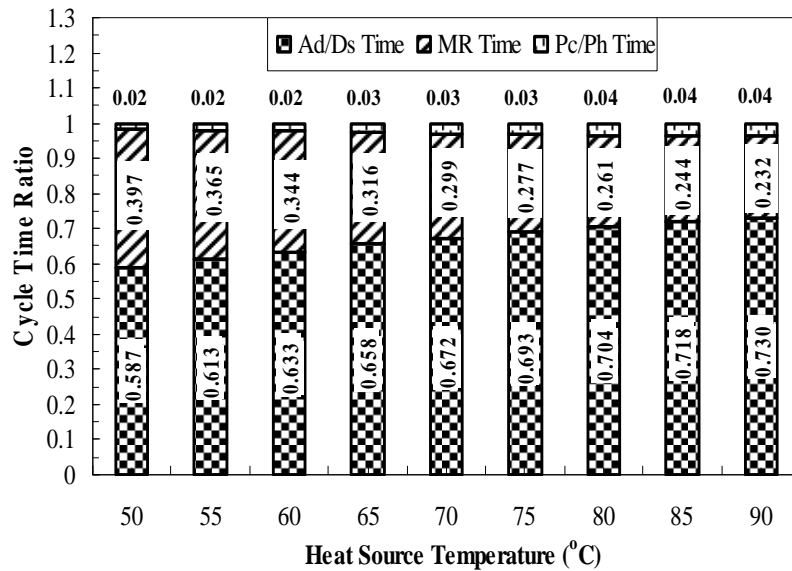


Fig. 4.3: Optimal cycle time ratio of cycle A for different heat source temperature.

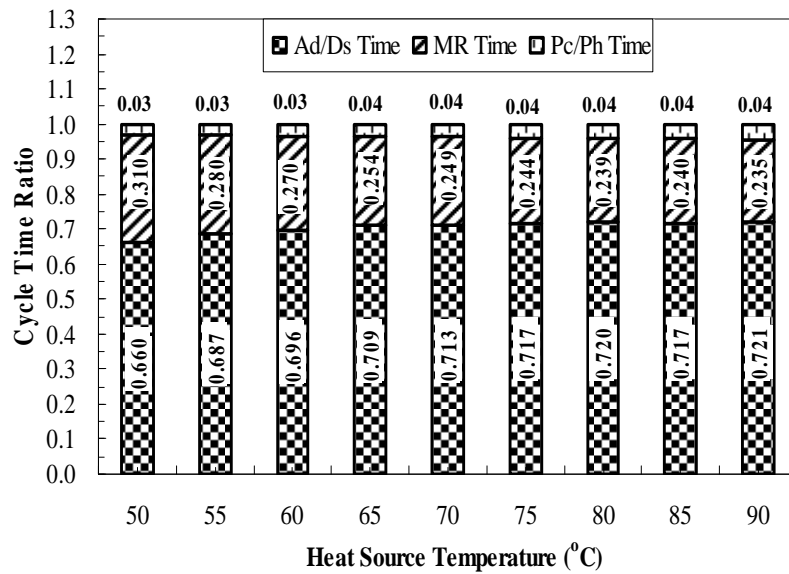


Fig. 4.4: Optimal cycle time ratio of cycle B for different heat source temperature.

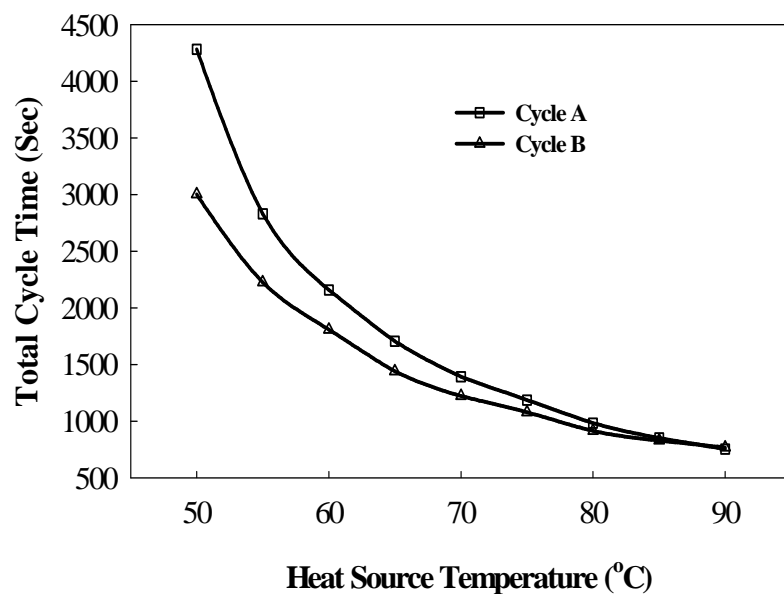


Fig. 4.5: Variation of optimal total cycle time of cycle A and cycle B with heat source temperature.

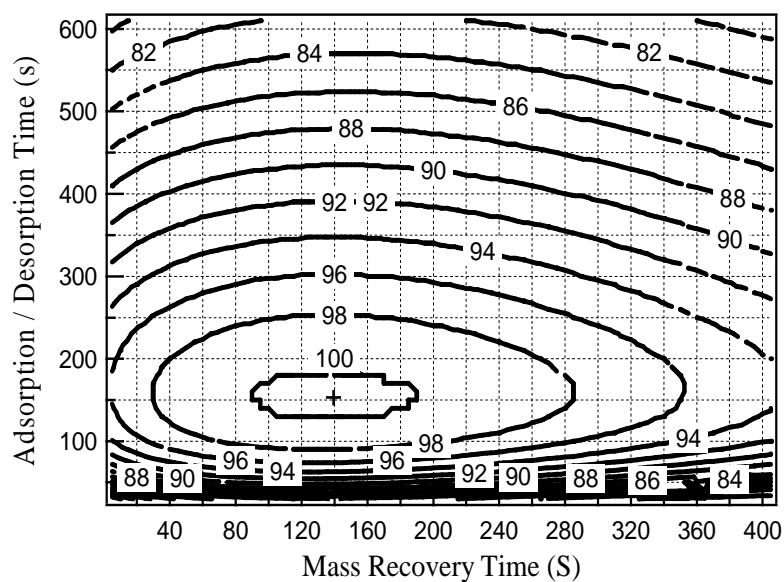


Fig. 4.6: Contour plot of SCP relating to adsorption/desorption time and mass recovery time for cycle A.

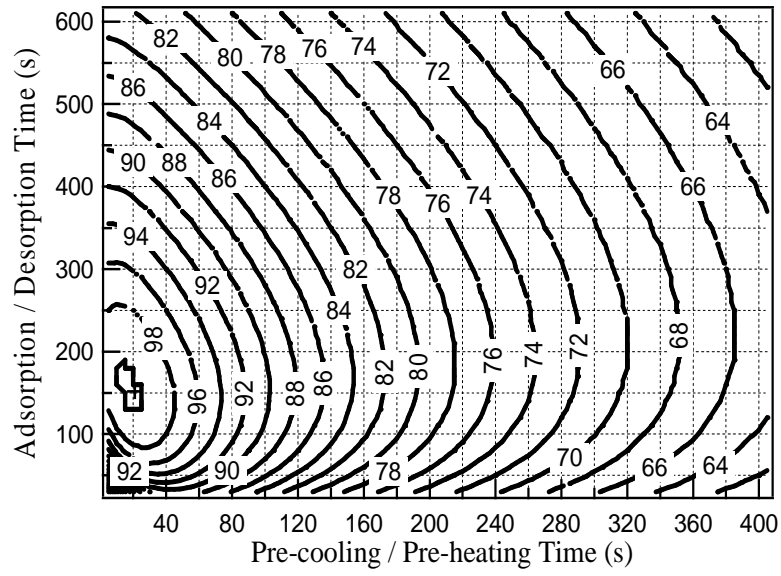


Fig. 4.7: Contour plot of SCP relating to adsorption/desorption time and pre-cooling/pre-heating time for cycle A.

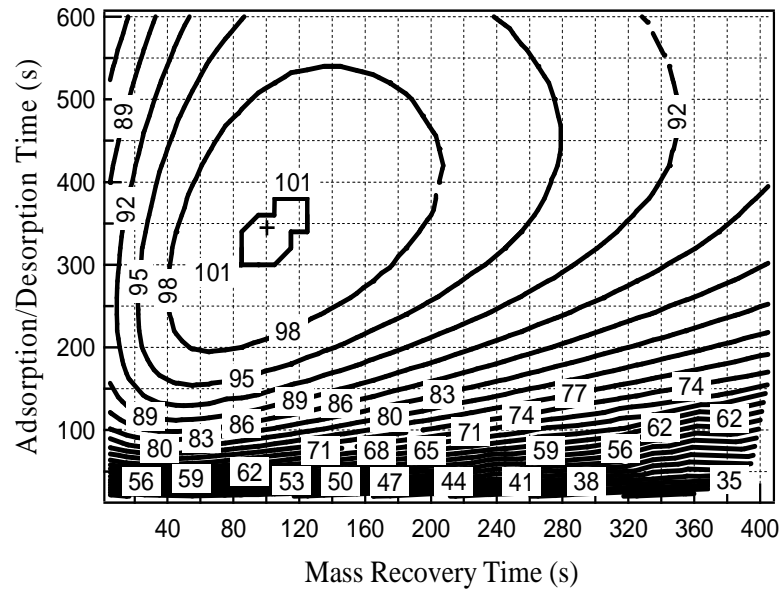


Fig. 4.8: Contour plot of SCP relating to adsorption/desorption time and mass recovery time for cycle B.

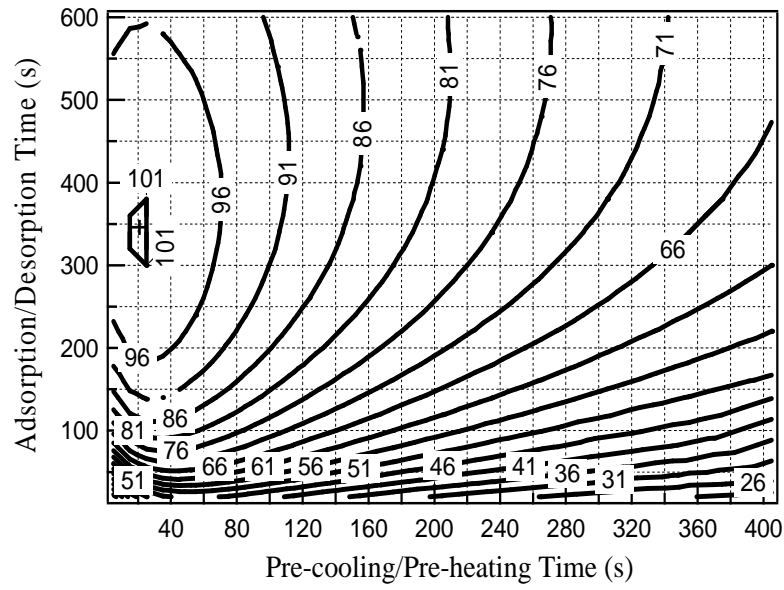


Fig. 4.9: Contour plot of SCP relating to adsorption/desorption time and pre-cooling/pre-heating time for cycle B.

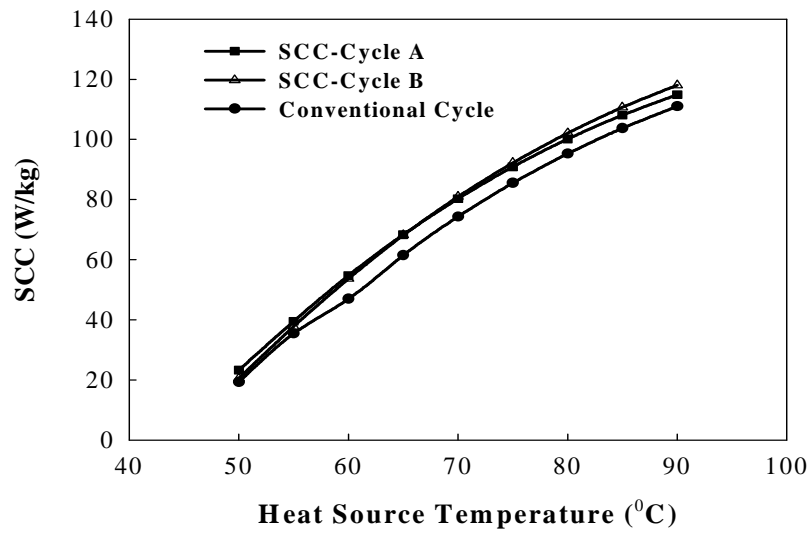


Fig. 4.10: Comparison of optimal SCP of cycle A, cycle B and conventional two bed system.

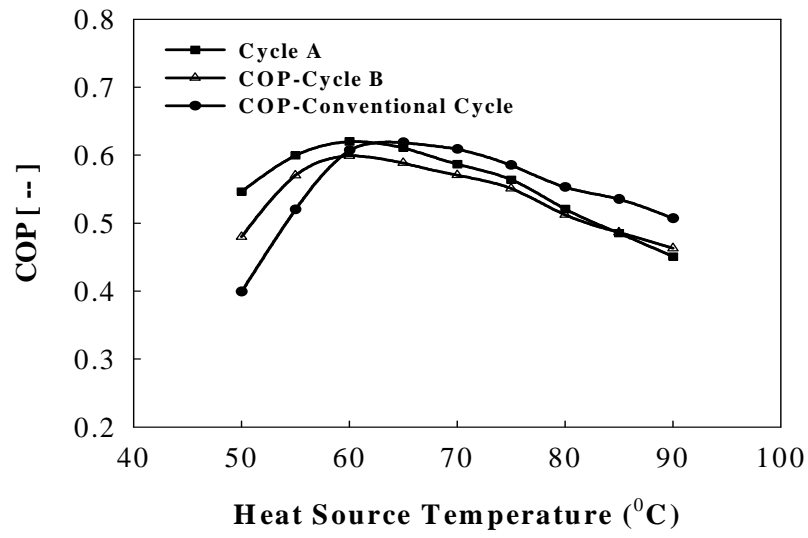


Fig. 4.11: Comparison of optimal COP of cycle A, cycle B and conventional two bed system.

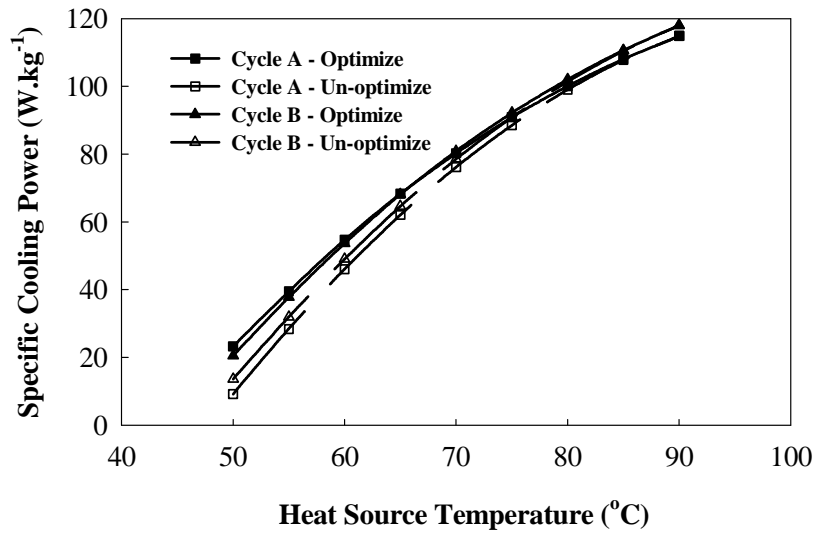


Fig. 4.12: Comparison of optimize and un-optimize SCP of cycle A and cycle B.

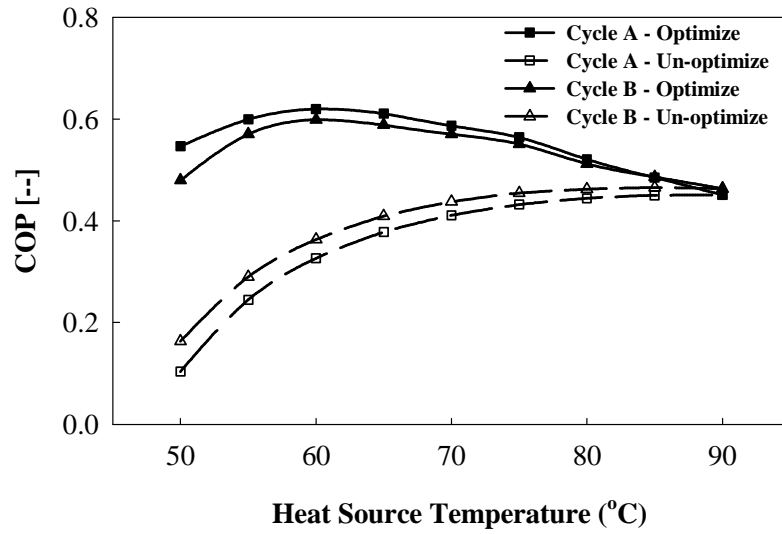


Fig. 4.13: Comparison of optimize and un-optimize COP of cycle A and cycle B.

Optimal cycle time as well as performance of a system is specific for each heat source temperature. It's means optimal cycle time for one heat source temperature is the un-optimize cycle time for other heat source temperatures. In order to understand the role of optimal cycle time settings, the authors conducted the simulations with the optimal time settings adjusted to heat source temperature and a given constant time setting. Based on optimal cycle time of 90 °C temperature the un-optimize SCP and COP was calculated for other heat source temperature, which is given in Table 4.5 and graphically shown in Figs. 4.12 and 4.13, respectively. From Fig. 4.12 it is obvious that optimal SCP of 50 °C heat source temperature is about 61 % and 34 % higher compare to un-optimize SCP for cycle A and cycle B, respectively. On the other hand optimal COP at the same temperature is about 82 % and 67 % higher compare to un-optimized COP for cycle A and cycle B, respectively (Fig. 4.13). Thus, it is illustrated from the results that specific cooling power with un-optimized cycle time setting is slightly smaller than the optimized cases while COP with un-optimized setting becomes significantly lower than that of the optimized cases. It suggests that optimal time setting is required to utilize heat source as much as possible at any temperature.

4.5 Conclusion

A simulation program has been developed for two different types of three-bed mass recovery with heating/cooling adsorption cooling systems. The particle swarm optimization

method was applied to optimize the cycle time as well as the performance of the analyzed adsorption systems. Based on PSO, the total optimal cycle time has been established for both cycle A and cycle B corresponding to the maximum values of SCP. The main conclusions are:

- i) Both three-bed mass recovery cycles have relatively higher COP at low heat source temperature of 50 °C than conventional single-stage adsorption cooling cycle. It indicates both cycle A and Cycle B are effective to recover low grade heat to produce cooling
- ii) Cycle A and cycle B have almost the same performance in terms of SCP. Both three-bed mass recovery cycles have better SCP than that of the conventional cycle over the whole range of heat source temperature.
- iii) COPs of cycle A and cycle B are almost the same except for low heat source temperature of 50 °C where COP of is slightly better than that of cycle B.
- iv) The proposed PSO based comparison method is useful to identify the best performance of adsorption cooling cycles with different configuration. It was found from the results of optimized cycle time that time allocation of cycle B is relatively insensitive compared with that of cycle A, which implies cycle B is considered to be robust against the variation of heat source temperature.

Chapter 5

Innovative Design and Performance of Three-bed Two-Stage Adsorption Cycle under Optimized Cycle Time

5.1 Introduction

Utilization of wasted heat or renewable energy is an urgent need to reduce the consumption of fossil fuels as well as environmental impact. One of the key technologies used to utilize relatively low grade heat sources is adsorption heat pump systems. Adsorption heat pumps can produce cooling using heat source temperature as low as 40 °C (Saha et al., 2003b) and this temperature can be easily found in wasted heat or renewable heat sources like solar thermal energy. Nowadays, adsorption heat pump and refrigeration systems have drawn a considerable attention due to their lower environmental impact and large energy-saving potentials. Moreover, these systems neither use ozone layer depleting gases such as CFCs/HCFCs and fossil fuel or electricity as their driving source. In this aspect, a number of researchers have investigated the performance of adsorption heat pump/ refrigeration systems driven by waste heat or renewable energy sources. A few examples of remarkable studies were demonstrated as in the field of solar cooling (Pons et al., 1986, Critoph, 1988, Sakoda et al., 1984, Wang et al., 2009), automobiles cooling system (Suzuki, 1993, Zhang, 1997) and in the field of waste heat utilization (Saha et al., 1995a, Chua et al., 1999).

Similarly, in the case of advanced adsorption systems utilizing heat and mass recovery cycles, there have been several attempts to improve the cooling performance and to utilize the low-temperature heat (Szarzynski, 1997, Akahira et al., (2004, 2005)), multi-stage cycles (Saha et al., 1995b, Alam et al., 2002) and multi-bed cycles (Chua et al., 2001, Saha et al., (2003a, 2006)). It has been shown that those advanced cycles would achieve better performances compared with that of the conventional adsorption system.

In order to utilize solar/waste heat with temperature below 70 °C, Saha et al. (2001) proposed a prototype design of a four-bed two-stage adsorption cycle. Subsequently, an extensive study was conducted (Alam et al., 2004, Hamamoto et al., 2005) to identify the influence of design and operating conditions on system performance. Moreover, the modification in design and operation procedure with re-heat scheme was done (Khan et al., (2005, 2006b, 2007c), Alam et al., 2007, Farid et al., 2011). Therefore, it was concluded that a two-stage adsorption cycle is well known and effective to utilize low grade heat sources.

In the above mentioned studies on two-stage cycle, two pairs of adsorption/desorption heat exchanger beds were used in the higher temperature and pressure cycle (i.e., upper cycle) and lower temperature and pressure cycle (i.e., lower cycle). However, the larger size of this adsorption cycle needs further modifications to make it more attractive to the users. In this study, the authors have focused on the reduction of the size of the four-bed two-stage adsorption cycle through reduce of a heat exchanger bed. Accordingly, a design was proposed via replacing the upper cycle two heat exchanger beds with one bed, whereas the lower cycle two beds were kept similar to the previous cycle. It can be said that the proposed cycle is the three-bed two-stage cycle, which is newly approached design with operational strategy. Previously investigated three-bed adsorption cycles (Saha et al., 2003a, Khan et al., 2007a, Uyun et al., 2009a) were single-stage and effective as low as 60 °C heat source temperature. On the other hand the proposed cycle is two-stage cycle, which will be applicable to utilize around 50 °C heat source temperature.

The objectives of this study are to investigate the performance of the proposed cycle and to clarify its advantage in comparison with the conventional four-bed two-stage cycle. It should be noted that cycle performance strongly depends on heat source temperature and cycle time that needs to be adjusted to maximize the performance in accordance with the temperature. Miyazaki et al., 2009 first attempted to optimize cycle time of two-bed single-stage adsorption cycle using a method called particle swarm optimization (PSO). The same method was adopted in this study to obtain the maximum cooling output. Finally, the results obtained from the proposed cycle were compared with the four-bed two-stage cycle in order to understand the influence of heat source temperature on specific cooling power (SCP) and coefficient of performance (COP).

5.2 Description of Three-bed Two-stage Adsorption Cycle

The three-bed two-stage adsorption cycle consists of three adsorber/desorber heat exchangers named Bed 1, Bed 2 and Bed 3, one evaporator and one condenser. The schematic diagram of the cycle is shown in Fig. 5.1. Silica-gel and water have been chosen as adsorbent-refrigerant pair because the regenerative temperature of silica gel is lower than that of other adsorbents and water has large latent heat of vaporization. The advantage of the two-stage cycle is to utilize the lower grade heat sources than single-stage adsorption cycle. For example, a temperature of 60 °C is enough to drive the two-stage cycle. However, such low temperature is not enough to pressurize the vapour from the evaporator up to the condenser pressure. The vapour needs to be pressurized twice in the cycle of two-stage

adsorption-desorption processes. The first stage pulls up the vapour from the evaporator pressure to the intermediate pressure and then the second stage pushes up the vapour from the intermediate pressure to the condenser pressure.

The proposed cycle is working in two-stages; Bed 1 and Bed 2 are working in low temperature and pressure (close to the evaporator temperature, T^e) while Bed 3 is working at higher temperature and pressure (close to the condenser temperature, T^c). The conceptual Dühring diagram is shown in Fig. 5.2. The cyclic diagrams a-b-c-d-a and e-f-g-h-e indicate the lower and upper cycle, respectively. All beds are completing four thermodynamic stages, i.e., pre-heating, desorption, pre-cooling and adsorption stage, which are accordingly followed by the sides a-b, b-c, c-d and d-a, and e-f, f-g, g-h and h-e for the lower and upper cycle, respectively.

To complete full cycle operation, each bed is to complete 8 modes, named A, B, C, D, E, F, G and H as shown in Table 5.1. In Mode A, Bed 1 and Bed 2 are in cooling state when cooling water is passed through both beds and are connected with evaporator to adsorb refrigerant vapour from evaporator. This process is called adsorption mode. At the same time evaporator's lower temperature and pressure is maintained so that water could easily vaporize by seizing heat from chilled water. Bed 2 remains in adsorption stage up to end of mode E. On the other hand Bed 3 is in heating state when hot water is passing through it and is connected with condenser to release its own refrigerant vapour and this process is called desorption mode. In desorption mode, adsorbed refrigerant is removed from adsorbent bed and goes to the condenser. Then refrigerant vapour is condensed inside condenser and condensation heat is removed by cooling water. Finally, condensed refrigerant goes to the evaporator via a U shape tube.

In mode B, Bed 1 is disconnected from the evaporator and Bed 3 from the condenser. Then Bed 1 is heated by hot water to increase its pressure, which is called pre-heating mode, and Bed 3 is cooled down by cooling water to reduce its pressure, which is called pre-cooling mode. When the pressure in both beds become nearly equal

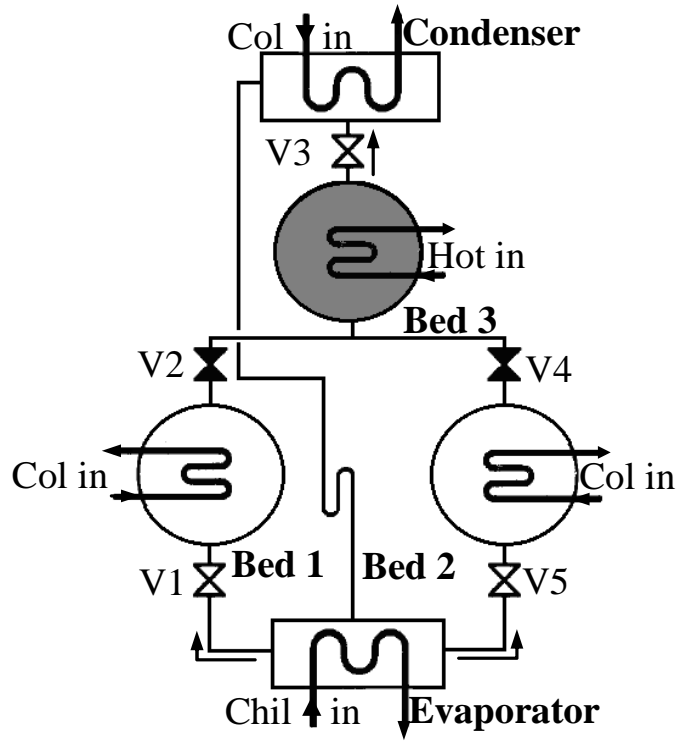


Fig. 5.1: Schematic of proposed three-bed two-stage adsorption cycle.

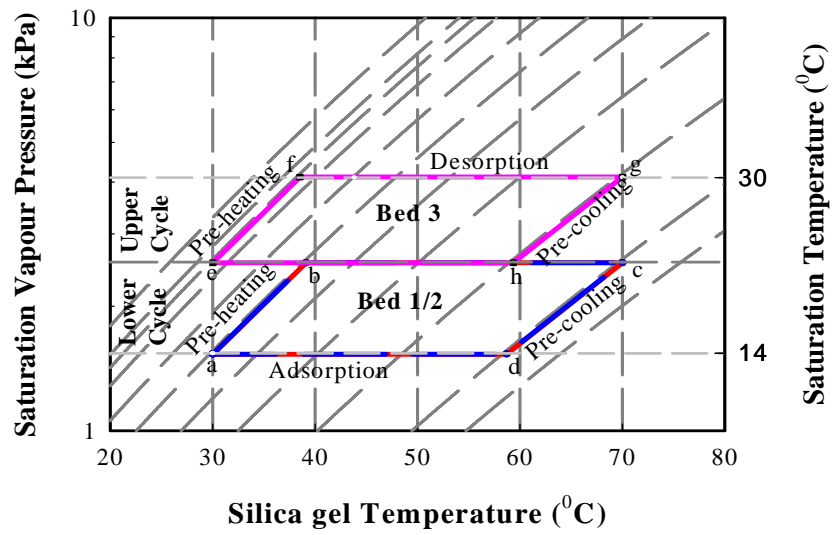


Fig. 5.2: Conceptual Dühring diagram of proposed three-bed two-stage adsorption cycle.

then both are connected with each other by opening the connecting valve (i.e., 'V2'), which is starting point for mode C. In this mode, Bed 1 is heated by hot water and Bed 3 is cooled by cooling water, which is called desorption mode for Bed 1 and adsorption mode for Bed 3. Bed 1 is desorbing its adsorbed vapour to the Bed 3 and Bed 3 is adsorbing vapour from Bed 1 during this mode. Mode D is called pre-cooling and pre-heating mode of Bed 1 and Bed 3, respectively, while both beds are isolated from other parts of the system. In this case Bed 1 is cooled by cooling water to reduce its pressure to the evaporator pressure and then it is connected with evaporator by opening the connecting valve ('V1'), which is called adsorption process and starting point for mode E. This will continue to the end of mode H. Meanwhile, Bed 3 is heated by hot water to increase its pressure up to condenser pressure and then connected with the condenser via valve, 'V3'. Through these modes the first half cycle (from mode A to D) of Bed 3 is completed and the second half cycle (from mode E to H) is started. The mechanism of modes E, F, G and H of Bed 3 is similar to the modes A, B, C and D, but during these modes, Bed 3 is connected with Bed 2 instead of Bed 1 (i.e., mode G) and vapour is transferred among Bed 2 and Bed 3.

The proposed cycle was modified from the four-bed two-stage cycle, which was proposed by Saha et al., 2001. The schematic diagram of former cycle is shown in Fig. 5.3 and its operation modes are given in Table 5.1. In previous case, two adsorption/desorption heat exchanger beds (i.e., Bed 1 and Bed 2) were used in lower cycle and other two beds (i.e., Bed 3 and Bed 4) were used in upper cycle. Upper cycle one bed is connected with lower cycle one bed, but in present case the upper two beds, Bed 3 and Bed 4 were replaced by one bed (i.e., Bed 3 of Fig. 5.1) to minimize the size of the cycle. To make the adsorption cycle competitive in the market, it is necessary to consider economical issues as well as the total size of system. In proposed case upper cycle only one bed can work instead of two beds in the previous cycle, which reduced one heat exchanger bed from the system. In first half cycle of proposed system, Bed 3 is connected with Bed 1 to transfer vapour and in second half cycle it is connected with Bed 2 for the same purpose. As a result Bed 3 is completing two full cycles, while Bed 1 and Bed 2 are completing only one full cycle operation at the same time. In Table 1 it is clear that in mode A and C beds are fully disconnected from evaporator for former cycle, but in the proposed case either Bed 1 or Bed 2 are always connected to the evaporator and produces continuous cooling supply. Consequently it can be expected that the proposed cycle keeps constant chilled water outlet temperature with less fluctuation.

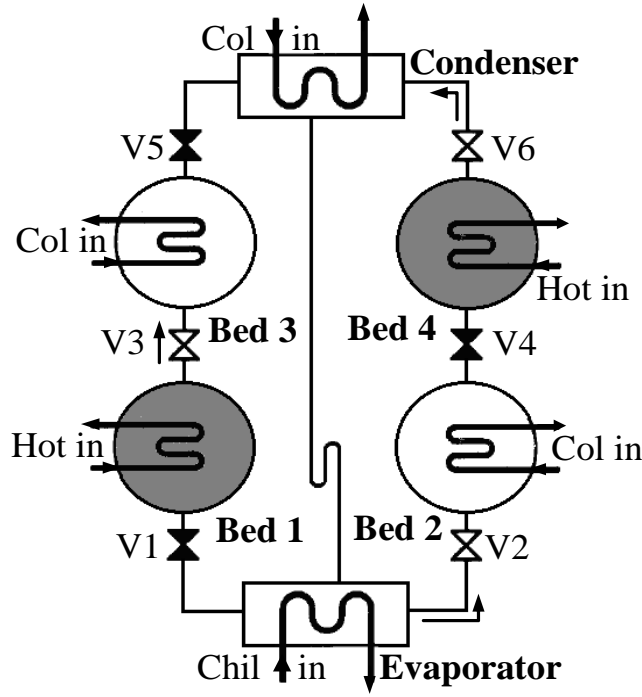


Fig. 5.3: Schematic of former four-bed two-stage cycle.

Table 5.1: Operation mode of proposed cycle and former two-stage cycle with optimal cycle time in second at 55 °C heat source temperature.

(a) Proposed three-bed two-stage cycle

Mode	A	B	C	D	E	F	G	H
	τ_1	τ_2	τ_1	τ_2	τ_1	τ_2	τ_1	τ_2
Bed 1	134.5	12.27	134.5	12.27	293.54			
Bed 2	428.04					12.27	134.5	12.27
Bed 3	134.5	12.27	134.5	12.27	134.5	12.27	134.5	12.27

(b) Former four-bed two-stage cycle

Mode	A	B	C	D
Bed 1	34.75	414.67	34.75	414.67
Bed 2	34.75	414.67	34.75	414.67
Bed 3	34.75	414.67	34.75	414.67
Bed 4	34.75	414.67	34.75	414.67

Desorption
 Pre-heating
 Adsorption
 Pre-cooling

5.3 Simulation Methods and Materials

Simulation methods and materials of three-bed two-stage adsorption system are details described in chapter 3 of section 3.4. Heading of the sub-sections from 3.4.1 to 3.4.6 are given below:

- ❖ Adsorption and Desorption Energy Balance
- ❖ Condenser energy balance
- ❖ Evaporator energy balance:
- ❖ Adsorption and desorption rate
- ❖ Mass balance:
- ❖ System performance

Optimization procedure

A complete simulation program was developed based on Matlab software to solve all equations mentioned in section 3.4. Adsorption/desorption rate equation, energy balance equation of beds, condenser and evaporator, and mass balance equation have been solved simultaneously using MATLAB ode45 solver. All input parameters such as adsorbent-refrigerant properties, flow rates of heat transfer fluids and heat exchangers specifications were initially given for which the system cyclic operation can be continued.

In this study, PSO was applied to optimize the cycle time based on maximum value of SCP, whereas SCP was chosen as the objective function and cycle time (i.e., τ_1 and τ_2) was chosen as the variable. In PSO, a particle holds the values of variables and updates the values toward the optimal solution. After a number of iterations, all the particles hold the same value and the objective function value is maximized. In this case, the number of particles and the number of iterations were considered as 24 and 1500, respectively. It was observed that all particles reached their best position around 500 iterations.

5.4 Results and Discussions

The simulation program developed for three-bed two-stage adsorption cycle was operated by adopting the basic input parameters and standard working conditions as presented in Table 5.2 (Moriyama, (2007)). The cycle time means operation time of each mode (i.e., τ_1 and τ_2) and it is one of the most important parameters of the system and influences the overall performance. The specific cooling power (SCP) represents the cooling capacity per unit quantity of adsorbent, and therefore it is a useful index for minimizing the

size of the system. At first, the cycle time was optimized based on the maximum value of SCP using PSO procedure. Cycle time of the system was optimized for different heat source temperatures varying from 45 to 90 °C by keeping average outlet temperature of the chilled water at 9 °C. Accordingly, the chilled water flow rate was optimized simultaneously with cycle time. Fig. 5.4 shows that optimum cycle time decreases with the increase in heat source temperature. Total optimal cycle time is the sum of the cycle time of all modes (Table 5.1). The cycle time ratio is defined as the ratio of each mode operation time to the total cycle time. Fig. 5.5 represents the optimal cycle time ratio of the system for different heat source temperatures. It was observed that cycle time ratio for τ_1 and τ_2 were constant at all heat source temperatures, which is an advantage of the proposed cycle. One setting can covers for all temperature range. Only total cycle time length needs to be controlled in operating system. The variation of chilled water flow rate with heat source temperature is shown in Fig. 5.6. It was observed that average chilled water flow rate increases with the increase in driving heat source temperature.

Table 5.2: Basic input parameters and standard working conditions

(a) Basic input parameters		
Parameters	Value	Units
Q_{st}	2.80×10^6	J kg^{-1}
E_a	4.2×10^4	J mol^{-1}
D_{so}	2.54×10^{-4}	$\text{m}^2 \text{s}^{-1}$
R	8.314	$\text{J mol}^{-1} \text{K}^{-1}$
R_p	0.30×10^{-3}	m
C_w	4.18×10^3	$\text{J kg}^{-1} \text{K}^{-1}$
C_{wv}	1.89×10^3	$\text{J kg}^{-1} \text{K}^{-1}$
L_w	2.50×10^6	J kg^{-1}
C_{Cu}	386.00	$\text{J kg}^{-1} \text{K}^{-1}$
C_{Al}	905.00	$\text{J kg}^{-1} \text{K}^{-1}$
C_s	924.00	$\text{J kg}^{-1} \text{K}^{-1}$
A_{hex}^b	0.61×16	m^2
A_{hex}^e	3.00	m^2
A_{hex}^c	1.00	m^2

U_{hex}^c	3900.00	$\text{W m}^{-2} \text{K}^{-1}$
U_{hex}^b (desorption)	750.00	$\text{W m}^{-2} \text{K}^{-1}$
U_{hex}^b (adsorption)	1000.00	$\text{W m}^{-2} \text{K}^{-1}$
U_{hex}^e	5800.00	$\text{W m}^{-2} \text{K}^{-1}$
W_s^b	16.00	kg
W_{hex}^b (Cu)	12.67	kg
W_{hex}^b (Al)	16.87	kg
W_{hex}^e	9.6	kg
W_w^e	61.32	kg
W_w^c	24.98	kg
W_{hex}^c	12.8	kg
(b) Standard working condition		
T_{in}^{hot}	45 - 90	$^{\circ}\text{C}$
\dot{m}_w^{hot}	1.0	kg s^{-1}
T_{in}^{col}	30	$^{\circ}\text{C}$
\dot{m}_w^{col}	1.0	kg s^{-1}
$T_{in}^{c,col}$	30	$^{\circ}\text{C}$
$\dot{m}_w^{c,col}$	0.8	kg s^{-1}
T_{in}^{chil}	14	$^{\circ}\text{C}$
T_{out}^{chil}	9	kg s^{-1}

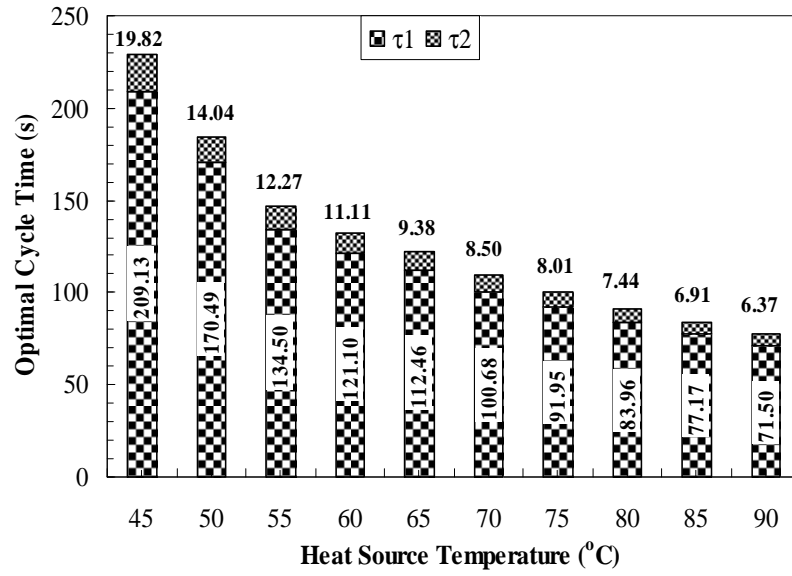


Fig. 5.4: Optimal cycle time of the cycle for different heat source temperatures.

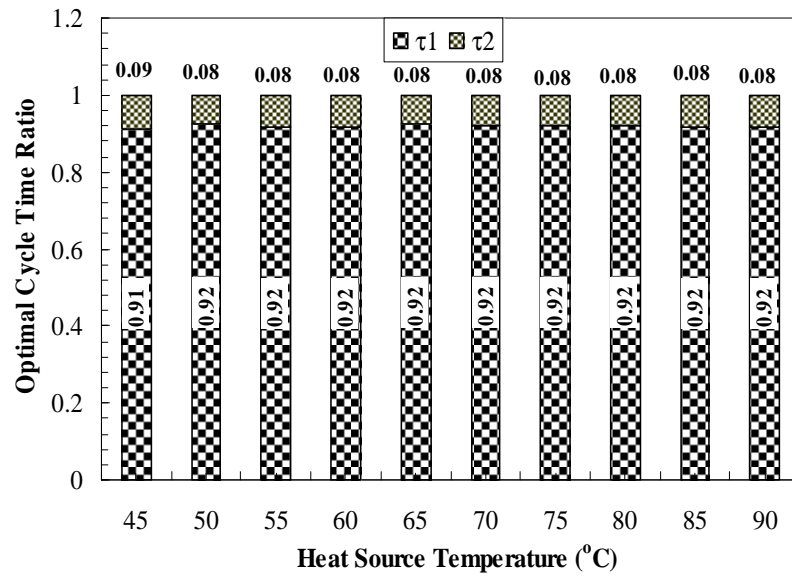


Fig. 5.5: Optimal cycle time ratio of the cycle for different heat source temperatures.

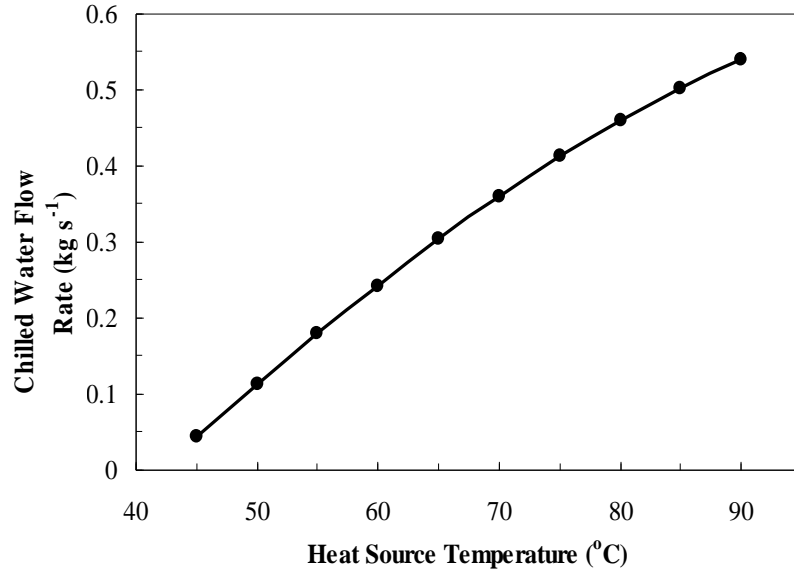


Fig. 5.6: Variation of chilled water flow rate with heat source temperature.

The variation of water contents in adsorption/desorption bed with cycle time at 55 °C heat source temperature is shown in Fig. 5.7. It is obvious from this figure that water contents were increased during adsorption time (i.e., mode D-H-A for Bed 1, mode A-E for Bed 2 and mode C with G for Bed 3) and was decreased during desorption time (i.e., mode C for Bed 1, mode G for Bed 2 and mode A with E for Bed 3). During pre-cooling and pre-heating time beds are fully disconnected from other parts of the system, therefore water contents are remained constant in this mode (i.e., mode B, D, F and H).

Temperature profile for all adsorbent beds, condenser and evaporator are shown in Fig. 5.8. It was observed that during adsorption stage, the beds temperatures were remained constant, since the beds are cooled by cooling water, but during desorption time beds temperatures were increased due to heating by hot water. Similarly, during pre-heating and pre-cooling stages beds temperatures were sharply increased and decreased, respectively. Condenser temperature was increased only during desorption time due to vapour transfer from Bed 3 to condenser. On the other hand evaporator temperature was nearly constant because of continuous cooling load.

Sensitivity of cycle time on SCP and chilled water outlet temperature was investigated for heat source temperature of 55 °C. These were calculated by varying the cycle time τ_1 from 20 to 500 s and cycle time τ_2 from 5 to 100 s. The increment steps for τ_1 was 5 s while for τ_2 was 2.5 s. Chilled water flow rate was kept constant 0.18 kg s⁻¹, which was observed using PSO for 55 °C

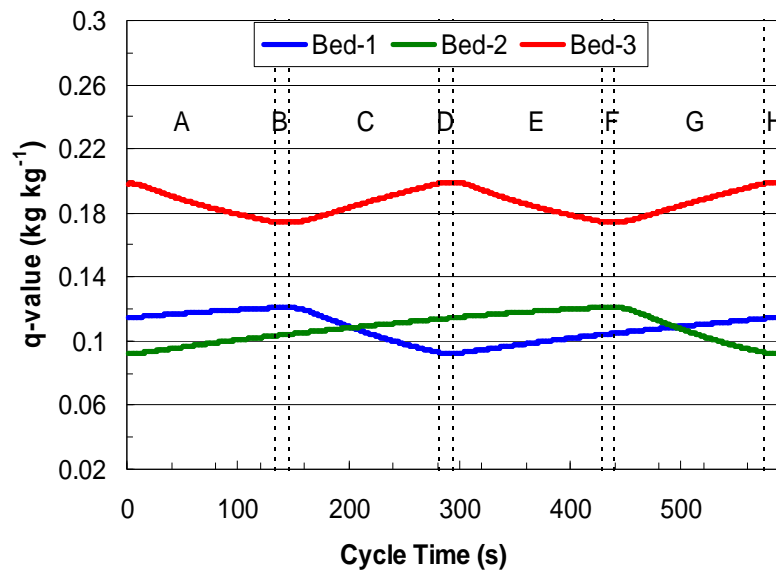


Fig. 5.7: Variation of water content in adsorption/desorption bed with cycle time at 55 °C heat source temperature.

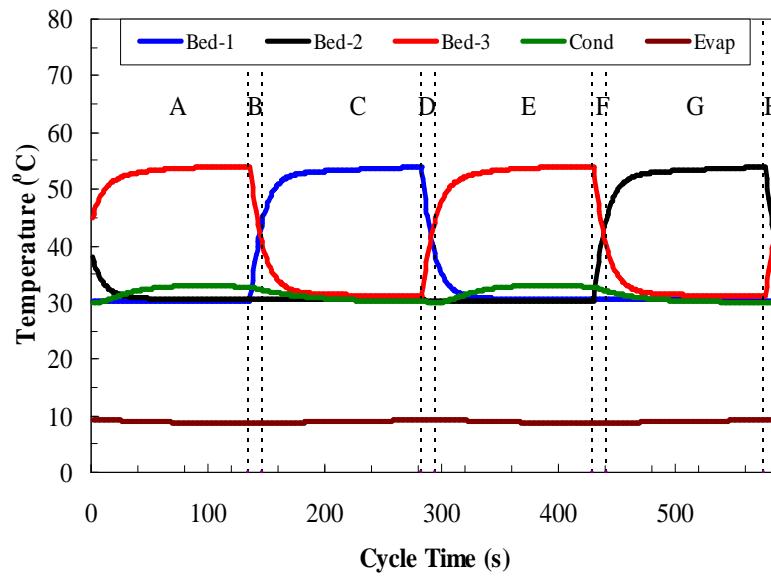


Fig. 5.8: Temperature profile of beds, condenser and evaporator at 55 °C heat source temperature.

temperature. Contour plot of SCP and averaged chilled water outlet temperature are shown in Figs. 5.9 and 5.10, respectively. It was clear that by increasing of τ_1 , the SCP increased to approximately 135 s when τ_2 is 12.5 s and after 135 s it was again decreased (Fig. 5.9). Whereas in the case of average chilled outlet temperature it was opposite (Fig. 5.10). Similarly, after 12.5 s to τ_2 value SCP was decreased and chilled water flow rate was increased along the line of 135 s of τ_1 . The contour plot of both parameters provided a singular pattern with cycle time. The centre of the contour was indicated the maximum SCP and minimum chilled water outlet temperature, which is exactly matching with PSO result.

The optimal performance of the cycle is shown in Fig. 5.11. It is apparent from the simulation that the cycle can operate at low temperature heat source as low as 45 °C with a coolant at 30 °C. The SCP increased with the increase of heat source temperature whereas COP increased sharply with heat source temperature up to 65 °C and then it decreased slightly with heat source temperature. An increase of heat source temperature with a fixed heat sink causes the system to increase the amount of refrigerant adsorption/desorption, resulting in higher SCP at higher heat source temperature. Due to similar effect, the total optimal cycle time was found to be decreased with heat source temperature as shown in Fig. 5.12. At lower temperature (<65 °C) the cycle time increased but the COP decreased. If the cycle time was not optimized, the performance at relatively low temperature must have been lower than the optimized result. It implies that the optimization of cycle time is necessary to utilize low temperature heat sources adaptively. The maximum COP was observed to be 0.34 at 65 °C heat source temperature.

The optimal performance of the proposed cycle was compared with optimal performance of the former four-bed two-stage cycle (Moriyama,(2007)) as shown in Fig. 5.11. It can be seen from Fig. 5.11 that the COP of proposed cycle is almost similar at higher heat source temperature and little bit lower for lower heat source temperature. On the other hand, SCP increased significantly over the whole range of studied heat source temperature. According to Fig. 5.12, it should be noted that the proposed cycle provides lower total optimal cycle time as compared to that of the four-bed two-stage system.

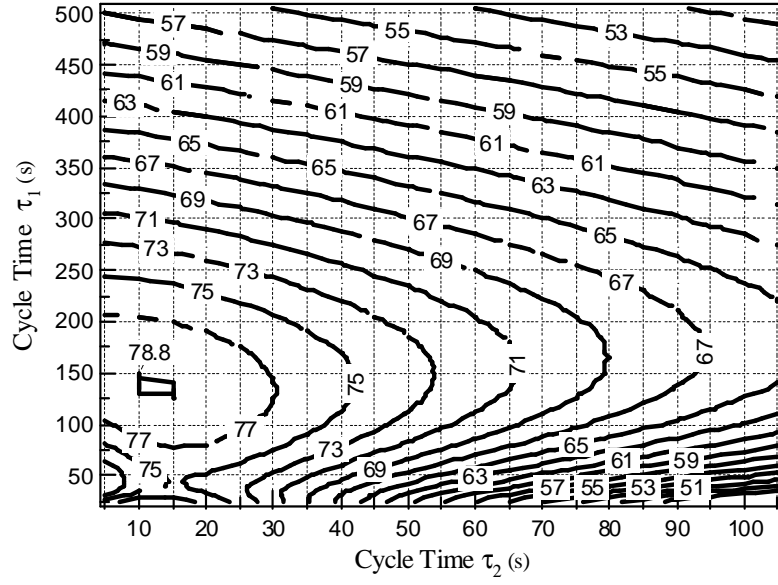


Fig. 5.9: Contour plot of SCP relating to cycle time τ_1 and τ_2 at 55 °C heat source temperature.

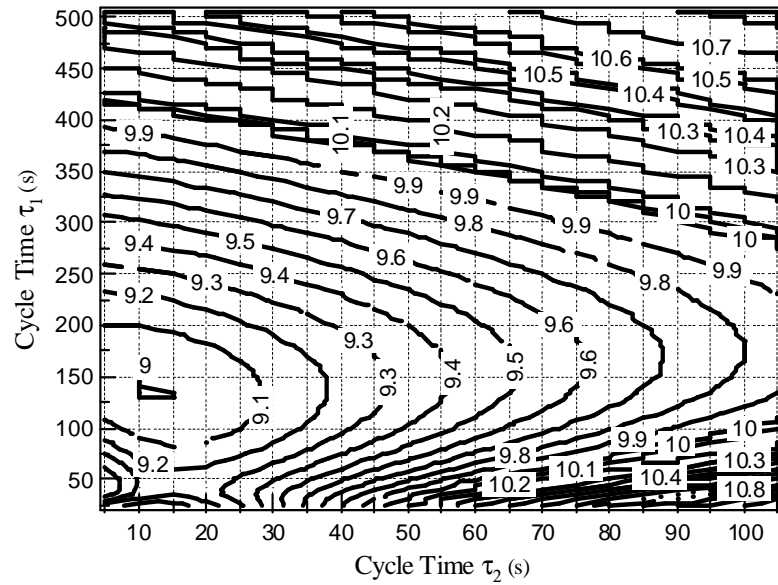


Fig. 5.10: Contour plot of average chilled water outlet temperature relating to cycle time τ_1 and τ_2 at 55 °C heat source temperature.

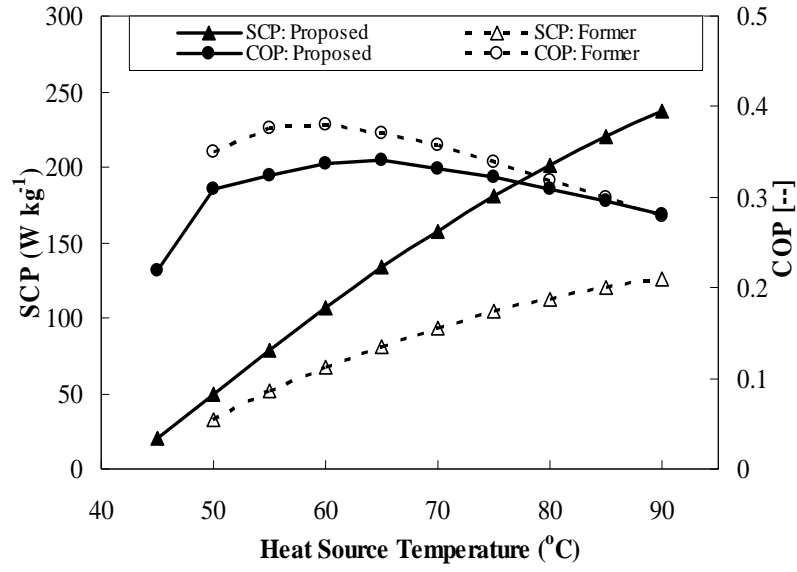


Fig. 5.11: Comparison of optimal SCP and COP of proposed cycle with the former four-bed two-stage cycle.

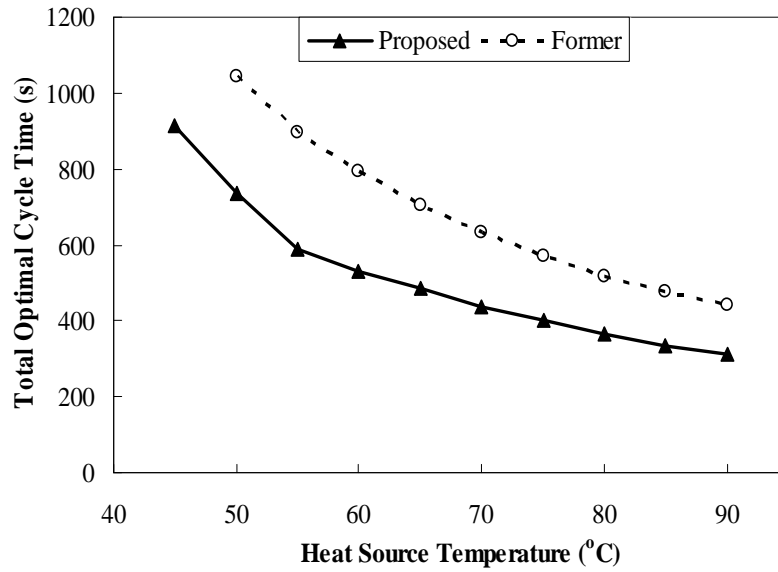


Fig. 5.12: Comparison of optimal cycle time of proposed cycle with the former four-bed two-stage cycle.

The higher SCP value of the proposed cycle is due to two kinds of effect. One is reduced mass of adsorbent (silica-gel) of the system and the other is shorter total cycle time.

Because the denominator values of SCP as described in Eq. 3.24 is lower as silica-gel mass of the three beds is smaller (i.e., 48 kg) than the mass of four beds (i.e., 64 kg). Heat release as described by the numerator is almost the same for both systems because both cycles have two beds in lower cycle and producing similar cooling effect to the evaporator. It is expected mathematically that the SCP of three bed system is larger than that of four bed system by the factor of 4/3. However, Fig. 5.11 shows the SCP of the proposed cycle presents much larger than the factor, even twice at the temperature of 90 °C. It is because the cycle time of the proposed cycle is shorter than that of the former four-bed two-stage cycle.

Although the total cycle time is shorter for the proposed cycle but it provides similar cooling output. The reason for this behavior is that the total adsorption time of the proposed cycle is longer than the former cycle as shown in Table 5.1. It can be seen from Table 5.1 that the adsorption and desorption time is same in all beds for the former cycle. However in the proposed cycle it was observed that adsorption time is more than twice time longer than desorption time as well as sum of desorption time, pre-cooling and pre-heating time. Aristov et al., (2012) was also given similar practical recommendations to manage cooling cycles with non-equal durations of adsorption and desorption time. Moreover, during pre-heating/pre-cooling time, Bed-1 and Bed-2 in the former cycle was fully disconnected from the evaporator, whereas in the proposed case, those beds were connected to the evaporator, thus producing continuous cooling. Therefore, the proposed cycle is capable to increase cooling output for relatively short cycle time.

Comparative study between former four-bed two-stage and proposed three-bed two-stage adsorption system along with improvements due to modification are given below;

	Former Four-bed Two-stage system	Proposed three-bed two-stage system
Number of evaporator	1	1
Number of condenser	1	1
Number of beds	4	3
Total mass of Adsorbent	64 kg	48 kg
Total mass of heat exchanger material in beds	12.67x4 kg (Cu)	12.67x3 kg (Cu)
	16.87x4 kg (Al)	16.87x3 kg (Al)
Improvement due to proposed modified design		
Number of bed(s) reduced		1
Reduction in total mass of silica gel		16

Reduction of heat exchanger material	12.67 kg Cu
	16.87 kg Al
SCP improved for different heat source temperature	35 to 47 %

Thus, it can be concluded that the proposed cycle can significantly reduce the overall size of the two-stage adsorption system along with an increase in the overall performance.

5.5 Conclusion

A new design of a three-bed two-stage adsorption cycle was introduced. The performance of the system was investigated by cycle simulations and the cycle time was optimized using particle swarm optimization method. It was observed that the specific cooling power of the proposed cycle increased with heat source temperature. The maximum coefficient of performance of the system was observed at 65 °C temperature. The optimal cycle time was largely dependent on the corresponding heat source temperature and it decreased with heat source temperature when chilled water outlet temperature was fixed at 9 °C. The cycle is effectively applicable for utilizing low grade heat source temperature as low as 45 °C. It was found that the SCP of the proposed cycle increased significantly over the whole range of heat source temperature compared with former four-bed two-stage cycle while the COP is slightly lower than the former cycle. This implies that the advantage of the proposed cycle is that the volume can be significantly reduced in comparison with the former cycle. Consequently, the proposed cycle is useful from the economical point of view due to its improved performance and smaller size.

Chapter 6

Design and Performance of an Innovative Four-bed, Three-stage Adsorption Cycle

6.1 Introduction

Utilization of waste heat and renewable energy can lead to significant contributions in the reduction of the consumption of fossil fuels. One of the key technologies that allow the utilization of relatively low-grade heat sources, typically below 100°C, are adsorption heat pump systems. It has been established that adsorption heat pumps can produce cooling power utilizing heat source consuming temperature as low as 40 °C along with a coolant at 30 °C if three-stage regenerative scheme is employed (Saha and Kashiwagi 1997a). Low-temperature waste heat is commonly found as part as any process in industry or in renewable heat sources, such as solar thermal energy, even in moderate solar radiation regions around the world. Moreover, in most cases, adsorption systems neither use ozone layer depleting gases such as CFCs/HCFs, nor it uses fossil fuel and electricity as its driving source. Therefore, it is widely considered that adsorption heat pump systems are environment-friendly and have energy-saving potential.

A basic conventional single-stage adsorption system comprises of two adsorbent beds, one condenser and an evaporator. Many researchers study advanced single-stage adsorption systems such as two-bed mass recovery, three-bed, three-bed mass recovery, and two-bed heat recovery adsorption cycle to improve the performance of the single-stage adsorption cooling system. However, the required driving temperature for advanced single-stage adsorption systems is 80 °C or higher.

Saha et al., 2001 proposed a design of a four-bed two-stage adsorption chiller to reduce the temperature of the heat source. They numerically showed that the chiller can utilize solar/waste heat of temperatures below 70 °C. Alam et al., 2004 and Hamamoto et al., 2005 identified the influence of design parameters and operating conditions on the performance of the chiller proposed by Saha et al., 2001. Moreover, the modification of the chiller in terms of operating condition such as re-heat scheme was investigated by Khan et al., (2005b, 2006b, 2007c), Alam et al., 2007 and Farid et al., 2011. These investigations identified that it can work with heat source temperature as low as 45°C (Rahman et al., 2012). Recently,

experimental study on a two-stage adsorption freezing machine driven by low temperature heat source was done by Wang et al., 2012. However, the coefficient of performance (COP) of two-stage adsorption cycle was found to be lower than that of the advanced single-stage chillers.

To increase the performance while keeping the heat source temperature around 45 °C, Saha et al., 1995b proposed a design of advanced three-stage chiller and then investigated the effect of different parameters (e.g. cycle time, heat exchanger flow rate and temperature) on system performance (Saha et al., 1997a). Khan et al., 2008 improved system performance by adding a re-heat scheme. It was shown that the COP of three-stage adsorption chiller reaches up to 0.3 at 70 °C heat source temperature with cycle time of 4400 s and longer, the heat source temperature can be reduced to as low as 40 °C along with a coolant at 30 °C.

The three-stage chiller has six beds (i.e., a pair of beds in each stage) and these beds occupy large space of the system. Accordingly, the footprint of the three-stage machine is larger than that of the single- and two-stage adsorption machine for the same cooling capacity. This is the drawback of multi-stage system. Therefore, the reduction of the number of adsorbent beds directly contributes to the reduction of system volume.

In the present study, first a design of a four-beds three-stage adsorption system was proposed, instead of six-beds three-stage adsorption system. Second, cycle time was optimized to maximize the performance of the proposed and former six-bed system to identify the best performance. The particle swarm optimization method was used to obtain the maximum cooling output under standard working conditions. Finally, the performance of the proposed cycle was compared with the optimal performance of former six-bed three-stage adsorption systems.

6.2 Description of Three-stage Adsorption Cycle

Advance single-stage adsorption system is used to achieve better performance, and two- and three-stage cycle were proposed to utilize lower heat source temperature. Single-stage adsorption cycle is not operational when heat source temperature is below 60 °C along with a coolant of temperature 30 °C or higher. For practical utilization of these temperatures in adsorption system operation, higher staged regeneration is necessary. In this regard, at first Saha et al., 1997b proposed six-bed three-stage adsorption cycle. The schematic diagram of the system is shown in Fig. 6.1(a) and its operation mode is given in Table 6.1(a). In this case, three pairs of adsorber/desorber heat exchanger beds i.e., Bed 1-Bed 2, Bed 3-Bed 4, and Bed

5-Bed 6 were used in lower cycle, intermediate cycle and upper cycle, respectively. To reduce the volume of the system, intermediate and upper cycle each pair of bed was replaced by one bed and it was proposed to modified the four-bed three-stage cycle. To make the adsorption cycle competitive in the market, it is necessary to consider economical issues as well as the total size of system. The schematic of proposed cycle with modification (indicated by arrow mark) is shown in Fig. 6.1(b). In proposed case Bed 3 and Bed 4 can work instead of Bed 3-Bed 4 and Bed 5-Bed 6 in the former cycle, respectively, whereas Bed 1 and Bed 2 was kept similar as former system. The operation mode of the proposed system is given in Table 6.1(b). Operation strategy was considered taken into account longer adsorption time compare to desorption time, whereas in former cycle adsorption and desorption time were chosen as equal. In first half cycle of proposed system, Bed 3 adsorbs vapour from Bed 1 and then it transfers to condenser via Bed 4. Similarly, in second half cycle, it adsorbs vapour from Bed 2 and then transfers to condenser in similar way. As a result, Bed 3 and Bed 4 are completing into two full cycles, while Bed 1 and Bed 2 are completing only one full cycle operation at the same time.

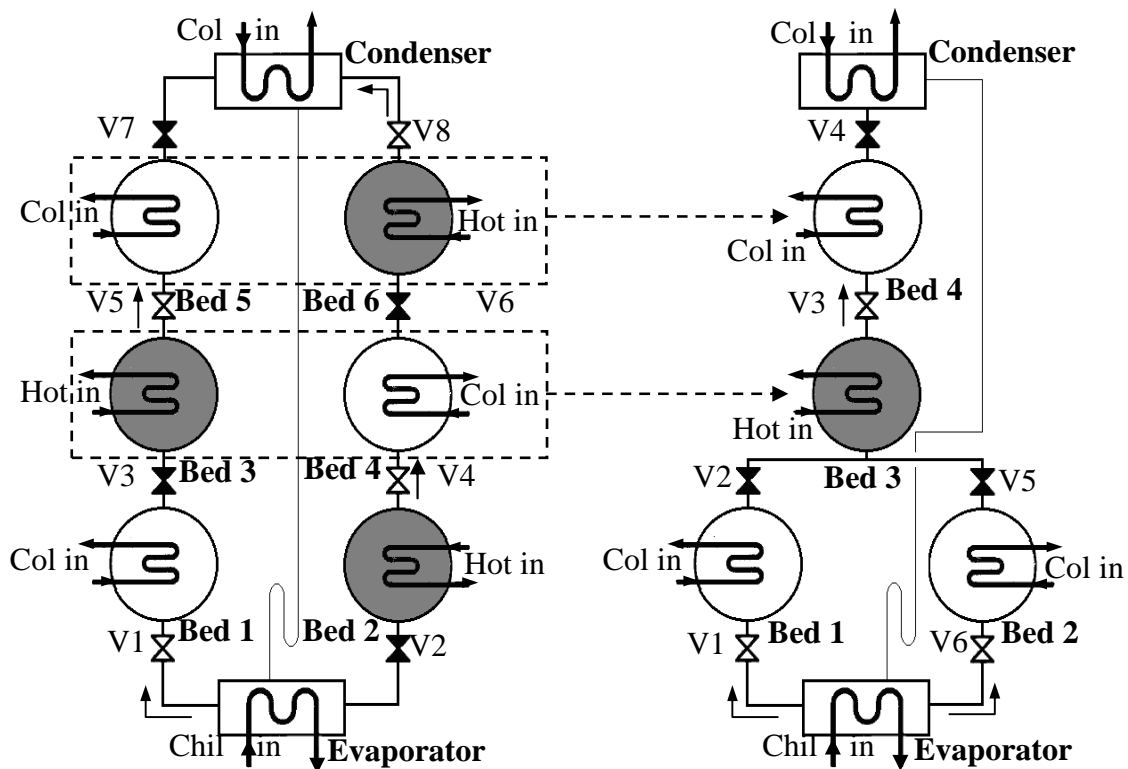


Fig. 6.1: Schemata of (a) six-bed, three-stage chiller of Saha et al., 1997a and (b) proposed design of four-bed, three-stage adsorption cycle.

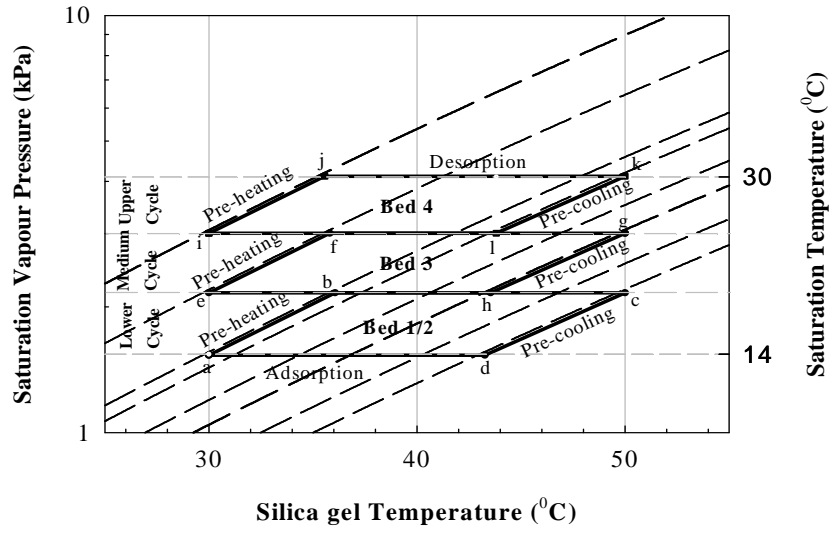


Fig. 6.2: Conceptual Dühring diagram of proposed cycle.

Table 6.1: Operation mode of former six-bed three-stage cycle and proposed four-bed three-stage cycle with optimal cycle time at 50 °C heat source temperature.

(a) Former six-bed three-stage cycle

Mode	A	B	C	D
	τ_1	τ_2	τ_1	τ_2
Bed 1	225.9	8.2	225.9	8.2
Bed 2	225.9	8.2	225.9	8.2
Bed 3	225.9	8.2	225.9	8.2
Bed 4	225.9	8.2	225.9	8.2
Bed 5	225.9	8.2	225.9	8.2
Bed 6	225.9	8.2	225.9	8.2

(b) Proposed four-bed three-stage cycle

Mode	A	B	C	D	E	F	G	H
	τ_1	τ_2	τ_1	τ_2	τ_1	τ_2	τ_1	τ_2
Bed 1	129.9	7.9	129.9	7.9	275.6			
Bed 2	405.5					7.9	129.9	7.9
Bed 3	129.9	7.9	129.9	7.9	129.9	7.9	129.9	7.9
Bed 4	129.9	7.9	129.9	7.9	129.9	7.9	129.9	7.9

Desorption
 Pre-heating
 Adsorption
 Pre-cooling

The proposed three-stage adsorption cycle consists of four adsorber/desorber heat exchangers namely Bed 1, Bed 2, Bed 3 and Bed 4, one evaporator and one condenser (Fig. 6.1(b)). Silica-gel and water have been chosen as adsorbent-refrigerant pair because the regenerative temperature of silica gel is lower than that of other adsorbents and water has large latent heat of vaporization. The advantage of the three-stage cycle is the utilization of the lower grade heat sources than single-stage and two-stage adsorption cycle. For example, the temperature of 50 °C is enough to drive the three-stage cycle. However, such low temperature is not enough to pressurize the vapour from the evaporator up to the condenser pressure in single-stage system. The vapour needs to be pressurized three times in the cycle through three-stage adsorption-desorption processes. The first stage pulls up the vapour from evaporator pressure to certain pressure level, second stage pulls up intermediate pressure and then the third stage pushes up the vapour from the intermediate pressure to the condenser pressure.

The Bed 1 and Bed 2 are working in low temperature and pressure (close to evaporator pressure), Bed 3 is working at intermediate temperature and pressure and Bed 4 is working at higher temperature and pressure (close to condenser pressure). The conceptual Dühring diagram is shown in Fig. 6.2. The cyclic diagrams a-b-c-d-a, e-f-g-h-e and i-j-k-l-i indicate the lower, intermediate and upper cycle, respectively. All beds are completing four thermodynamic stages, i.e., pre-heating, desorption, pre-cooling and adsorption stage, which are accordingly followed by the sides a-b, b-c, c-d and d-a, and e-f, f-g, g-h and h-e for the lower and intermediate cycle, respectively. Similarly, the sides i-j, j-k, k-l and l-i indicate the modes pre-heating, desorption, pre-cooling and adsorption stage of Bed 4, respectively.

To complete full cycle operation, each bed is to complete eight operational modes, namely A, B, C, D, E, F, G and H as shown in Table 6.1 (b), whereas former cycle it is needed four operation modes. Number of operation mode was increased to choose the longer adsorption time compare to desorption time. In Mode A, Bed 1 and Bed 2 are in cooling state when cooling water is passed through both beds and are connected with evaporator to adsorb refrigerant vapour from evaporator. This process is called adsorption mode. At the same time evaporator's lower temperature and pressure is maintained so that water could easily vaporize by seizing heat from chilled water. Bed 2 remains in adsorption stage up to end of mode E. On the other hand Bed 3 and Bed 4 is connected each other and Bed 3 is heated with hot water to released it own refrigerant vapour to Bed 4. At the same time Bed 4 is cooled with cooling water passing through it to release the adsorption heat.

In mode B, Bed 1 is disconnected from evaporator and other two beds (i.e., Bed 3 and

Bed 4) are disconnected each other by closing the connecting valve `V3`. Then the Bed 1 and Bed 4 are heated by hot water to increase its pressure, which is called pre-heating mode and Bed 3 is cooled down by cooling water to reduce its pressure, which is called pre-cooling mode. When the pressure of Bed 1 and Bed 3 become nearly equal then both are connected each other by opening the connecting valve (i.e., V2), which is starting point of mode C. In this mode, Bed 1 is heated by hot water and Bed 3 is cooled by cooling water, which is called desorption mode for Bed 1 and adsorption mode for Bed 3. Bed 1 is desorbing its adsorbed vapour to the Bed 3 and Bed 3 is adsorbing vapour from Bed 1 during this mode. On the other hand when the pressure of Bed 4 becomes equal to condenser pressure then it connected with condenser by opening the connecting valve (`V4`) to release its own refrigerant vapour to condenser and it is called the desorption of Bed 4 (i.e., mode C). In this mode, adsorbed refrigerant is removed from bed and goes to the condenser. Then refrigerant vapour is condensed inside condenser and condensation heat is removed by cooling water. Finally, condensed refrigerant goes to the evaporator via U shape tube.

Mode D is called pre-cooling for Bed 1 and Bed 4, and pre-heating mode for Bed 3, while beds are isolated from other parts of the cycle. In this case Bed 1 is cooled by cooling water to reduce its pressure to the evaporator pressure and then it is connected with evaporator by opening the connecting valve (`V1`), which is called adsorption process and starting point for mode E. This process will continue to the end of mode H. Meanwhile, Bed 3 is heated by hot water to increase its pressure and Bed 4 is cooled with cooling water passing through it. When the pressure of both beds are become equal then both are connected each other by opening connecting valve `V3`. It is the starting point of Mode E, which is similar as the mode A. Through these modes the first half cycle (from mode A to D) of Bed 3 and Bed 4 are completed and the second half cycle (from mode E to H) is started. The mechanism of modes E, F, G and H of Bed 3 is similar to the modes A, B, C and D, but during these modes, Bed 3 is connected with Bed 2 instead of Bed 1 (i.e., mode G) and vapour is transferred among Bed 2 and Bed 3. In second half cycle Bed 4 acts exactly similar as first half cycle.

6.3 Simulation Methods and Materials

Simulation methods and materials of four-bed three-stage adsorption system are details described in chapter 3. Heading of the sub-sections from 3.4.1 to 3.4.6 are given below:

- ❖ Adsorption and Desorption Energy Balance

- ❖ Condenser energy balance
- ❖ Evaporator energy balance:
- ❖ Adsorption and desorption rate
- ❖ Mass balance:
- ❖ System performance

Optimization procedure

A complete simulation program was developed based on Matlab software to solve all equations mentioned in section 3.4. Adsorption/desorption rate equation, energy balance equation of beds, condenser and evaporator, and mass balance equation have been solved simultaneously using MATLAB ode45 solver. All input parameters such as adsorbent-refrigerant properties, flow rates of heat transfer fluids and heat exchangers specifications were initially given for which the system cyclic operation can be continued.

In this study, PSO was applied to optimize the cycle time based on maximum value of SCP, whereas SCP was chosen as the objective function and cycle time (i.e., τ_1 and τ_2) was chosen as the variable. In PSO, a particle holds the values of variables and updates the values toward the optimal solution. After a number of iterations, all the particles hold the same value and the objective function value is maximized. In this case, the number of particles and the number of iterations were considered as 24 and 1500, respectively. It was observed that all particles reached their best position around 500 iterations.

6.4. Results and Discussions

The simulation program developed for proposed four-bed three-stage adsorption cycle was operated by adopting the basic input parameters and standard working conditions as presented in Table 6.2 (Moriyama, 2007). The cycle time, operating time of each mode (i.e., τ_1 and τ_2), is one of the most important parameters of the system and influences on the overall performance effectively. The specific cooling power (SCP) represents the cooling capacity per unit quantity of adsorbent, and therefore it is a useful index for minimizing the size of the system. At first the cycle time was optimized based on the maximization of SCP using PSO procedure. Cycle time of the system was optimized using various heat source temperatures varying from 40 to 70 °C with the increment of 5 °C by keeping outlet temperature of the chilled water at 9 °C. Accordingly, the chilled water flow rate was optimized simultaneously with cycle time to adjust chilled water outlet at constant temperature. Fig. 6.3 shows that

optimum cycle time of the proposed system decreases with the increase of heat source temperature. Total optimal cycle time is the sum of the cycle time of all modes (Table 6.1). The cycle time ratio is defined as the ratio of each mode operation time to the total cycle time. Fig. 6.4 represents the optimal cycle time ratio of the system for different heat source temperatures. It was observed that cycle time ratio for τ_1 and τ_2 were slightly decreased and increased with heat source temperature, respectively. Similar, decreasing behaviour of optimal cycle time with heat source temperature was also observed for former six-bed three-stage cycle, which is shown in Fig. 6.5. But in optimal cycle time ratio of former cycle indicated opposite nature, i.e. τ_1 and τ_2 were decreased and increased with heat source temperature, respectively (Fig. 6.6). It is noted that both systems are giving shorter pre-cooling/pre-heating (i.e. τ_2) time.

Table 6.2: Basic input parameters and standard working conditions

(a) Basic input parameters		
Parameters	Value	Units
Q_{st}	2.80×10^6	$J\ kg^{-1}$
E_a	4.2×10^4	$J\ mol^{-1}$
D_{so}	2.54×10^{-4}	$m^2\ s^{-1}$
R	8.314	$J\ mol^{-1}\ K^{-1}$
R_p	0.30×10^{-3}	m
C_w	4.18×10^3	$J\ kg^{-1}\ K^{-1}$
C_{wv}	1.89×10^3	$J\ kg^{-1}\ K^{-1}$
L_w	2.50×10^6	$J\ kg^{-1}$
C_{Cu}	386.00	$J\ kg^{-1}\ K^{-1}$
C_{Al}	905.00	$J\ kg^{-1}\ K^{-1}$
C_s	924.00	$J\ kg^{-1}\ K^{-1}$
A_{hex}^b	0.61×16	m^2
A_{hex}^e	6.00	m^2
A_{hex}^c	2.00	m^2
U_{hex}^c	3070	$W\ m^{-2}\ K^{-1}$
U_{hex}^b (desorption)	4898	$W\ m^{-2}\ K^{-1}$

U_{hex}^b (adsorption)	3347	$\text{W m}^{-2} \text{K}^{-1}$
U_{hex}^e	1251	$\text{W m}^{-2} \text{K}^{-1}$
W_s^b	16.00	kg
W_{hex}^b (Cu)	12.67	kg
W_{hex}^b (Al)	16.87	kg
W_{hex}^e	674.0	kg
W_w^e	61.0	kg
W_w^c	24.98	kg
W_{hex}^c	12.8	kg
(b) Standard working condition		
T_{in}^{hot}	40 - 70	$^{\circ}\text{C}$
\dot{m}_w^{hot}	1.0	kg s^{-1}
T_{in}^{col}	30	$^{\circ}\text{C}$
\dot{m}_w^{col}	1.0	kg s^{-1}
$T_{in}^{c,col}$	30	$^{\circ}\text{C}$
$\dot{m}_w^{c,col}$	0.8	kg s^{-1}
T_{in}^{chil}	14	$^{\circ}\text{C}$
T_{out}^{chil}	9	kg s^{-1}

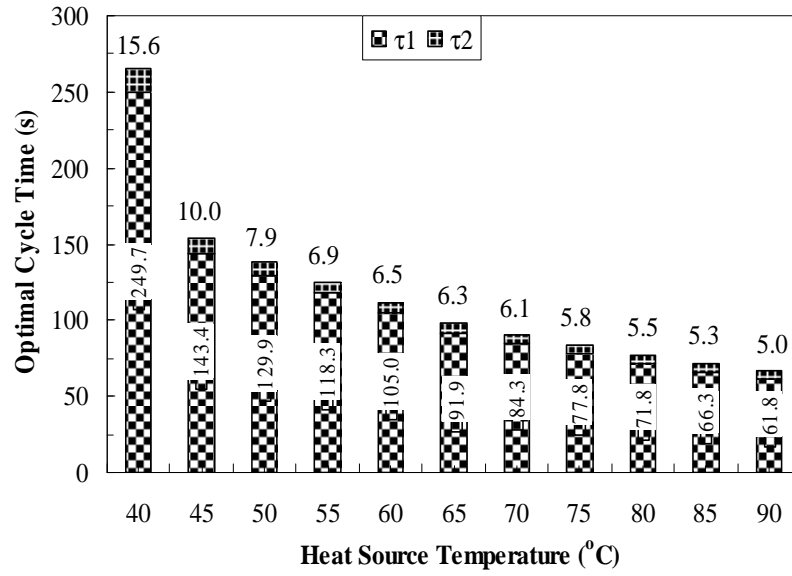


Fig. 6.3: Optimal cycle time of the proposed cycle for different heat source temperature.

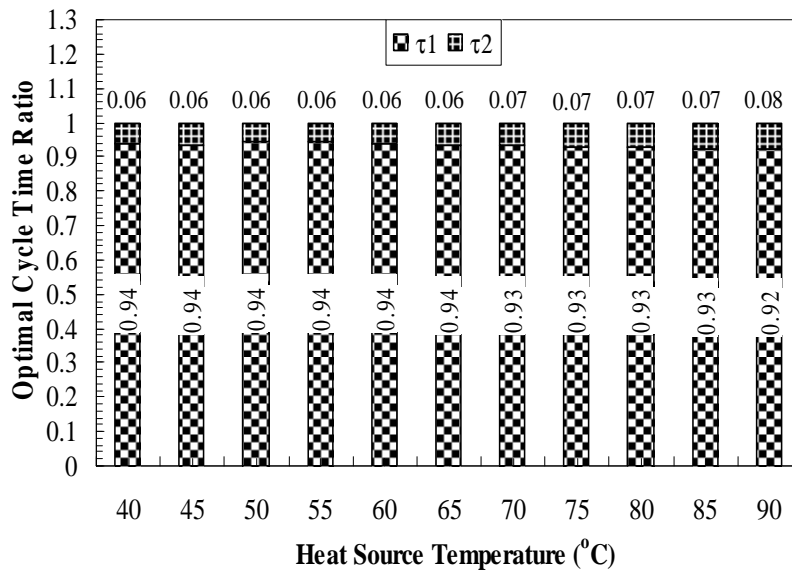


Fig. 6.4: Optimal cycle time ratio of the proposed cycle for different heat source temperature.

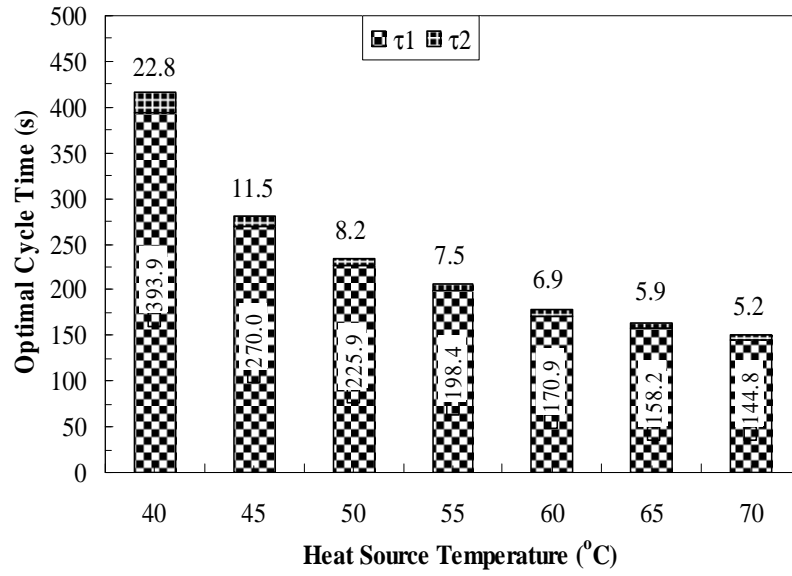


Fig. 6.5: Optimal cycle time of former six-bed three-stage cycle for different heat source temperature.

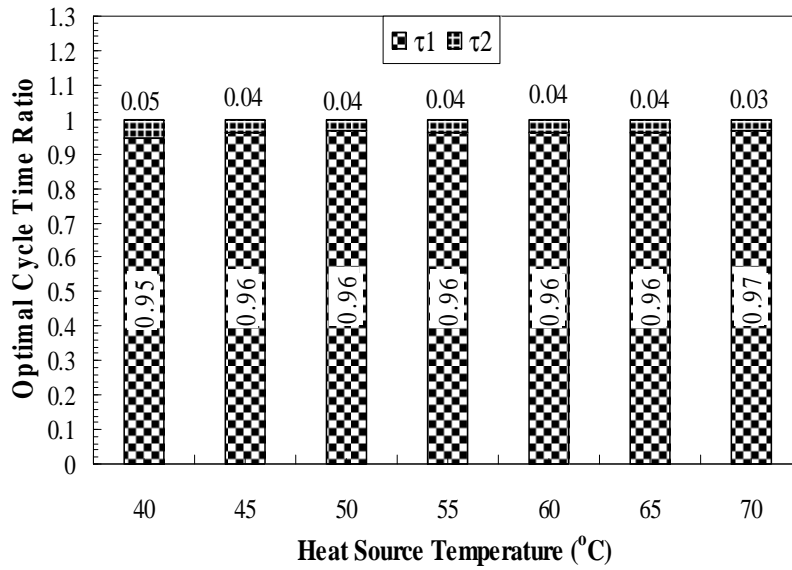


Fig. 6.6: Optimal cycle time ratio of former six-bed three-stage cycle for different heat source temperature.

The variation of chilled water flow rate with heat source temperature for both cycles are shown in Fig. 6.7. It was observed that average chilled water flow rate increases with the increase of driving heat source temperature. Since, ceasing heat from chilled water increased with heat source temperature and to keep constant average chilled water outlet temperature at 9 °C, chilled water flow rate was increased. It was observed that chilled water flow rate was similar for both cycles. It is due to both systems have two beds (i.e., Bed 1 and Bed 2) in bottom cycle with equal mass of silica gel and producing similar effect.

Sensitivity of cycle time on SCP of both systems was investigated for heat source temperature of 60 °C. SCP was calculated by varying the cycle time τ_1 from 20 to 500 s and cycle time τ_2 from 5 to 100 s. The increment steps for τ_1 was 5 s while for τ_2 was 2.5 s. Chilled water flow rate was kept constant 0.281 and 0.304 kg.s⁻¹ for proposed and former cycle, respectively. These values were observed using PSO procedure for 60 °C heat source temperature. Contour plot of SCP of both systems are shown in Figs. 6.8 and 6.9, respectively. It was clear that by increasing of τ_1 , the SCP increased to approximately 100 s and after 100 s, it was again decreased (Fig. 6.8). On the other hand, SCP was decreased with the increases of τ_2 . Similar profile was also observed in case of former system (Fig. 6.9). The contour plot of both systems provided a singular pattern with cycle time. The centre of the contour indicates the maximum SCP and corresponding cycle times indicate the optimal cycle time, which is exactly matching with PSO result.

The optimal performance of the proposed system is shown in Figs. 6.10 and 6.11. It is apparent that the cycle can operate at low temperature heat source as low as 40 °C with a coolant at 30 °C. The SCP increased with the increase in heat source temperature whereas COP increased with heat source temperature up to 55 °C and then it was decreased slightly with heat source temperature. An increase of heat source temperature with a fixed heat sink causes the system to increase the amount of refrigerant adsorption/desorption promptly, resulting in higher SCP at higher heat source temperature. Due to similar effect, the total optimal cycle time was found to be decreased with heat source temperature as shown in Fig. 6.12. It is generally observed that the behaviour of COP of adsorption cycle increased with longer cycle time. However at lower temperature (<55 °C), cycle time was found to be increased, whereas COP was found to be decreased because at lower driving heat source temperature longer time is needed for effective desorption. The maximum COP was observed to be 0.218 at 55 °C heat source temperature.

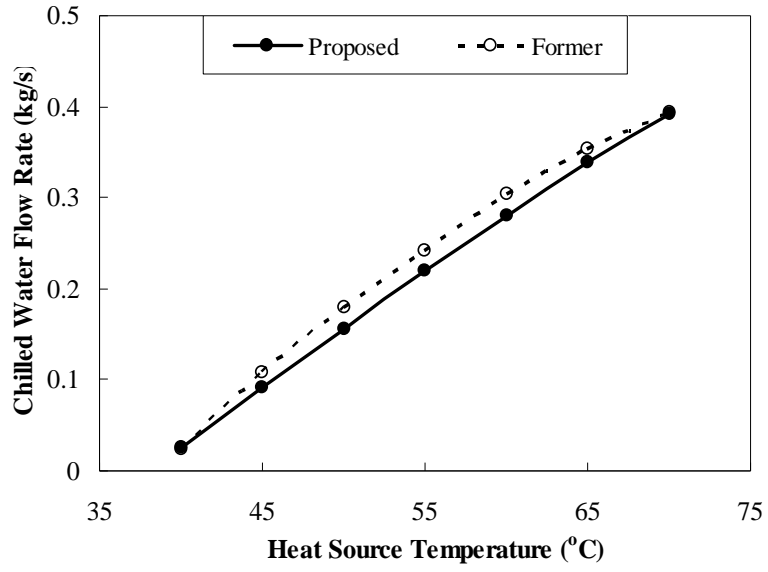


Fig. 6.7: Variation of chilled water flow rate with heat source temperature.

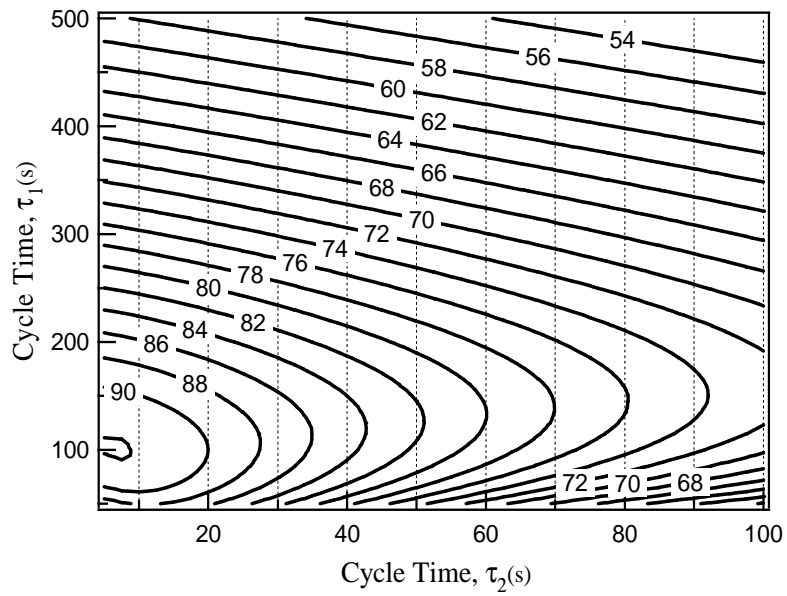


Fig.6.8: Contour plot of SCP relating to processing time τ_1 and τ_2 at 60 °C heat source temperature of proposed system.

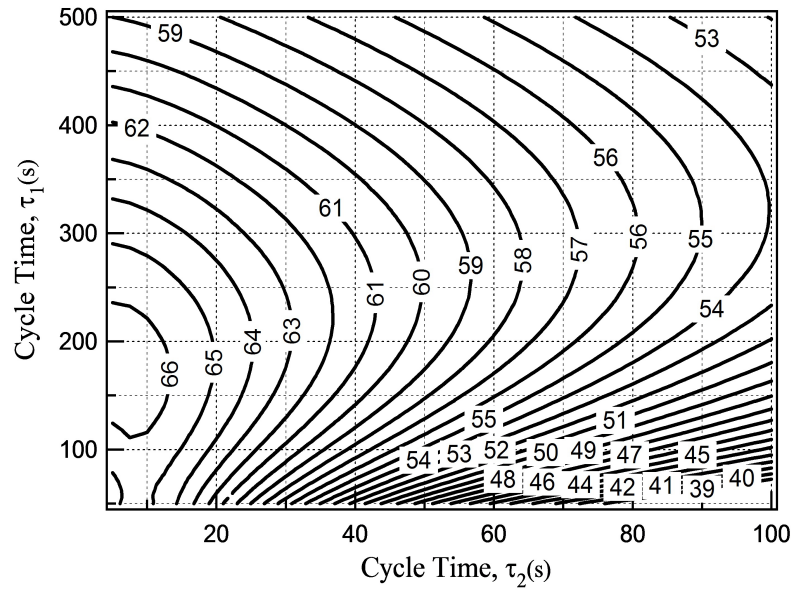


Fig.6.9: Contour plot of SCP relating to processing time τ_1 and τ_2 at 60 °C heat source temperature of former system.

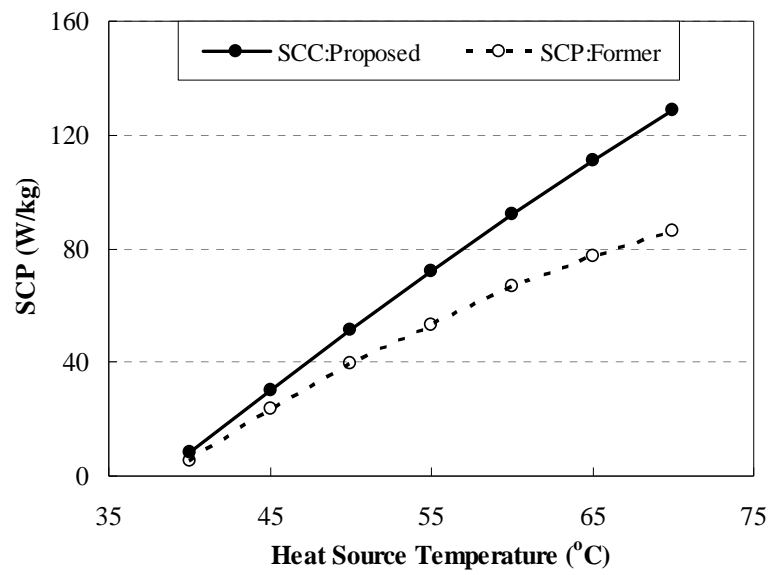


Fig. 6.10: Comparison of optimal SCP of proposed cycle with the former six-bed three-stage cycle.

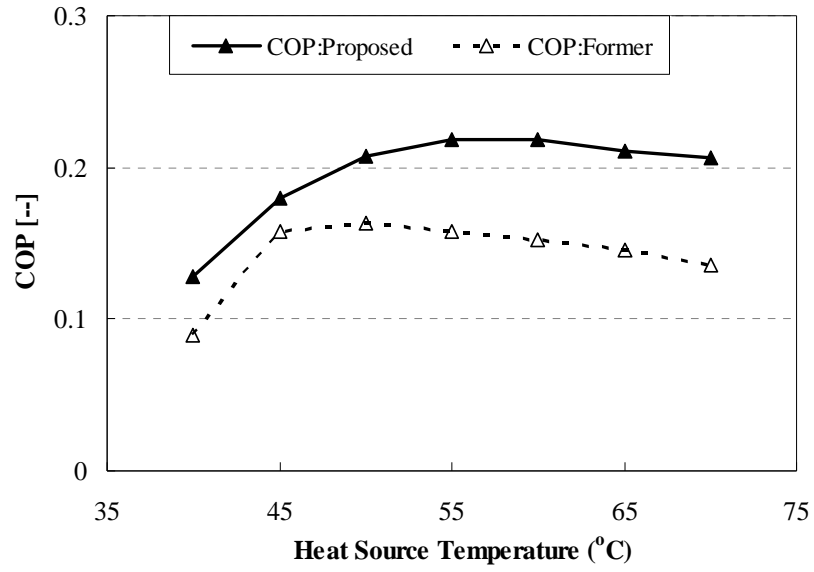


Fig. 6.11: Comparison of optimal COP of proposed cycle with the former six-bed three-stage cycle.

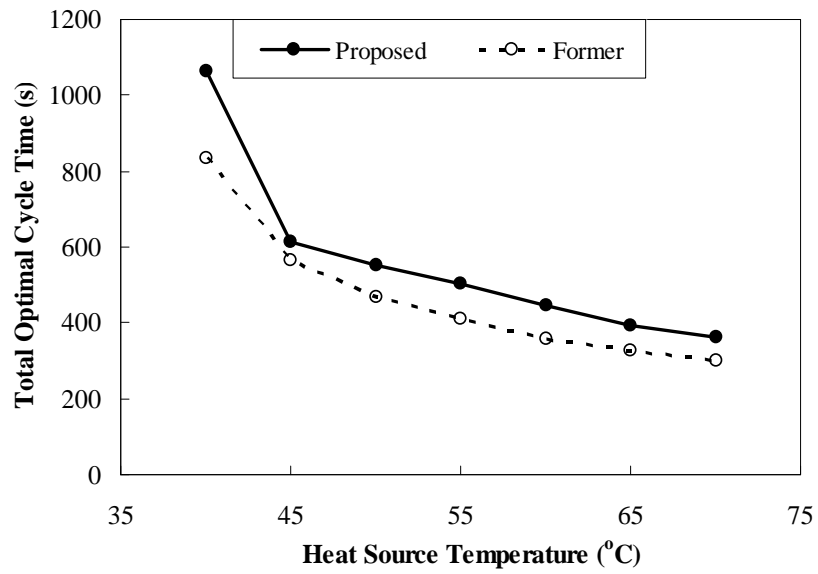


Fig. 6.12: Comparison of optimal cycle time of proposed cycle with the former six-bed three-stage cycle.

The optimal performance of the proposed cycle was compared with optimal performance of the former six-bed three-stage cycle as shown in Figs. 6.10 and 6.11. It can be seen from these figures that both SCP and COP of proposed cycle were found to be increased significantly over the whole range of studied heat source temperatures, which is the great benefit of the proposed cycle. Comparison of optimal total cycle time of proposed cycle with the former six-bed three-stage cycle is also shown in Fig. 6.12. It was observed that proposed cycle provided little bit longer optimal cycle time at each heat source temperature.

The higher SCP value of the proposed cycle is due to effects of lower total mass of adsorbent (silica-gel) of the system. Because the denominator values as described in equation (Eq. 3.24) is lower as four beds silica-gel mass is smaller (i.e., 64 kg) than six beds silica-gel (i.e., 96 kg). Heat release as described in numerator is same for both systems because both cycles have two beds in lower cycle and producing similar cooling effect to evaporator. It is expected mathematically that the SCP of four-bed system is larger than that of six-bed system by the factor of $3/2$, which was exactly achieved in proposed case.

Although the total cycle time of proposed system is little bit longer but the proposed cycle provided around 12 to 34 % higher COP value compare to former cycle. It is due to longer adsorption time as well as shorter desorption time, which is shown in Table 6.1. Not only that in proposed case, it was observed that adsorption time is more than twice time longer than desorption time as well as sum of desorption time, pre-cooling and pre-heating time. Aristov et al., (2012) was also given similar practical recommendations to manage cooling cycles with non-equal durations of adsorption and desorption time. Due to longer adsorption time total adsorption of proposed cycle is higher than the former cycle. As a result COP as well as SCP was increased over the whole range of heat source of temperature.

Comparison of optimal performance of proposed three-bed two-stage adsorption system was compared with the proposed four-bed three-stage adsorption system, which is shown in Figs. 6.13 and 6.14. In these case basic input parameter and standard working condition was chosen as same for both system but main different was in total number of beds and total mass of adsorbent. From these figures it is obvious that two-stage system is capable to utilize the waste heat as low as 45 °C whereas three-stage system is capable to utilize as low as 40 °C heat source temperature. Moreover both SCP and COP of two-stage system is better than three-stage system.

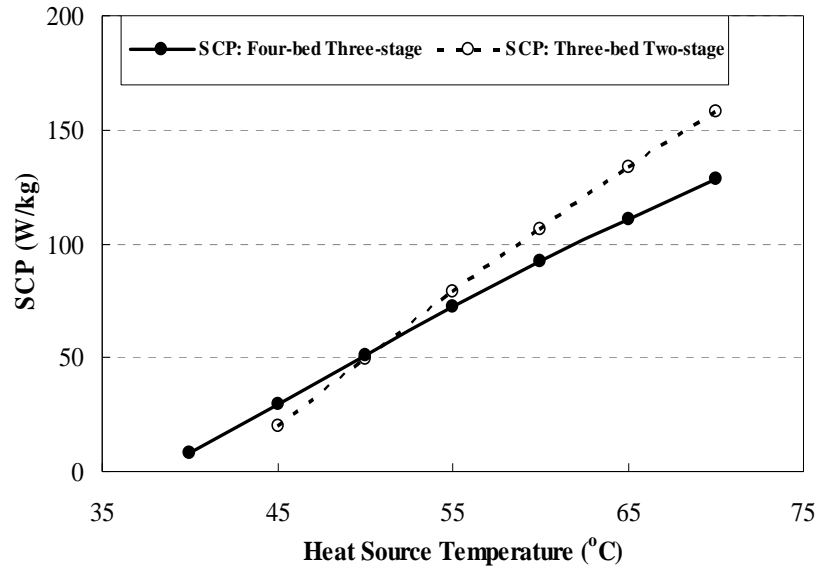


Fig.6.13: Variation of SCP of two-stage and three-stage adsorption system at different heat source temperature.

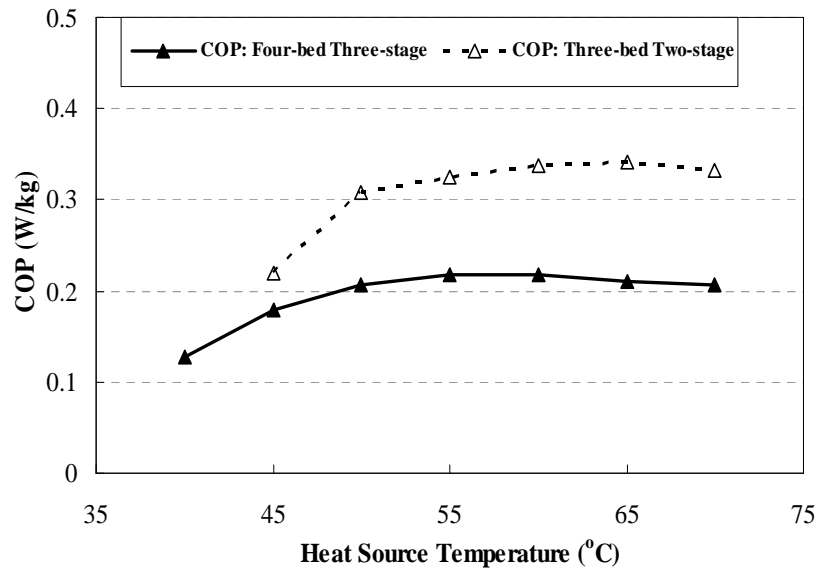


Fig.6.14: Variation of COP of two-stage and three-stage adsorption system at different heat source temperature.

Comparative study between former six-bed three-stage and proposed four-bed three-stage adsorption system along with improvements due to modification are given below.

	Former six-bed three-stage system	Proposed four-bed three-stage system
Number of evaporator	1	1

Number of condenser	1	1
Number of beds	6	4
Total mass of adsorbent	96 kg	64 kg
Total mass of heat exchanger material in beds	12.67x6 kg (Cu)	12.67x4 kg (Cu)
	16.87x6 kg (Al)	16.87x4 kg (Al)
Improvement due to proposed modified design		
Number of bed(s) reduced		2
Reduction in total mass of silica gel		32 kg
Reduction of heat exchanger material	25.34 kg (Cu)	
	33.74 kg (Al)	
COP increased for different heat source temperatures		12 to 34 %
SCP increased for different heat source temperatures		21 to 35 %

Thus, it can be concluded the proposed cycle can significantly reduce the overall size of the three-stage adsorption system along with an increase in the overall performance.

6.5 Conclusions

A modified design of a four-bed, three-stage adsorption cycle which can be powered by low-temperature thermal energy source as low as 40 °C has been introduced. A simulation program has been developed to investigate the performance of the system and cycle time was optimized using particle swarm optimization method. It was observed that the specific cooling power of the proposed innovative cycle increased with heat source temperature. The maximum coefficient of performance of the system was observed for regeneration temperature at 55 °C. The optimal cycle time was observed to be largely depending on the corresponding heat source temperature and it decreased with higher heat source temperature when the chilled water outlet temperature was fixed at 9 °C. With the present innovative design, the overall system footprint can be significantly reduced compared to the six-bed three-stage cycle. Moreover, both SCP and COP were also increased significantly over the whole range of heat source temperature as compared to that of six-bed three-stage cycle. The proposed cycle could be useful from the economical point of view due to its higher performance and significant reduction in system footprint.

Chapter 7

7.1 Overall Conclusions

In this dissertation, innovative designs of three-bed two-stage and four-bed three-stage adsorption system are introduced. A computational simulation program has been developed for three-bed mass recovery with heating/cooling adsorption system based on Matlab software. Modification has been done to make the simulation program suitable for three-bed two-stage and four-bed three-stage adsorption system. The PSO method was applied to optimize the cycle time to know the best performance of the analyzed adsorption systems. It was observed that optimal cycle time is specific for each heat source temperature, which was decreased with heat source temperature. Optimal result shown that SCP was increased with heat source temperature for all investigated adsorption system. On the other hand COP was first increased up to certain heat source temperature after that it was decreased with temperature. Maximum COP was observed at 60 °C heat source temperature for three-bed single-stage system whereas maximum COP was observed at 65 and 55 °C temperature for three-bed two-stage and four-bed three-stage adsorption system, respective. In comparison of two different adsorption system it is necessary to compare the best performance of each system, which has been done in every aspect of comparison of this work. Sensitivity of cycle time on SCP was investigated base on contour plot to make the PSO result reliable. The contour of SCP relating to cycle time was provided unique pattern wherein the center of the contour indicated the maximum SCP and corresponding cycle time indicated the optimal cycle time, which was matched with PSO value. Investigation on two different type of three-bed single-stage with mass recovery with heating/cooling adsorption can be summarize as

- i) Previous all investigation was based on un-optimize cycle time, which was fixed for all heat source temperature. While the present investigation is based on optimal cycle time. It was observed that optimal cycle time is specific for each heat source temperature, which was decreased with heat source temperature.
- ii) Comparison of optimized and up-optimized result illustrated that SCP with un-optimized cycle time setting is slightly lower than the optimized cases while COP with un-optimized cycle becomes significantly lower than that of the optimized cases. It suggests that optimal time setting is required to utilize heat source as much as possible at any temperature.
- iii) The proposed PSO based comparison method is useful to identify the best performance of adsorption system with different configuration. It was found from the results of optimized

cycle time that time allocation of cycle B is relatively insensitive compared with that of cycle A, which implies cycle B is considered to be robust against the variation of heat source temperature.

For two-stage system, a new design of a three-bed two-stage adsorption system was introduced. The cycle is effectively applicable for utilizing low grade heat source temperature as low as 45 °C. It was found that the SCP of the proposed cycle increased significantly over the whole range of heat source temperature compared with former four-bed two-stage cycle while the COP is slightly lower than the former cycle. This implies that the advantage of the proposed cycle is that the volume can be significantly reduced in comparison with the former cycle. Consequently, the proposed cycle is useful from the economical point of view due to its improved performance and smaller size.

A modified design of a four-bed, three-stage adsorption cycle which can be powered by low-temperature thermal energy source as low as 40 °C has been introduced. With the present innovative design, the overall system footprint can be significantly reduced compared to the six-bed three-stage cycle. Moreover, both SCP and COP were also increased significantly over the whole range of heat source temperature as compared to that of former six-bed three-stage cycle. The proposed cycle could be useful from the economical point of view due to its higher performance and significant reduction in system footprint.

It can be conclude that three-bed two-stage and four bed three-stage adsorption system recognized as multi stage adsorption refrigeration cycle is one step advance of refrigeration system for simple design, optimal size and better performance as well as the technique of investigation. Therefore, it is expected that this multi-stage adsorption refrigeration system will be more attractive to the consumers.

7.2 Remarks

In order to further development, the following investigation can be done for the proposed adsorption system

1. Optimization of total mass allocation as well as mass allocation of upper cycle bed and lower cycle beds of three-bed two-stage and four-bed three-stage system.
2. Three-bed two-stage adsorption can be modified as a dual mode system means it will work as single-stage as well as two-stage mode. Details investigation can be done to know the performance of dual mode cycle (Appendix A).
3. Four-bed three-stage system can be modified to four stage and above. Investigation can be done to know the real performance of higher stage system (Appendix B).

Appendix A

Study on a Three-bed Dual Mode Adsorption Cycle

Synopsis

The design and operation of a three-bed mass recovery silica gel-water based adsorption cooling cycle has been outlined along with the performance evaluation of the system. The system can operate in dual-mode, either single-stage mode or two-stage mode without any change of its physical configuration. Cycle time of the system is optimized to maximize the specific cooling power (SCP) using particle swarm optimization (PSO) method. It is evident that in single-stage operation mode the proposed system can effectively utilize low grade heat source as low as 55 °C along with a coolant at 30 °C, whereas two-stage mode can utilize heat source as low as 45 °C. The optimal performance of the system with single-stage operation mode is compared with the optimal performance of two-stage operation mode. Accordingly, the coefficient of performance (COP) of the system in single-stage operation mode is found to be more effective than that of the two-stage operation mode over the whole range of heat source temperature. However, SCP is observed to be to some extent lower than the two-stage mode. The system could be operated in single-stage operation mode when the regeneration temperature remains between 60 and 90 °C, and in two-stage mode when the available regeneration temperature lingers between 45 and 60 °C

A.1. Introduction

Adsorption heat pump is one of the advance technologies to utilize waste heat and solar thermal energy. Consequently it contributes to reduce global warming potential as well as consumption of primary energy sources, which is global argent need. It uses solid adsorbent such as silica-gel instates of liquid adsorbent i.e. CFC/HCFC of vapor compression system as a result it has no contribution for depleting of ozone layer. The adsorption technology was used in refrigeration equipment in the late 1920s, as reported by Hulse, 1929. Last few decades scientists were given a considerable effort to use adsorption (solid/vapor) process for cooling/heating and other different applications. Waste heat driven silica gel-water based two-bed adsorption chillers was successfully commercialized in Japan (Critoph et al., 2005) and then Wang et al., 2005 was built a prototype silica gel-water based adsorption chiller and tested the performance in details.

Silica gel-water based two-bed adsorption system is the basic and fundamental system and well suited for low-temperature waste heat utilization to produce effective cooling power. Considerable efforts were given on two-bed adsorption system by Cho et al., 1992, Saha et al., 1995a, Boelman et al., 1995 and Chua et al., 1999. To improve the cooling power of conventional system mass recovery process was introduced and investigated by Pons et al., 1999 and Wang et al., 2001, which is more effective for the high evaporating pressure lift as well as for the low regenerating temperature. In this regard, Akahira et al., (2004, 2005) investigated the mass recovery process of silica gel-water based two-bed single-stage adsorption chiller theoretically as well as experimentally. Miyazaki et al., (2009a, 2009b) optimized cycle time using particle swarm optimization to utilize the waste heat below 100 °C as well as to increase the performance of two-bed adsorption system.

Advance three-bed non-regenerative silica gel-water adsorption chiller was proposed and analyzed by Saha et al., 2003a, which is effective for utilization of low-temperature waste heat between 60 and 95 °C and got better performance compared to two-bed adsorption cycles. Khan et al., (2006a, 2007a) and Uyun et al., (2009a, 2009b) modified the three-bed system by adapting mass recovery as well as heat recovery process and observed better performance compared to the three-bed system without mass recovery. The cycle time of both systems were optimized by Rahman et al., 2013 using particle swarm optimization process. Overall it was observed that three-bed mass recovery system is applicable as low as 50 °C heat source temperature to 90 °C and maximum performance was observed around 70 °C heat source temperature.

To utilize solar/waste heat with temperatures below 70 °C, Saha et al., 2001 proposed a design of prototype four-bed two-stage chiller. After that an extensive study was conducted by Alam et al., 2004 and Hamamoto et al., 2005 to identify the influence of design and operating condition on the system performance. Moreover, the modification in design and operation procedure with re-heat scheme was done by Khan et al., (2005b, 2006, 2007), Alam et al., 2007 and S.K. Farid et al., 2011. It was observed that two-stage chiller effectively work as low as heat source temperature 45 °C whereas advance single-stage chiller can not. On the other hand the performance of two-stage chiller at higher temperature is lower than single-stage adsorption chiller.

That is why in this study a design of three-bed adsorption system has been proposed which can be worked as single-stage as well as two-stage by switching only operation mode. The proposed system was modified from four-bed two-stage adsorption system to three-bed two-stage system for minimizing the overall size. In this paper, the design and operation of same system in single-stage was only introduced whereas two-stage operation was introduced in our previous paper (Rahman et al., 2012) and then the performance was investigated numerically in terms of specific cooling power (SCP) and coefficient of performance (COP) for different heat source temperatures. After that the cycle time of the system was optimized using practical swarm optimization method to maximize the SCP. Finally, the optimal performance of single-stage and two-stage operation of the system were compared.

A.2. Description of the Cycle

Three-bed adsorption system becomes attractive as it can be utilized low temperature waste heat and solar thermal energy, moderate size, low operation cost and provide stable chilled water outlet temperature. Smaller size of a system is becoming popular day by day. That is why optimization of overall size without reducing the performance is great important. Four-bed two-stage adsorption system was modified to three-bed two-stage system. It can also work as single-stage only switching the operation mode. The schematic diagram of proposed system is shown in Fig.A.1. It consists of three adsorber/desorber heat exchangers namely Bed 1, Bed 2 and Bed 3, one evaporator and one condenser. During two-stage operation Bed 3 is fully disconnected from evaporator by closing valve 'V5'. On the other hand, for single-stage operation Bed 3 is connected with evaporator through same valve. Operation modes of single-stage and two-stage are fully different, which can be changed by switching (Table A.1).

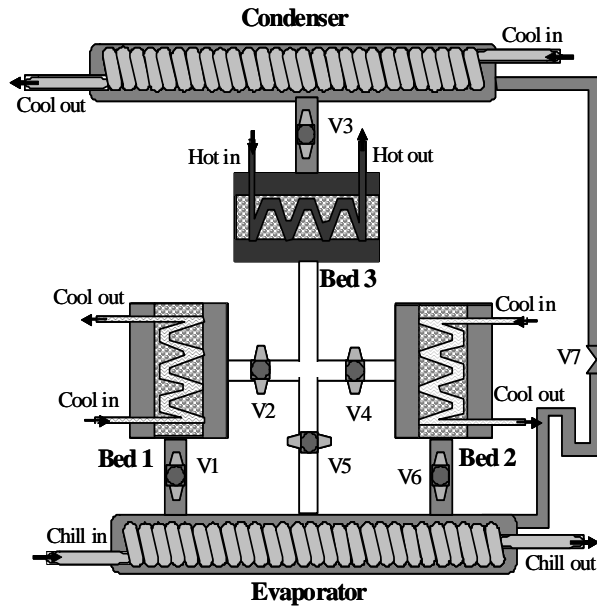


Fig. A.1: Schematic diagram of a proposed three-bed dual mode adsorption cycle.

The conceptual single-stage Dühring diagram of the system is shown in Fig. A. 2. The cyclic diagram a-b-c-d-g-a indicates the stages of mass recovery cooling, pre-heating, desorption, pre-cooling and adsorption modes of Bed 3. On the other hand, Bed 1/2 only complete the process of mass recovery heating/desorption, pre-cooling and adsorption process, which is shown by the cyclic diagram a-e-f-a. The conceptual diagram for two-stage mode is shown in Fig. A.3. In this case all beds are following pre-heating, desorption, pre-cooling and adsorption modes and Bed 1 and Bed 2 works in lower temperature/pressure level and Bed 3 works in upper temperature/pressure.

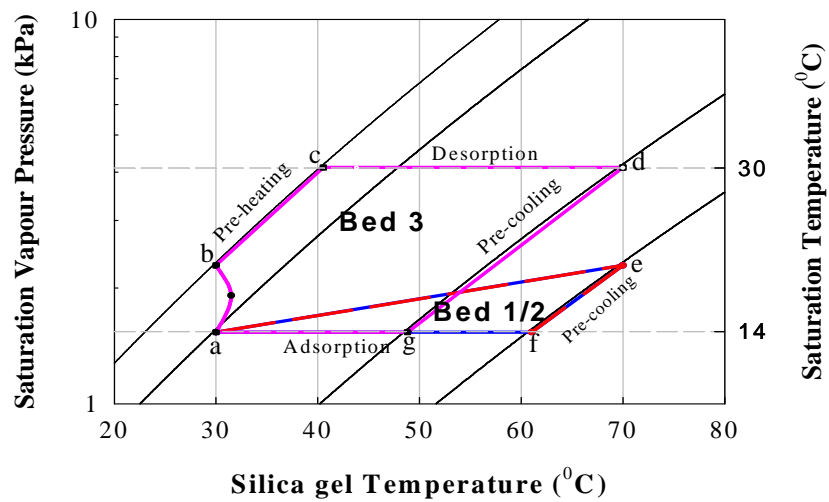


Fig. A.2: Conceptual Dühring diagram of single-stage operation of the system.

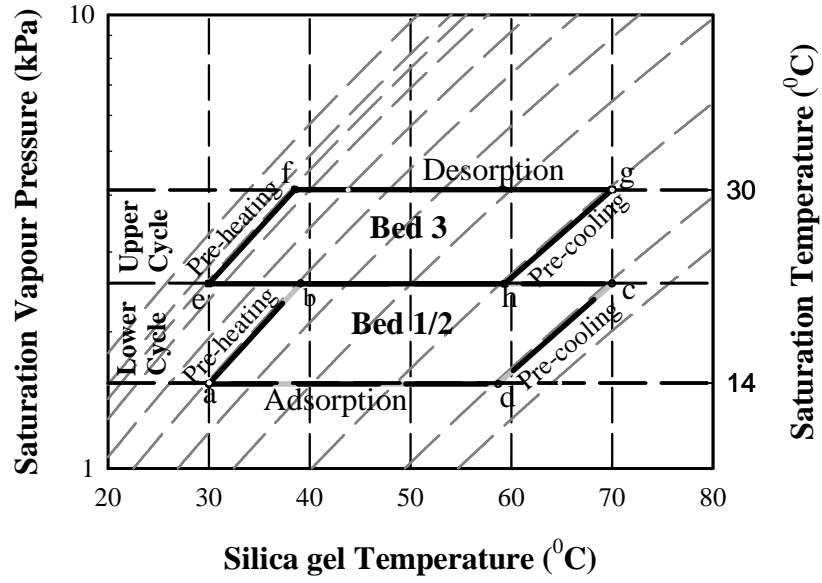


Fig. A.3: Conceptual Dühring diagram of two-stage operation of the system.

TableA.1: Operation modes of the system with optimal time allocation at 60 °C heat source temperature.

(a) Single-stage operation modes										
Mode	A τ_1	B τ_3	C τ_1	D τ_2	E τ_3	F τ_1	G τ_3	H τ_1	I τ_2	J τ_3
Bed 1	325			413	15	753				
Bed 2	1078								413	15
Bed 3	155	15	155	413	15	155	15	155	413	15
(b) Two-stage operation modes										
Mode	A τ_1	B τ_2	C τ_1	D τ_2	E τ_1	F τ_2	G τ_1	H τ_2		
Bed 1	134.5	12.27	134.5	12.27	293.54					
Bed 2	428.04							134.5	12.27	
Bed 3	134.5	12.27	134.5	12.27	134.5	12.27	134.5	12.27	134.5	12.27
<div><div><div></div><div>Desorption</div></div><div><div></div><div>Adsorption</div></div><div><div></div><div>Mass recovery heating</div></div><div><div></div><div>Mass recovery cooling</div></div><div><div></div><div>Pre-heating</div></div><div><div></div><div>Pre-cooling</div></div></div>										

To complete full cycle single-stage operation, each bed is to complete 10 operation modes, i.e. A to J. Operation modes and time allocation of each mode of the system are given in Table 1(a). In mode A, Bed 1 and Bed 2 are in cooling state when cooling water is passed through both beds and are connected with evaporator to adsorb refrigerant vapor from evaporator. This process is called adsorption mode. At the same time, evaporator's lower temperature and pressure maintained in such a way that water could easily be vaporized by seizing heat from chilled water. Bed 1 continues this process up to end of mode C whereas Bed 2 continues up to end of mode H. On the other hand, Bed 3 is in heating state when hot water passes through it and connects with the condenser to release its own refrigerant vapor and this process is called desorption. In desorption process, adsorbed refrigerant is removed from adsorbent bed and goes to the condenser. Then refrigerant vapor is condensed inside condenser and condensation heat is removed by cooling water. Finally, condensed refrigerant go to the evaporator via U shape tube.

In mode B, Bed 3 is disconnected from condenser via closing the connecting valve ('V3') and at the same time it is cooled with cooling water to reduce pressure by reducing the temperature as it was in higher temperature and pressure in previous mode. This mode is known as pre-cooling mode. In this mode no vapor will be transferred as it is fully disconnected from other parts of the system. When its pressure reduces to evaporator pressure then it connects with evaporator via opening the connecting valve 'V5' to adsorb refrigerant vapor from evaporator. It is the starting point of mode C and the adsorption mode of Bed 3. At the end of mode C, valve 'V5' becomes close and connects with Bed 1 via opening the connecting valve ('V2') and at the same time Bed 1 is heated with hot water and Bed 3 is cooled with cooling water. As a result vapor will transfer form Bed 1 to Bed 3. The process is known as mass recovery process. Bed 1 never connects with condenser that is why it remove adsorbed vapor to Bed 3 via this process. This process will be continued upto end of mode D.

Mode E is called pre-cooling and pre-heating mode for Bed 1 and Bed 3, respectively. After pre-cooling Bed 1 goes to adsorption process, which will continue up to end of mode J. At the same time Bed 3 is heated with hot water to increase its temperature and pressure. When its pressure becomes equal to the pressure of the condenser then connect with condenser by opening the connecting valve 'V3' and desorption process starts, which is the starting point of mode F. The operation process of Bed 3 from modes F to J is similar as the operation process of modes A to E. However, in case of mass recovery happened between Bed 3 and Bed 2 instead of Bed 1. It is clear that Bed 3 completes two full cycle operation within one full cycle operation of Bed 1/Bed 2

3. Methods and Materials

Simulation methods and materials of three-bed dual mode adsorption system are details described in section 3.4 of chapter 3. Heading of the sub-sections from 3.4.1 to 3.4.6 are given below:

- ❖ Adsorption and desorption energy balance
- ❖ Condenser energy balance
- ❖ Evaporator energy balance:
- ❖ Adsorption and desorption rate
- ❖ Mass balance:
- ❖ System performance

Optimization procedure

A complete simulation program was developed based on Matlab software to solve all equations mentioned in section 3.4 of chapter 3. Heat and energy balance equations, mass balance equation and equation for adsorption/ desorption rates were solved simultaneously using matlab ode-45 solver. In the beginning of the solution process, initial values are assumed and finally, those are adjusted by the iteration process. Once the satisfactory convergence criterion is achieved, then the process goes for the next step and continues until reaching to its last step of the cycle.

In this investigation, PSO was applied to optimize the cycle time based on maximum value of SCP, whereas SCP was chosen as the objective function and cycle time (i.e., adsorption/desorption time and pre-cooling/pre-heating time) was chosen as the variable. In PSO, a particle holds the values of variables and updates the values toward the optimal solution. After a number of updating calculations, all the particles hold the same value and the objective function value is maximized. In this case, the number of particles and the number of iterations were considered as 24 and 1500, respectively. It was observed that all particles reached their best position before 500 iterations.

A.4. Results and Discussions

A simulation program was developed for the proposed three-bed adsorption system. Numerical analysis has been done based on standard working condition, shown in Tables A.3. The basic input parameters are given in Table A.4, which is taken from the literature (Rahman et al., 2012). Cycle time indicates the time duration of each mode such as τ_1 , τ_2 and τ_3 , which are directly influence the performance of the system. τ_1 is indicted the desorption time for

Bed 3, τ_2 is the mass recovery/desorption for Bed 1/Bed 2 and τ_3 is the pre-cooling/pre-heating time for all beds. Cycle time of the system was optimized to find the maximum SCP of the system. Observed cycle time are shown in Fig.A.4 and cycle time ratio is define as the ratio of each mode time to the total time, which is shown is Fig. A.5. It is observed that cycle time is decreasing with heat source temperature as desorption occurred faster with temperature. Cycle time ratio of τ_3 was slightly increased with temperature but τ_1 was increased and τ_2 was decreased around 60 - 65 °C heat source temperature. Total cycle time is the sum of cycle time of all modes which was decreased with temperature (Fig. A.6). Chilled water flow rate was varied simultaneously with cycle time to keep constant chilled water outlet temperature at 9 °C. It is obvious that chilled water flow rate was increased with heat source temperature to maintain the chilled water outlet temperature at constant temperature (Fig.A.7).

Table A.3: Standard working conditions

Hot water inlet		Cooling water inlet		Chilled water inlet	
Temp (°C)	Flow rate (kg/s)	Temp (°C)	Flow rate (Ads + Con) (kg/s)	Temp (°C)	Flow rate (kg/s)
50-90	1.0	30	1.0+0.8	14	--

Table A.4: Basic input parameters

Parameters	Value	Units
Q _{st}	2.80E+6	J/kg
L _w	2.50E+6	J/kg
E _a	4.2E+4	J/mol
R	8.314	J/mol.K
D ₀	2.54E-4	m ² /s
R _p	0.30E-3	m
C _w	4.18E+3	J/kg.K
C _{wv}	1.89E+3	J/kg.K
C _{cu}	386	J/kg.K
C _{al}	905	J/kg.K
C _s	924	J/kg.K
A _{hex}	0.61x16	m ²
A _{evp}	3.0	m ²
A _{cond}	1.0	m ²

U_{cond}	3900	$\text{W/m}^2.\text{K}$
U_{hexd}	1000	$\text{W/m}^2.\text{K}$
U_{hexa}	750	$\text{W/m}^2.\text{K}$
U_{evp}	5800	$\text{W/m}^2.\text{K}$
W_s	16	kg
W_{khex}	12.67	kg
W_{fhex}	16.87	kg
W_{evp}	9.6	kg
W_{ew}	61.0	kg
W_{cw}	24.98	kg
$W_{\text{c,hex}}$	12.8	kg

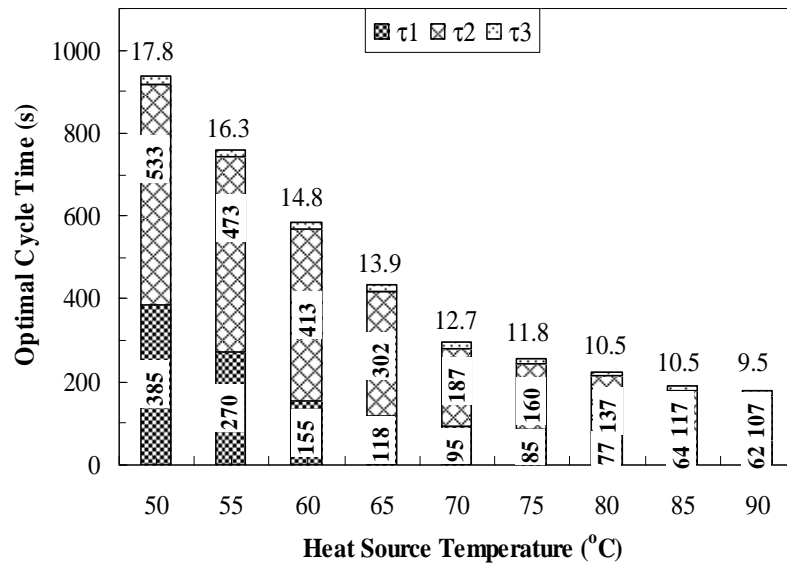


Fig. A.4: Variation optimal cycle time with heat source temperature.

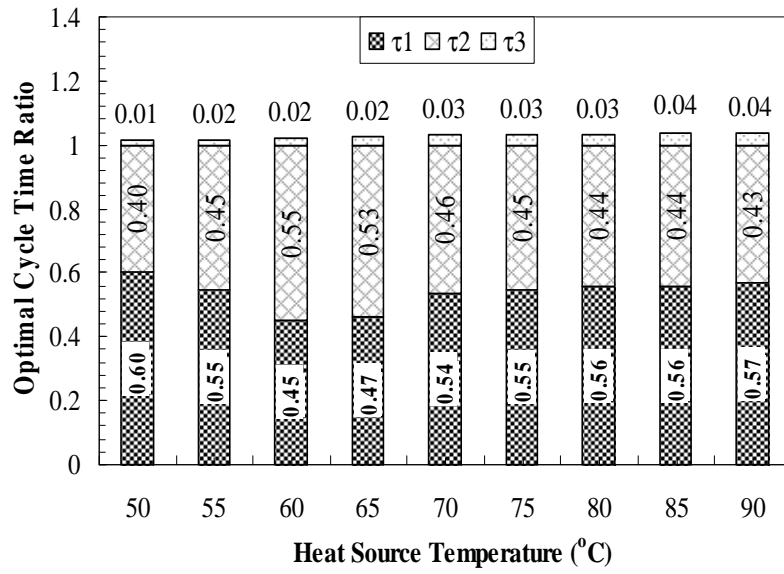


Fig. A.5: Variation of optimal cycle time ratio with heat source temperature.

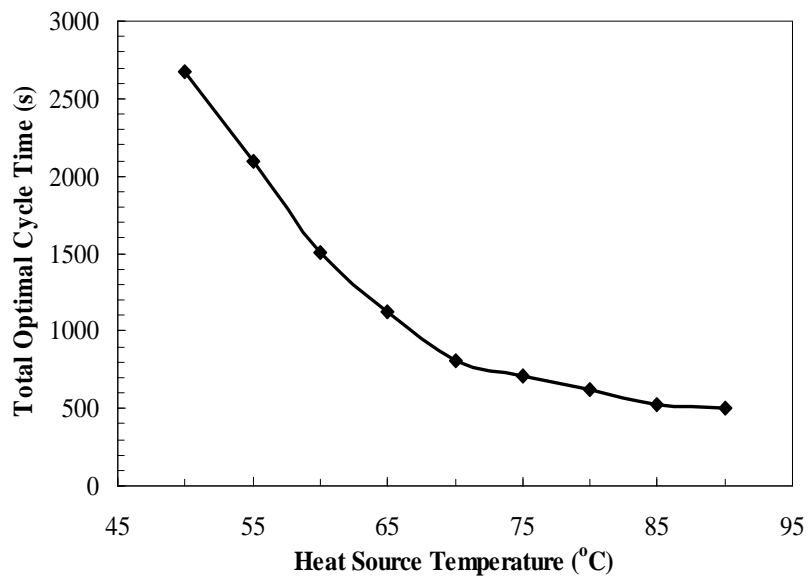


Fig. A. 6: Variation of total optimal total cycle time with heat source temperature.

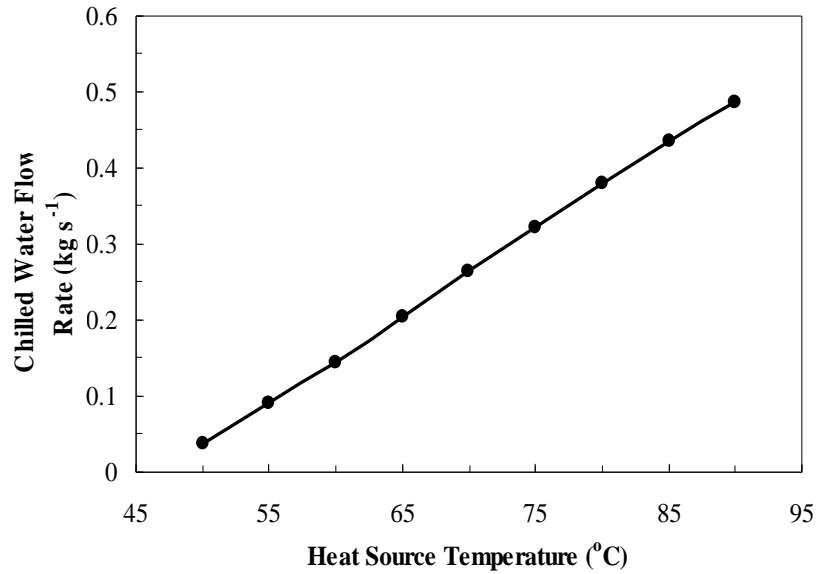


Fig. A.7: Variation of chilled water flow rate with heat source temperature.

The simulated water content in beds with optimal cycle time at 60 °C heat source temperature is shown in Fig. 8. From these figure, it is clear that q -value was increased with adsorption time (e.g., modes A to C and modes F to J for Bed 1, and modes A-H for Bed 2) and was decreased with desorption time (e.g., modes A and F for Bed 3) due to adsorption and desorption process. During pre-heating/pre-cooling time, q -value was not changed because in this stage bed was fully disconnected from other part of the system, e.g. modes E and J for Bed 1 and Bed 2, respectively. One the other hand, the vapor was transferred between two beds in the mass recovery process and consequently the q -value increased for one bed and decreased for other bed, e.g. modes D and I.

The temperature profile of the proposed system in single-stage operation is presented in Fig.A.9. During desorption/desorption time, temperature was not changed significantly. In case of pre-heating mode, temperature was increased and it was decreased during pre-cooling mode promptly. During mass recovery, one bed temperature was increased due to heated by hot water to remove vapour and other bed temperature initially was slightly increased due to adsorption vapour after that decrease due to cool by cooling water. Condenser temperature was little bit increased in the modes A and F because in this case, Bed 3 was connected with condenser for desorbing vapour. On the other hand evaporator temperature was fully constant over the whole cycle because Bed 1 and Bed 2 were continuously produced cooling lead to the evaporator.

Optimal performance of the system is shown in Fig. 10. It is clear for this figure that

single-stage operation the system can effectively work as low as 50 °C heat source temperature. SCP was increase with heat source temperature and COP at first was increased up to 60°C heat source temperature after that again decreased with higher temperature.

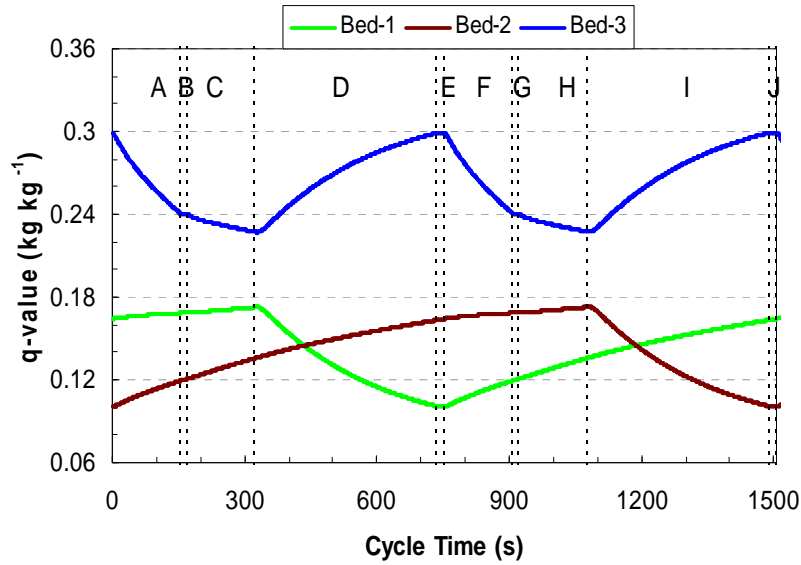


Fig.A.8: Variation of q-value in beds with cycle time at 60 °C heat source temperature.

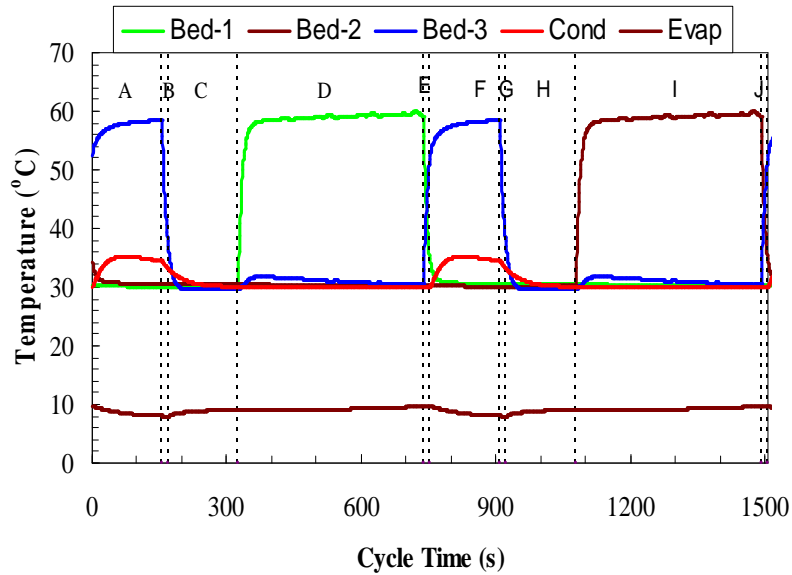


Fig.A.9: Temperature profile of the system at heat source temperature was at 60 °C.

Optimal performance of two-stage operation was compared in Fig. A.10, which is taken from (Rahman et al., 2012). It is noted that basic input parameter and standard working condition were chosen same during optimization for both operation process. It is obvious that COP of single-stage operation is higher than two-stage operation whereas SCP shown as lower value.

It is also clear that two-stage operation can work as low as 45 °C temperature but single-stage operation can't. If the system is operate from 60 to 90 °C in single-stage operation instate of two-stage operation mode then the COP will be increased around 15 to 25 %. Thus, it can be conclude that to get maximum benefit from the proposed dual mode adsoeption system, it should be operate form 45 to 60 °C in two-stage operation mode and from 60 to 90°C in single-stage operation mode. Combined performance of the dual mode system is shown in Fig. A.11.

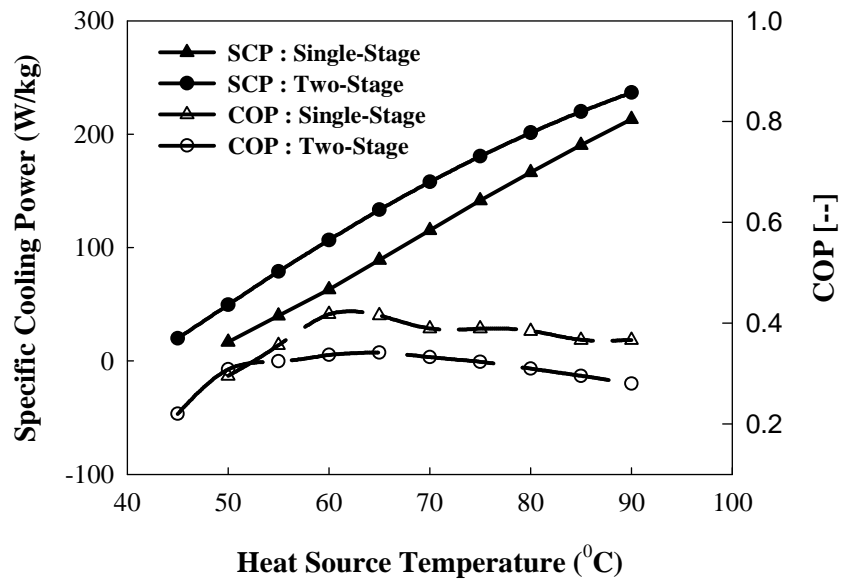


Fig.A.10: Optimal performance of the cycle in single-stage and two-stage operation mode.

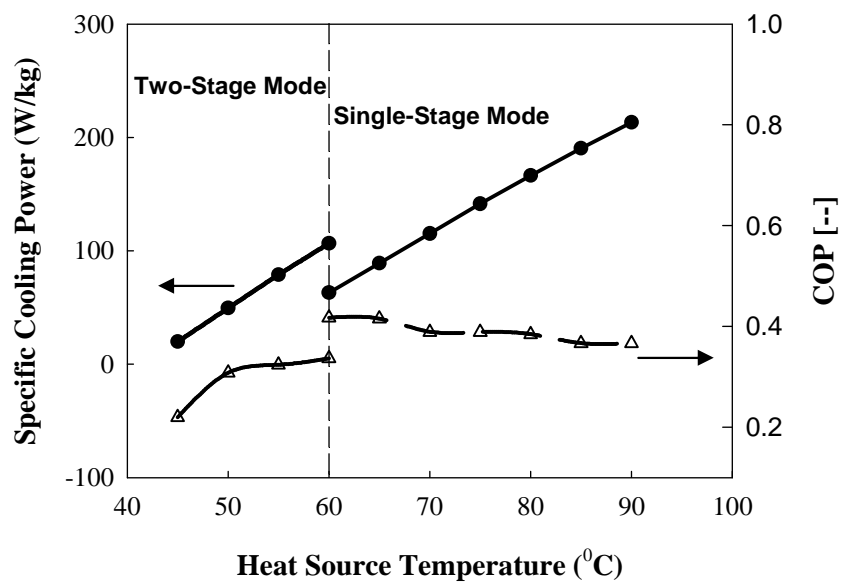


Fig.A.11: Combined performance of the system.

A.5. Conclusion

A silica gel-water based three-bed, dual-mode adsorption cooling cycle has been proposed to increase the overall performance as well as to utilize low temperature heat source for cooling applications. The effect of cycle time on the system performance was analyzed numerically for different heat source temperatures using PSO method. The main findings are:

1. The proposed system is capable to work as single-stage and two-stage operation modes;
2. COP of single-stage operation mode is higher than that of the two-stage operation mode. However, SCP is found to be lower;
3. Single-stage operation mode can utilize heat source as low as 55 °C but two-stage mode is operational with heat source temperature as low as 45 °C;
4. To achieve maximum performance of the three-bed, dual-mode cycle, it should operate in single-stage mode when available regeneration temperature is between 60 to 90 °C, and it should work in two-stage mode if the available heat source temperature is within 45 to 60 °C.

Appendix B

Design and Performance of Four-Stage Adsorption Refrigeration Cycle

Synopsis

A design of four-stage adsorption system was proposed to utilize very low temperature waste heat or solar heat. A simulation model for the proposed system was developed to analyse the influence of cycle time and driving heat source temperature on the performance of system identifying the specific cooling power (SCP) and coefficient of performance (COP). It was found that the proposed cycle could be driven by waste heat temperature as low as 35°C with the coolant at 30°C. Both SCP and COP of the proposed system is very low at lower heat source temperature, which can be improved through optimization of cycle time with other design parameters.

B.1. Introduction

Adsorption heat pump is one of the key technology to utilize waste heat or solar heat. It is neither use ozone layer depleting gases such as CFCs/HFCs, and fossil fuel or electricity as its driving source. Therefore, it has environmental friendliness and energy-saving potentials. There are different types of adsorption systems such as single-stage, two-stage and three-stage adsorption system. A basic conventional single-stage adsorption system has two beds: each of them has one heat exchanger, one condenser and one evaporator. Moreover advanced single-stage adsorption systems, such as two-bed mass recovery, three-bed, three-bed mass recovery, and heat recovery type were proposed. The performance of advance single-stage systems is better than that of the basic two-bed adsorption system (Akahira et al., 2005, Khan et al., 2007a, Uyun et al., 2009a).

To reduce the temperature of the heat source, Saha et al., 2001 proposed a design of a four-bed two-stage adsorption system. They numerically showed that their system can utilize solar/wasted heat with temperature below 70 °C. Alam et al., 2004 and Hamamoto et al., 2005 identified the influence of design parameters and operating conditions on the performance of the system proposed by Saha. Moreover, the modification of the system in operation procedure such as re-heat scheme was investigated by Khan et al., (2005b, 2006b, 2007c), Alam et al., 2007 and S.K. Farid et al., 2011. As a result of these investigations, it can work with the heat source having the temperature as low as 45 °C but the coefficient of performance (COP) of two-stage adsorption system is lower than that of the advanced single-stage systems.

To increase performance with keeping the heat source temperature around 45 °C, Saha et al., 1995b proposed a design of three-stage system and then investigated the effect of different parameters (e.g., cycle time, heat exchanger flow rate and temperature) on the system performance (Saha et al., (1997b, 2003b)). They shown that three-stage adsorption system can work as low as 40 °C heat source temperature. It has three pair of adsorber/desorber heat exchangers in each stage as a result volume of system is larger, which was modified to four-bed three-stage system to reduce the over all size. In this work a innovative design of a system was proposed by adding one heat exchanger bed on upper side of four-bed three-stage adsorption system, which has converted to five bed four stage adsorption system. Main intention to utilize very low

grade waste heat with keeping fixed the heat sink temperature. Finally, the effect of cycle time on the system performance was investigated for different heat source temperature.

B.2. Description of Three-stage Adsorption Cycle

It is well known that conventional single-stage adsorption cycle is not operational when heat source temperature is below 60 °C with a coolant of temperature 30 °C or higher. For practical utilization of these temperatures in adsorption system operation, two or three-stage regeneration is necessary. Because lower heat source temperature is not sufficient enough to drive vapour from evaporator pressure to condenser pressure. It was observed higher stage system can utilize lower heat source temperature. For example two-stage system can work as low as 45 °C and three-stage system can work as low as 40 °C. That is why four-stage system was proposed to utilize more lower temperature waste heat. The schematic diagram of the system is shown in Fig. 1 and its operation mode is given in Table 1. It consists of five adsorber/desorber heat exchanger beds namely Bed 1, Bed 2, Bed 3, Bed 4 and Bed 5, one condenser and one evaporator. Bed 1 and Bed 2 work as lower temperature and pressure (near to evaporator pressure) and Bed 5 works in upper temperature and pressure (near to condenser pressure). Bed 3 and 4 work in two separate level in between evaporator and condenser pressure level. Only Bed 1 and 2 are to connect with evaporator and Bed 5 connect with condenser. In first half cycle, Bed 3 is adsorbed vapour from Bed 1 and then transfer to Bed 4 and finally to condenser via Bed 5. Similarly, in second half cycle Bed 3 adsorbed vapour from Bed 2 and then transfer to condenser through Bed 4 and Bed 5. As a result Bed 3, Bed 4 and Bed 5 are completing two full cycles, while Bed 1 and Bed 2 are completing only one full cycle operation at the same time of operation.

The conceptual Dühring diagram of the proposed four-stage adsorption system is shown in Fig.2. The cyclic diagrams a-b-c-d-a, e-f-g-h-e, i-j-k-l-i and m-n-o-p-m indicate the four different stages (i.e., first, second, third and fourth stage) in between condenser and evaporator pressure level. Bed 1 and 2 work in first stage and other three beds work in three different stages. All beds are completing four thermodynamically modes, i.e., pre-heating, desorption, pre-cooling and adsorption modes, which are accordingly followed by the sides a-b, b-c, c-d and d-a, and e-f, f-g, g-h and h-e for Bed

1/2 and Bed 3, respectively. Similarly, the sides i-j, j-k, k-l and l-i, and m-n, n-o, o-p and p-m indicate the modes pre-heating, desorption, pre-cooling and adsorption modes for Bed 4 and Bed 5, respectively. On the other hand, to complete a full cycle operation of the system, each bed is to complete 8 operational modes, namely A, B, C, D, E, F, G and H, which is shown in Table B.1.

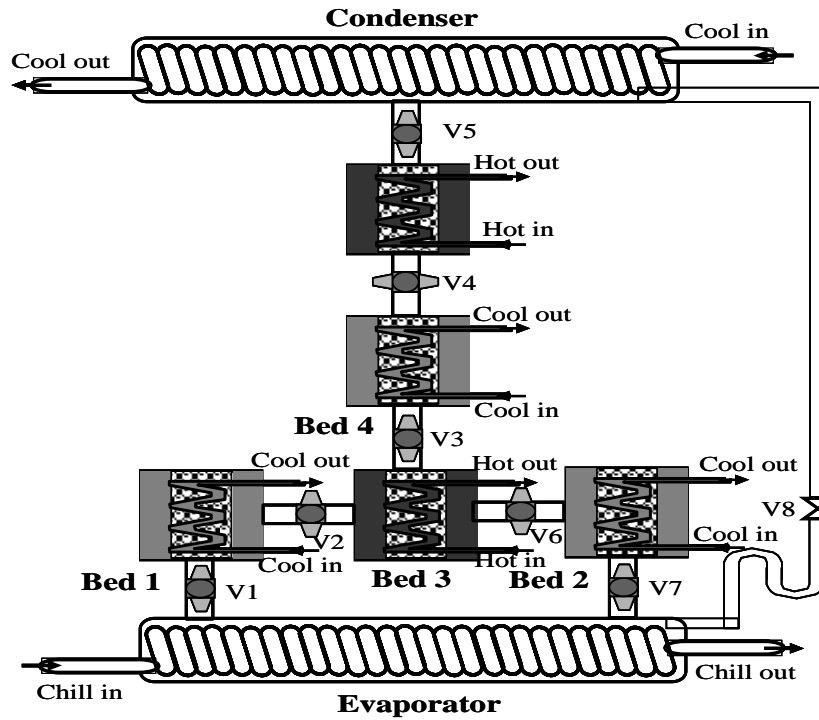


Fig. B.1: Schemata diagram of proposed four-stage adsorption system.

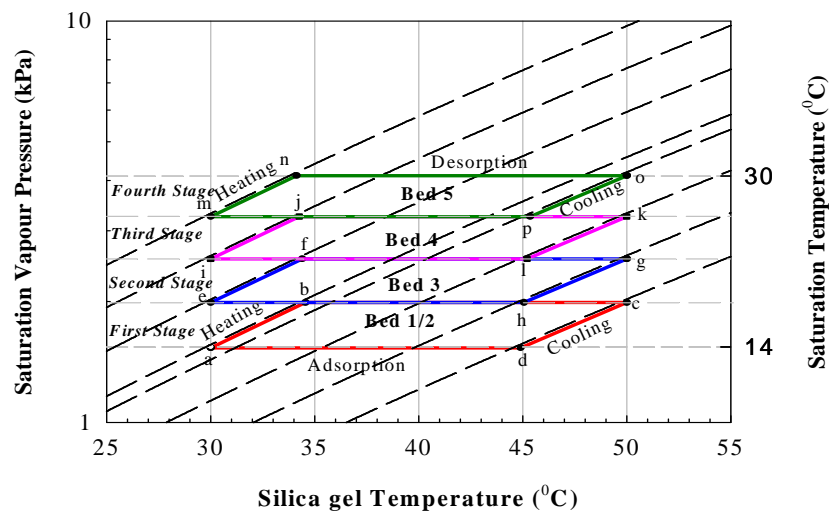


Fig. B.2: Conceptual Dühring diagram of proposed four-stage cycle.

Table B.1: Operation mode and cycle time of four stage adsorption system.

Mode	A τ_1	B τ_2	C τ_1	D τ_2	E τ_1	F τ_2	G τ_1	H τ_2
Bed 1	400	30	400	30	860			
Bed 2	1260					30	400	30
Bed 3	400	30	400	30	400	30	400	30
Bed 4	400	30	400	30	400	30	400	30
Bed 5	400	30	400	30	400	30	400	30

AdsorptionPre-heatingDesorptionPre-cooling

B.3. Simulation Methods and Materials

Simulation methods and materials of five-bed four stage adsorption system are details described in section 3.4 of chapter 3. Heading of the sub-sections from 3.4.1 to 3.4.6 are given below:

- ❖ Adsorption and Desorption Energy Balance
- ❖ Condenser energy balance
- ❖ Evaporator energy balance:
- ❖ Adsorption and desorption rate
- ❖ Mass balance:
- ❖ System performance

A complete simulation program was developed based on Matlab software to solve all equations mentioned in section 3.4 of chapter 3. Adsorption/desorption rate equation, energy balance equation of beds, condenser and evaporator, and mass balance equation have been solved simultaneously using MATLAB ode45 solver. All input parameters such as adsorbent-refrigerant properties, flow rates of heat transfer fluids and heat exchangers specifications were initially given for which the system cyclic operation can be continued.

B.4. Results and Discussions

The simulation program developed for proposed system was operated by adopting the basic input parameters and standard working conditions as presented in Table B.2 (Moriyama 2007). The variation of water contents in adsorber/desorber beds with cycle

time at 50 °C heat source temperature is shown in Fig. B.3. It is obvious from this figure that water contents were increased during adsorption time (i.e., mode E-H-A for Bed 1, mode A-E for Bed 2, mode C with G for Bed 3, mode A with E for Bed 4 and mode C with G for Bed 5) and was decreased during desorption time (i.e., mode C for Bed 1, mode G for Bed 2, mode A with E for Bed 3, mode C with G for Bed 4 and mode A with E for Bed 5). During pre-cooling and pre-heating time beds are fully disconnected from other parts of the system, therefore water contents are remained constant in this mode (i.e., mode B, D, F and H for Bed 3, 4 and 5).

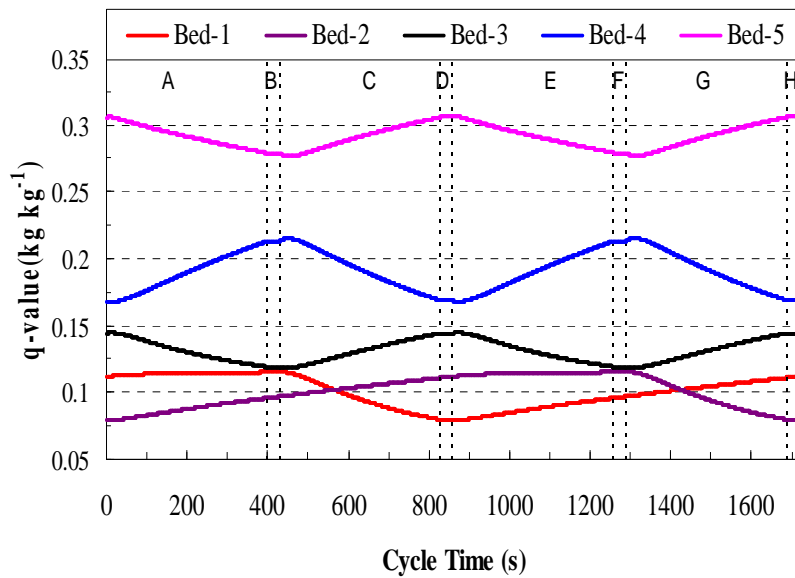


Fig. B.3: Variation of water content in beds with cycle time at 50 °C heat source temperature.

Table B.2: Basic input parameters and standard working conditions

Parameters	Value	Unit
Q_{st}	2.80×10^6	$J \text{ kg}^{-1}$
E_a	4.2×10^4	$J \text{ mol}^{-1}$
D_{so}	2.54×10^{-4}	$m^2 \text{ s}^{-1}$
R	8.314	$J \text{ mol}^{-1} \text{ K}^{-1}$
R_p	0.30×10^{-3}	m
C_w	4.18×10^3	$J \text{ kg}^{-1} \text{ K}^{-1}$
C_{wv}	1.89×10^3	$J \text{ kg}^{-1} \text{ K}^{-1}$

L_w	2.50×10^6	$J\ kg^{-1}$
C_{Cu}	386.00	$J\ kg^{-1}\ K^{-1}$
C_{Al}	905.00	$J\ kg^{-1}\ K^{-1}$
C_s	924.00	$J\ kg^{-1}\ K^{-1}$
A_{hex}^b	0.61×16	m^2
A_{hex}^e	3.00	m^2
A_{hex}^c	1.00	m^2
U_{hex}^c	3900.00	$W\ m^{-2}\ K^{-1}$
U_{hex}^b (desorption)	750.00	$W\ m^{-2}\ K^{-1}$
U_{hex}^b (adsorption)	1000.00	$W\ m^{-2}\ K^{-1}$
U_{hex}^e	5800.00	$W\ m^{-2}\ K^{-1}$
W_s^b	16.00	kg
W_{hex}^b (Cu)	12.67	kg
W_{hex}^b (Al)	16.87	kg
W_{hex}^e	2x4.8	kg
W_w^e	2x30.66	kg
W_w^c	2x12.49	kg
W_{hex}^c	2x6.4	kg
Standard working condition		
T_{in}^{hot}	35 - 85	$^{\circ}C$
\dot{m}_w^{hot}	1.0	$kg\ s^{-1}$
T_{in}^{col}	30	$^{\circ}C$
\dot{m}_w^{col}	1.0	$kg\ s^{-1}$
$T_{in}^{c,col}$	30	$^{\circ}C$
$\dot{m}_w^{c,col}$	0.8	$kg\ s^{-1}$
T_{in}^{chil}	14	$^{\circ}C$
\dot{m}_w^{chil}	0.3528	$kg\ s^{-1}$

Temperature profile for all adsorbent beds, condenser and evaporator are shown in Fig. B.4. It was observed that during adsorption stage, the beds temperatures at first sharply decreased after that it became saturated, since the beds are cooled by cooling water, but during desorption time beds temperatures at first sharply increased after that it became saturated due to heating by hot water. Similarly, during pre-heating and pre-cooling stages beds temperatures were sharply increased and decreased, respectively. Condenser temperature was increased only during desorption time of Bed 5 due to vapour transfer from bed to condenser. On the other hand evaporator temperature was nearly constant with cycle time. In Table 1 it is clear that either Bed 1 or Bed 2 are always connected to the evaporator and produces continuous cooling supply. Consequently it was observed that the proposed cycle keep constant evaporator temperature with less fluctuation.

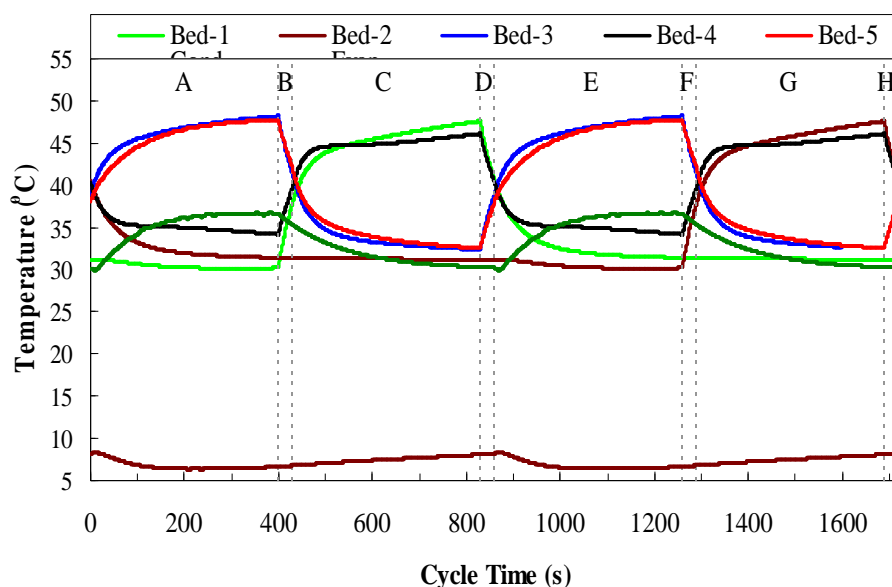


Fig. B.4: Temperature profile of beds, condenser and evaporator at 50 °C heat source temperature.

Effect of total cycle time on the system performance was investigated at 50 °C heat source temperature, which is shown in Fig. B.5. In this case only desorption time, τ_1 was increased from 50 s to 1000 s whereas pre-cooling/pre-heating, τ_2 was kept constant at 30 s. It is obvious that initially SCP was increased with cycle time after that it was decreased. Similar effect of total cycle time was observed on COP. Maximum performance was observed at cycle time 1720 s. This cycle time was chosen for

investigation the effect of heat source temperature on the system performance.

The performance of the proposed system at different heat source temperature is shown in Fig. B.6. It is apparent that the system can work at very low temperature as low as 35 °C with a coolant temperature at 30 °C. The SCP was increased with the increase of heat source temperature whereas COP was increased sharply with heat source temperature up to 50 °C and then it was decreased with temperature. The maximum COP was observed 0.12 at 50 °C heat source temperature whereas both SCP and COP are very low at lowest temperature. An increase of heat source temperature with a fixed heat sink causes the system to increase the amount of refrigerant adsorption/desorption promptly, resulting in higher SCP at higher heat source temperature. Due to similar reason chilled water outlet temperature was decreased with heat source temperature, which is shown in Fig. B.7. In this case total cycle time and chilled water flow rate was kept constant where as only heat source temperature was varied from 35 °C to 90 °C.

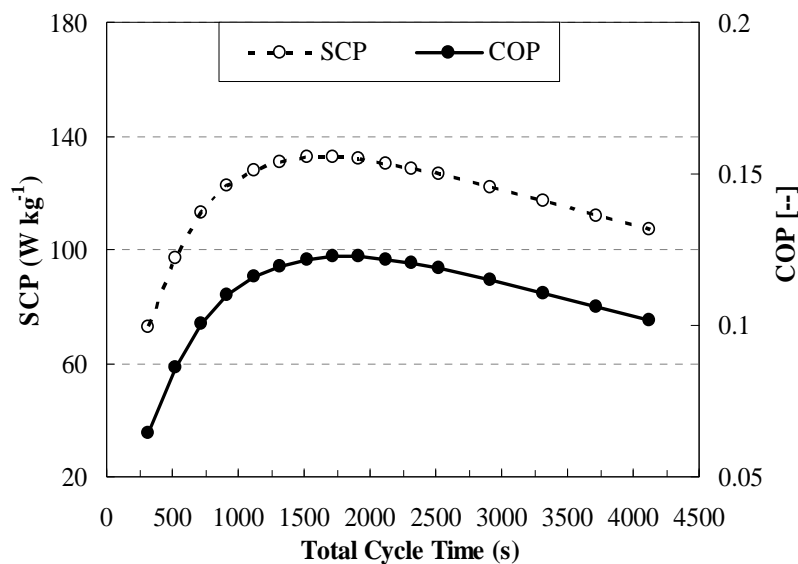


Fig. B.5: Effect of total cycle time on the system performance at 50 °C heat source temperature.

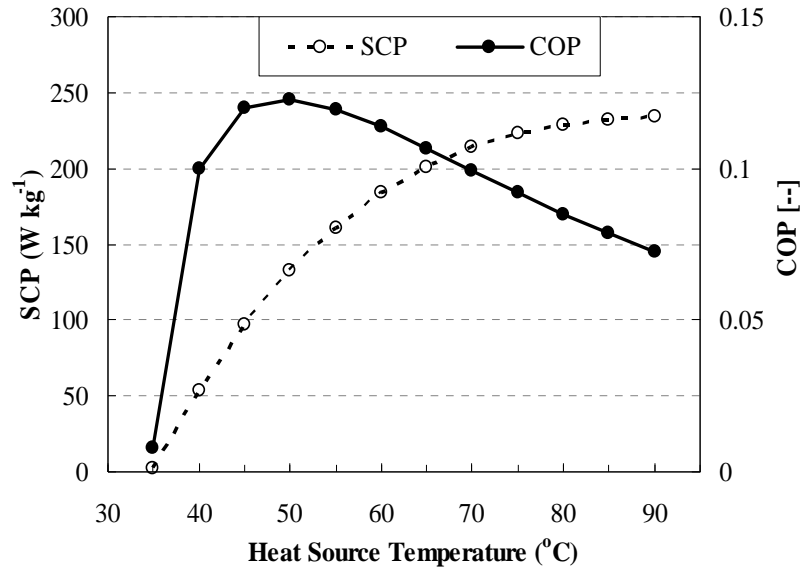


Fig. B.6: Variation of SCP and COP of proposed cycle with heat source temperature.

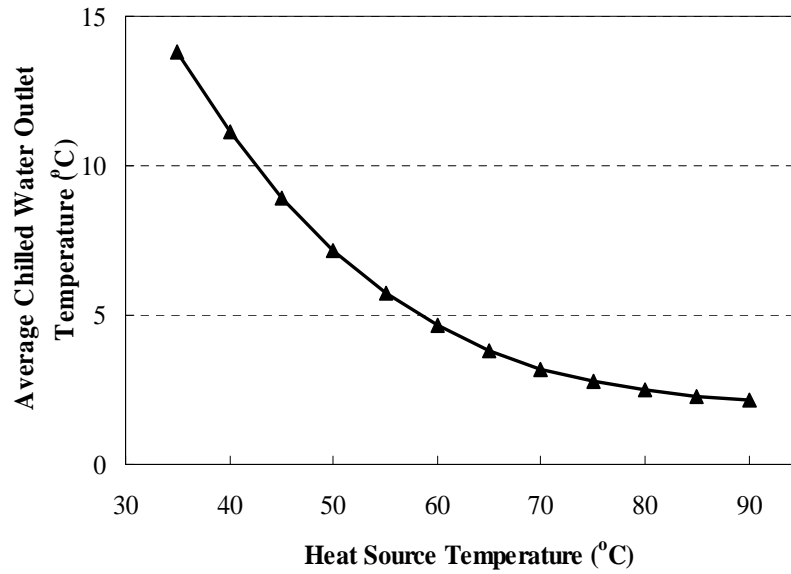


Fig. B.7: Variation of average chilled water outlet temperature with heat source temperature.

B.5. Conclusion

An innovative design of four-stage adsorption system was introduced. A simulation program was developed to investigate the performance of the system for different heat source temperature and cycle time. Maximum performance of the system was observed when cycle time was 1720s. The cycle is effectively applicable to utilize waste heat

source from 35 °C to 90 °C temperature. It was observed that the specific cooling power of the proposed cycle increased with heat source temperature. The maximum coefficient of performance of the system was observed at 50 °C temperature. Both SCP and COP are very low at lowest heat source temperature, more investigation can be done to improve the performance such cycle time optimization with other design parameter and optimization of mass allocation of upper beds and lower beds.

References

1. Akahira A., 2004. Research on the advanced adsorption refrigeration cycles with vapour recovery, Ph.D. Thesis, Tokyo University of Agriculture and Technology, Tokyo, Japan.
2. Akahira A., Alam K.C.A., Hamamoto Y., Akisawa A. and Kashiwagi T., 2004. Mass recovery adsorption refrigeration cycle-improving cooling capacity, *Int. J. Refrigeration*, 27, pp. 225-234.
3. Akahira A., Alam K.C.A., Hamamoto Y., Akisawa A. and Kashiwagi T., 2005. Experimental investigation of mass recovery adsorption refrigeration cycle, *Int. J. Refrigeration*, 28, pp. 565-572.
4. Alam K. C. A., Saha B. B., Akisawa A. and Kashiwagi T., 2004. Influence of design and operating conditions on the system performance of a two-stage adsorption chillier, *Chem. Eng. Commun.*, 191, 981-997.
5. Alam K.C.A., Hamamoto Y., Akisawa A., Kashiwagi T., Saha B.B., Koyma S., Ng K.C., Chua H.T., (2002). Multi-bed multi-stage adsorption refrigeration cycle-reducing driving heat source temperature, *JSHRAE Transactions*, Vol. 20, No. 3, pp. 413-420.
6. Alam K.C.A., Khan M.Z.I., Uyun A.S., Hamamoto Y., Akisawa A. and Kashiwagi T., 2007. Experimental study of a low temperature heat driven re-heat two-stage adsorption chiller, *Appl. Therm. Eng.* 27, pp. 1686-1692.
7. Aristov Y.I., Sapienza A., Ovoshchnikov D.S., Freni A. and Restuccia G., 2012. Reallocation of adsorption and desorption times for optimization of cooling cycles, *Int. J. Refrigeration*, 35, pp. 525-531.
8. Barrer R.M. and Whiteman J.L., 1967. *J. Chem. Soc. A*, pp. 13.
9. Boelman E.C., Saha BB and Kashiwagi T., 1995. Experimental investigation of a silica gel-water adsorption refrigeration cycle the influence of operating conditions on cooling output and COP, *ASHRAE Transactions*, 39(2), pp. 358-66.
10. Boelman, E.C. and Kashiwagi T., 1995. Closed-cycle solid sorption refrigerant, *Trans. of the JAR*, 12(3), pp. 241-252.
11. Brunauer S., Deming L.S., Deming W.E. and Teller E.J., 1940. *J. Am. Chem. Soc.* 62, pp. 1723.

12. Brunauer S., Emmett P.H. and Teller E., 1938. J.Am. Chem.Soc. 60, pp. 309.
13. Cacciola G. and Restuccia G., 1995. Reversible adsorption heat pump: a thermodynamic model, , Int. J. Refrigeration, 18(2), pp. 100-106.
14. Chen C.J., Wang R.Z., Wang L.W., Lu Z.S., 2007. Studies on cycle characteristics and application of split heat pipe adsorption ice maker, Energy Convers Manage, 48, pp. 1106-12.
15. Cho S.H., Kim J.N.1992. Modeling of a silica gel/water adsorption-cooling system, Energy 17 (9), pp. 829-839.
16. Chua H.T., Ng K.C., Malek A., 1999. Modeling the performance of two-bed, silica gel-water adsorption chillers. Int. J. Refrigeration, 22, pp. 194-204.
17. Chua H.T., Ng K.C., Malek A., Kashiwagi T., Akisawa A. and Saha B.B., 2001. Multi-bed regenerative adsorption chiller-improving the utilization of waste heat and reducing the chilled water outlet temperature fluctuation, Int. J. Refrigeration, 24 pp. 124-136
18. Chua H.T., Ng K.C., Malek A., Kashiwagi T., Akisawa A. and Saha B.B., 2001. Multi-bed regenerative adsorption chiller-improving the utilization of waste heat and reducing the chilled water outlet temperature fluctuation, Int. J. Refrigeration, 24, pp. 124-136.
19. Chua H.T., Ng K.C., Malek A., Kashiwagi T., Akisawa A., Saha B.B., 1999. Modelling the performance of two-bed, silica gel-water adsorption chillers, Int. J. Refrigeration, 22, pp. 194 - 204.
20. Chua H.T., Ng K.C., Wang W., 2004. Transient modeling of a two-bed silica gel-water adsorption chiller, Int. J. Heat Mass Transfer, 47, pp. 659-69.
21. Chua H.T., Ng K.C., Wang W., Yap C. and Wang X.L., 2004. Transient modeling of a two-bed silica gel - water adsorption chiller, Int. J. Heat Mass Transfer, 47(4), pp. 659-669.
22. Clausse M., Meunier F., Coulie J. and Herail E., 2008. Comparison of adsorption systems for poly generation systems based on fuel cells, International Sorption Heat Pump Conference 2008.
23. Critoph R.E, 1988. Performance limitations of adsorption cycles for solar cooling, Solar Energy, 41(1), pp. 21-31.

24. Critoph R.E. and Zhong Y., 2005. Review of trends in solid sorption refrigeration and heat pumping technology, *Proc. IMechE, Part E: J. Process Mech. Eng.*, 219(3), pp. 285-300.
25. Critoph R.E., 2002. Carbon-ammonia systems-previous experience, current projects and challenges for the future. In: *Proceedings of the international sorption and heat pump conference (ISHPC 2002)*, China.
26. Critoph R.E. and Metcalf S.J., 2004. Specific cooling power intensification limits in ammonia-carbon adsorption refrigeration systems, *Appl. Therm. Eng.*, 24(5-6), pp. 661-678.
27. Critoph R.E. and Thorpe R., 1996. Thermal compressive device, PCT publication no. WO96/09504.
28. Critoph R.E. and Thorpe R., 2004. Test results of a convective thermal wave adsorption air conditioning system, *Proceedings of HPC04*, Larnaca.
29. Critoph R.E., 1994. Forced convection enhancement of adsorption cycles, *Heat Recovery Systems and CHP*, Vol. 14 (4), pp. 343-350.
30. Critoph R.E., 1998. Forced convection adsorption cycles, *Appl. Therm. Eng.*, 18 (9-10), pp. 799-807.
31. Douss N., Meunier F. and Sun L.M., 1988. Predictive model and experimental results for a two adsorber solid adsorption heat pump, *Ind. Eng. Chem. Res.*, 27, pp. 310-16.
32. Fan Y., Luo, L. and Souyri, B., 2007. Review of solar sorption refrigeration technologies: Development and applications, *Renewable and Sustainable Energy Reviews*, 11, pp. 1758-1775.
33. Farid S.K., Billah M.M., Khan M.Z.I., Rahman M.M. and Sharif U. M., 2011. A numerical analysis of cooling water temperature of two-stage adsorption chiller along with different mass ratios. *Int. Commun. Heat Mass Transfer*, 38, pp. 1086-1092.
34. Gong L.X., Wang R.Z., Xia Z.Z., Chen C.J., 2011. Design and performance prediction of a new generation adsorption chiller using composite adsorbent, *Energy Convers Manage*, 52(6), pp. 2345-50.

35. Hamamotoa Y., Alam K.C.A., Akisawa A. and Kashiwagi T., 2005. Performance evaluation of a two-stage adsorption refrigeration cycle with different mass ratio. *Int. J. Refrigeration* 28(3), pp. 344-352.
36. Hidaka H., Kakiuchi H., Iwade Y., Takewaki T., Yamazaki M., Watanabe N., 2005. JP2005098647.
37. Hulse G.E., 1929. Refroidissement d'un wagon frigorifique a marchandises par un system a adsorption utilisant le gel de silice, *Revue Generale de Froid*, 10, pp. 281-7.
38. Kennedy J. and Eberhart R., 1995. Particle Swarm Optimization. *Proc. IEEE Int. Conf. Neural Networks*, IV, pp. 1942-1948.
39. Khalifa A.H.N., 2011. Experimental Study on Two Beds Adsorption Chiller with Regeneration, *Modern Applied Science*, 5(4), pp. (43-52).
40. Khan M.Z.I., Saha B.B., Alam K.C.A., Akisawa A. and Kashiwagi T., 2005a. Performance investigation on mass recovery three-bed adsorption cycle, *Proceedings of the International Conference on Mechanical Engineering 2005 (ICME2005)*, 28 - 30 December 2005, Dhaka, Bangladesh.
41. Khan M.Z.I., Saha B.B., Miyazaki T., Akisawa A. and Kashiwagi T., 2005b. Study on a two-stage adsorption chiller using re-heat, *Proceedings of JSRAE annual conference-10*, Tokyo, Japan, pp. 23 - 27.
42. Khan M.Z.I., Saha B.B., Alam K.C.A., Miyazaki T., Akisawa A. and Kashiwagi T., 2006a. Multi-bed mass recovery adsorption cycle-improving performance, *Trans. of the JSRAE*, Vol 23, No.4, pp. 399-408.
43. Khan M.Z.I., Alam K.C.A., Saha B.B., Hamamoto Y., Akisawa A. and Kashiwagi T., 2006b. Parametric study of a two-stage adsorption chiller using re-heat - the effect of overall thermal conductance and adsorbent mass on system performance, *Int. J. therm. Sci.*, 45, pp. 511-519.
44. Khan M.Z.I., Saha B.B., Alam K.C.A., Akisawa A., Kashiwagi T., 2007a. Study on solar/waste heat driven multi-bed adsorption chiller with mass recovery, *Renewable Energy*, Vol. 32, pp. 365 - 381.
45. Khan M.Z.I., 2007b. Study on advanced adsorption cycle employing re-heat and mass recovery scheme, *Ph.D. thesis*, Tokyo University of Agriculture and Technology, Tokyo, Japan.

46. Khan M.Z.I., Alam K.C.A., Saha B.B., Akisawa A. and Kashiwagi T., 2007c. Study on a re-heat two-stage adsorption chiller - the influence of thermal capacitance ratio, overall thermal conductance ratio and adsorbent mass on system performance. *Appl. Therm. Eng.*, 27, pp. 1677-1685.
47. Khan M.Z.I., Alam K.C.A., Saha B.B., Akisawa A. and Kashiwagi T., 2008. Performance evaluation of multi-stage, multi-bed adsorption chiller employing re-heat scheme, *Renewable Energy*, 33 pp. 88-98.
48. Kubota M., Ueda T., Fujisawa R., Kobayashi J., Watanabe F., Kobayashi N. and Hasatani M., 2008. Cooling output Performance of a prototype adsorption heat pump with fin-type silica gel tube module, *App. Therm. Eng.*, 28(2-3), pp. 87-93.
49. Langmuir I., 1918, *J. Chem. Soc.*, 40, pp. 1361.
50. Li S.L., Wu J.Y., Xia Z.Z., Wang R.Z., 2011. Study on the adsorption isosteres of the composite adsorbent CaCl_2 and expanded graphite, *Energy Convers Manage*, 52, pp. 1501-6.
51. Liu Y. and Leong K.C., 2006. Numerical study of a novel cascading adsorption cycle, *Int. J. Refrigeration*, 29 pp. 250-259.
52. Lu Y.Z., Wang R.Z., Zhang M., Jiangzhou S., 2003. Adsorption cold storage system with zeolite-water working pair used for locomotive air conditioning, *Energy Convers Manage*, 44, pp. 1733-43.
53. Marletta, L., Maggio, G., Freni, A., Ingrassiotta, M., and Restuccia, G., 2002. A non-uniform temperature non-uniform pressure dynamic model of heat and mass transfer in compact adsorbent beds, *Int. J. Heat Mass Transfer*, 45(16), pp. 3321-3330.
54. Marlinda, Uyun A.S., Miyazaki T., Ueda Y. and Akisawa A., 2010. Performance Analysis of a Double-effect Adsorption Refrigeration Cycle with a Silica Gel/Water Working Pair, *Energies*, 3, pp. 1704-1720.
55. Meunier F., 1978. Utilisation des cycle a sorption pour la production de froid par l'énergie solaire, *Cahiers de l'AFEDDES*, 5, pp. 57-67.
56. Miles D.J. and Shelton S.V., 1996. Design and testing of a solid-sorption heat-pump system, *Appl. Therm. Eng.*, 16 (5), pp. 389-394.
57. Miller E.B., 1929. The development of silica-gel, refrigerating engineering, the American society of refrigerating engineers, 17(4), pp. 103-108.

58. Mittelbach W., Büttner T., and Herrmann R., 2008. Compact adsorption chillers with coated adsorber heat exchangers, International Sorption Heat Pump Conference 2008.
59. Miyazaki T. and Akisawa A., 2009. The influence of heat exchanger parameters on the optimum cycle time of adsorption chillers, *Appl. Therm. Eng.*, 29, pp. 2708-2717.
60. Miyazaki T., Akisawa A., Saha B.B., El-Sharkawy I.I., Chakraborty A., 2009. A new cycle time allocation for enhancing the performance of two-bed adsorption chillers, *Int. J. Refrigeration*, 32, pp. 846-853.
61. Monma, T., Mizota, T., 2005. JP2005299974.
62. Moriyama K., 2007. Performance Improvement of Adsorption Chillers by the Optimization of Cycle time Component, MS Thesis, Tokyo University of Agriculture Technology, Tokyo, Japan.
63. Ng K.C., Wang X., Lim Y.S., Saha B.B., Chakraborty A., Koyama S., Akisawa A. and Kashiwagi T., 2006. Experimental study on performance improvement of a four-bed adsorption chiller by using heat and mass recovery. *Int. J. Heat Mass Transfer*, 49, pp. 3343-3348
64. Papadopoulos A.M., Oxizidis S. and Kyriakis N., 2003. Perspectives of solar cooling in view of the developments in the air-conditioning sector, *Renewable and Sustainable Energy Reviews*, 7(5), pp. 419-438.
65. Patzner N., 2001. EP1154208.
66. Pons M. and Guilleminot J.J., 1986. Design of an experimental solar powered, solid-adsorption ice maker, *Journal of Solar Energy Engineering*, 108, pp.332-337.
67. Rahman A.F.M.M., Miyazaki T., Ueda Y., Saha B.B. and Akisawa A., 2013. Performance comparison of three-bed adsorption cooling system with optimal cycle time setting, *Heat Transfer Engineering*, 34 (11-12), pp 1-10.
68. Rahman A.F.M. M., Ueda Y., Akisawa A., Miyazaki T. and Saha B.B., 2012. Innovative design and performance of three-bed two-stage adsorption cycle under optimized cycle time, *Journal of Environment and Engineering* 7(1), pp. 92-108.
69. Ruthven D. M., 1984. Principles of adsorption and adsorption processes, John Wiley and Sons, Inc. publication, pp. 30- 34.

70. Saha B.B., Boelman E.C. and Kashiwagi T., 1995a. Computer simulation of a silica gel-water adsorption refrigeration cycle the influence of operating conditions on cooling output and COP, ASHRAE Transactions, 39(2), pp. 348-57.
71. Saha B.B, Boelman E.C. and Kashiwagi T., 1995b. Computational analysis of an advanced adsorption-refrigeration cycle, Energy 20 (10), pp. 983-994.
72. Saha, B.B. and Kashiwagi T., 1997a. Experimental investigation of an advanced adsorption refrigeration cycle, ASHRAE Transactions 103(2), pp. 50-58.
73. Saha B. B., Akisawa A. and Kashiwagi T., 1997b. Silica gel water advanced adsorption refrigeration cycle, Energy, 22(4), pp. 437 - 447.
74. Saha B.B., Akisawa A. and Kashiwagi T., 2001. Solar/waste heat driven two-stage adsorption chiller: the prototype. Renewable Energy, 23, pp. 93-101.
75. Saha B.B., Koyama S., Lee J.B., Kuwahara K., Alam K.C.A., Hamamoto Y., Akisawa A. and Kashiwagi T., 2003a. Performance evaluation of a low-temperature waste heat driven multi-bed adsorption chiller, Int. J. Multiphase Flow, 29, pp. 1249-1263.
76. Saha B.B., Koyama S., Kashiwagi T., Akisawa A., Ng K.C., Chua H.T., 2003b. Waste heat driven dual-mode, multi-stage, multi-bed regenerative adsorption system, Int. J. Refrigeration, 26, 749-757.
77. Saha B.B., El-Sharkawy I.I., Koyama S., Lee J.B. and Kuwahara T., 2006. Waste heat driven multi-bed adsorption chiller: heat exchangers overall thermal conductance on chiller performance, Heat Transfer Eng., 27 (5), pp. 80-87.
78. Saha B.B., El-Sharkawy I.I., Chakraborty A., Koyama S. 2007, Study on an activated carbon fiber-ethanol adsorption chiller: Part I - system description and modeling, Int. J. Refrigeration, 30, pp. 86-95.
79. Sakoda A. and Suzuki M., 1984. Fundamental study on solar powered adsorption cooling system, Journal of Chemical Engineering of Japan, 17(1), pp. 52-57.
80. San J.Y., 2006. Analysis of the performance of a multi-bed adsorption heat pump using a solid-side resistance model, Appl. Therm. Eng., 26, pp. 2219-2227.
81. Santamouris M, Argiriou A., 1994. Renewable energies and energy conservation technologies for buildings in southern Europe, Int. J. Sol. Energy, 15, pp. 69-79.
82. Schicktanz M., and Núñez T., 2008. Modeling of an adsorption chiller for dynamic system simulation, International Sorption Heat Pump Conference 2008.

83. Srivastava N.C., Eames I.W., 1998. A review of adsorbents and adsorbates in solid - vapour adsorption heat pump systems, *App. Therm. Eng.*, 18, pp. 707-714.
84. Sun L. M., Feng Y. and Pons M., 1997. Numerical investigation of adsorptive heat pump systems with thermal wave heat regeneration under uniform-pressure conditions, *International Journal of Heat and Mass Transfer*, 40(2), pp. 281-293.
85. Suzuki M., 1993. Application of adsorption cooling system to automobiles, *Heat Recovery Systems and CHP*, 13(4), pp. 335-340.
86. Sward, B.K., Douglas LeVan, M. and Meunier, F., 2000. Adsorption heat pump modeling: the thermal wave process with local equilibrium, *Appl. Therm. Eng.*, 20(8), pp. 759-780.
87. Szarzynski S., Feng Y. and Pons M., 1997. Study of different internal vapor transports for adsorption cycles with heat regeneration, *Int. J. Refrigeration*, 20 (6), pp. 390-401.
88. Szarzynski S., Feng Y. and Pons M., 1997. Study of different internal vapour transports for adsorption cycles with heat regeneration, *Int. J. Refrigeration*, 20 (6), pp. 390-401.
89. Uyun A.S., Akisawa A., Miyazaki T., Ueda Y. and Ksahiwagi T., 2009a. Numerical analysis of an advanced three-bed mass recovery adsorption refrigeration cycle, *Appl. Therm. Eng.*, 29, pp. 2876-2884.
90. Uyun A.S., Miyazaki T., Ueda Y. and Akisawa A., (2009b). Experimental investigation of a three-bed adsorption refrigeration chiller employing an advanced mass recovery cycle, *Energies*, 2, pp. 531-544; doi:10.3390/en20300531.
91. Uyun A.S, Miyazaki T., Ueda Y. and Akisawa A., 2009c. High Performance Cascading Adsorption Refrigeration Cycle with Internal Heat Recovery Driven by a Low Grade Heat Source Temperature, *Energies*, 2, pp. 1170-1191.
92. Vasta S., Sapienza A., Freni A., and Restuccia G., 2008. A new adsorbent bed for automotive applications: experimental test in a full scale laboratory chiller, *International Sorption Heat Pump Conference 2008*.
93. Wang D.C., Wu J.Y., 2005. Influence of intermittent heat source on adsorption ice maker using waste heat, *Energy Convers Manage*, 46, pp. 985-98.

94. Wang, J.; Wang, L.W.; Luo, W.L.; Wang, R.Z., 2012. Experimental study of a two-stage adsorption freezing machine driven by low temperature heat source, *Int. J. Refrigeration*, xxx 1-8.
95. Wang R.Z., Ge T.S., Chen C.J., Ma Q. and Xiong Z.Q., 2009. Solar sorption cooling systems for residential applications: Options and guidelines, *Int. J. Refrigeration*, 32, pp. 638 - 660.
96. Wang X., Chua H.T., 2007. A comparative evaluation of different heat-recovery schemes as applied to a two-bed adsorption chiller, *Int J Heat Mass Transfer*, 50, pp 433-43.
97. Wu J.Y., Wang R.Z., Xu Y.X., 2002. Dynamic analysis of heat recovery process for a continuous heat recovery adsorption heat pump, *Energy Convers Manage*, 43, pp. 2201-11.
98. Yang G.Z., Xia Z.Z., Wang R.Z., Keletigui D., Wang D.C., Dong Z.H. Yang X. 2006. Research on a compact adsorption room air conditioner, *Energy Convers Manage*, 47, pp. 2167-77.
99. Zhang L.Z. and Wang L., 1997. Performance estimation of an adsorption cooling system for automobile waste heat recovery, *Appl. Therm. Eng.*, 17, pp. 1127-1139.
100. Zhang, L.Z., and Wang, L., 1997. Performance estimation of an adsorption cooling system for automobile waste Heat Recovery, *Appl. Therm. Eng.*, 17(12), pp. 1127-1139.

Dissertation Related Author's Publication

Patent

1. A patent of title "**Multi Stage Adsorption Refrigerator (多段吸着冷凍機)**" has been submitted to the Tokyo University of Agriculture and Technology on 2012-03-01 (under process).

International Journal

1. A.F.M. Mizanur Rahman, T. Miyazaki, Y. Ueda, B.B. Saha and A. Akisawa, "Performance Comparison of Three-bed Adsorption Cooling System with Optimal Cycle Time Setting", **Heat Transfer Engineering**, **34 (11-12)**, pp 1-10, 2013.

2. A.F.M. Mizanur Rahman, Y. Ueda, A. Akisawa, T. Miyazaki and B.B. Saha, "Innovative Design and Performance of Three-bed Two-Stage Adsorption Cycle under Optimized Cycle Time", **Journal of Environment and Engineering** **7(1)**, pp. 92-108, 2012.

3. A.F.M. Mizanur Rahman, Y. Ueda, A. Akisawa, T. Miyazaki and B.B. Saha, "Design and Performance of an Innovative Four-bed, Three-Stage Adsorption Cycle", **Submitted to the International journal of Energies (under review)**.

4. A.F.M. Mizanur Rahman, Y. Ueda, A. Akisawa, T. Miyazaki and B.B. Saha, "Study on a Silica gel-Water based Three-bed Dual-Mode Adsorption Cooling Cycle", **will be submitted soon to the international journal of Heat Transfer Research**.

Proceedings of Conference

1. A.F.M. Mizanur Rahman, T. Miyazaki, Y. Ueda, B.B. Saha and A. Akisawa, "Optimal Performance of Three Bed Mass Recovery With Heating/Cooling Adsorption Cooling System", published in the proceeding of 'International Symposium on Innovative Materials for Processes in Energy Systems 2010' (IMPRES2010), pp. 79-85.